

ABSTRACT

Title of Dissertation: GENETIC ENGINEERING AND
NANOTECHNOLOGICAL APPROACHES TO
ENHANCE LIPID PRODUCTION IN *FREMYELLA*
DIPLOSIPHON, A MODEL CYANOBACTERIUM

Somayeh Gharaie Fathabad, Doctor of Philosophy, May 2019

Dissertation Chair: Viji Sittther, Doctor of Philosophy
Department of Biology

In recent years, cyanobacteria have gained great importance as a potential source of biofuel due to their fast generation time and ability to directly convert carbon dioxide into free fatty acids. In this study, the sterol desaturase (SD) gene was overexpressed on the model cyanobacterium *Fremyella diplosiphon* B481 to enhance total lipid content and fatty acids. The effort resulted in a transformant designated as B481-SD with a 64-fold increase in mRNA transcript level. Results of gravimetric analysis and gas

chromatography-mass spectrometry (GC-MS) revealed a 27.3% increase in total lipid content and a 23% increase in unsaturated fatty acid methyl esters (FAMES) from B481-SD transesterified lipids relative to wild type (WT).

In the second phase, the effect of salinity stress on B481-SD growth, total lipid content, and fatty acid composition was examined. The halotolerant strain designated as B481-SDH exhibited a 38-fold increase in mRNA transcript level when compared to the WT. In addition, proteomic analysis revealed a band near the expected size of sterol desaturase in all strains. Four spots that potentially represent SD up-regulated in B481-SD and B481-SDH were identified using 2D-PAGE. In the third phase, the effect of various concentrations (0.05-3.2 mg L⁻¹) of two iron nanoparticles (Nanofer 25 and 25s) on growth, photosynthetic pigmentation, total lipid content, and fatty acid composition of *F. diplosiphon* was investigated. Results of the study revealed a significant increase ($P \leq 0.05$) in growth of *F. diplosiphon* treated with Nanofer 25s ranging from 0.2-1.6 mg L⁻¹ compared to the control; however, no significant difference was observed in growth of *F. diplosiphon* treated with Nanofer 25 relative to the control. Photosynthetic pigment quantification revealed no significant increases in *chl a* and carotenoid accumulations in *F. diplosiphon* exposed to Nanofer 25s ranging from 0.4-1.6 mg L⁻¹. Results of gravimetric analyses and GC-MS revealed significant increases in total lipid content and unsaturated fatty acid methyl esters in *F. diplosiphon* nano-treated transesterified lipids. The presence of iron nanoparticles inside *F. diplosiphon* was visualized using optical microscopy and transmission electron microscopy. Our findings address a key challenge in lipid productivity of cyanobacterial cultivation systems by increasing total lipid content and

essential unsaturated fatty acids to maximize the potential of *F. diplosiphon* as a large-scale biofuel agent.

GENETIC ENGINEERING AND NANOTECHNOLOGICAL APPROACHES TO
ENHANCE LIPID PRODUCTION IN *FREMYELLA DIPLOSIPHON*, A MODEL
CYANOBACTERIUM

by

Somayeh Gharaie Fathabad

A Dissertation Submitted in Partial Fulfillment
of the Requirements for the Degree
Doctor of Philosophy

MORGAN STATE UNIVERSITY

May 2019

GENETIC ENGINEERING AND NANOTECHNOLOGICAL APPROACHES TO
ENHANCE LIPID PRODUCTION IN *FREMYELLA DIPLOSIPHON*, A MODEL
CYANOBACTERIUM

by

Somayeh Gharai Fathabad

has been approved

January 2019

DISSERTATION COMMITTEE APPROVAL:

_____, Chair
Viji Sittther, Ph.D.

AnithaChristy S. Arumanayagam, Ph.D.

Birol Ozturk, Ph.D.

Kadir Aslan, Ph.D.

Kenneth Samuel, Ph.D.

Michael Koban, Ph.D.

Dedication

This work is dedicated to my parents Homa Motamedi and Alireza Gharai
Fathabad, sisters Hayedeh, Bahareh and Samaneh Gharai Fathabad, and brother
Amirhossein Gharai Fathabad.

Acknowledgements

I would like to express my sincere gratitude to my advisor, Dr. Viji Sittther, for her instruction, guidance, patience, motivation, immense knowledge, and encouragement throughout the research, and providing valuable suggestions. I also greatly appreciate the suggestions provided by my committee members, Drs. AnithaChristy S. Arumanayagam (external), Birol Ozturk, Kadir Aslan, Kenneth Samuel, and Michael Koban. I would also like to acknowledge the support from the Strengthening Historically Black Graduate Institutions, Title III funding, A student-centered entrepreneurship development (ASCEND), and The School of Graduate Studies.

I am grateful to Dr. Huan Chen and Mr. Jie Lu at the National High Magnetic Field Laboratory, Florida, for their help in lipidomics. I also acknowledge the help provided by Drs. Yucheng Lan and Pumtiwitt McCarthy, and Mr. Kevin Swinson for standardizing certain experimental procedure.

I would like to thank my lab members Dr. Behnam Tabatabai (Research Associate), Afua Adusei, Dy'mon Walker, Shaveen McKeen, and Ebunoluwa Oni (Ungergraduates) for their valuable help during my dissertation research. My sincere thanks to Dr. Solomon Tadesse and Mr. Cole Grinnell in the Department of Chemistry for their technical help and support in transesterification procedures.

Table of Contents

List of Figures	xi
List of Tables	xxi
CHAPTER I: INTRODUCTION	1
1.1 Objectives	9
CHAPTER II: LITERATURE REVIEW	14
2.1 Cyanobacteria, a photosynthetic prokaryote.....	14
2.1.1 Cyanobacterial photosynthetic pathway	15
2.1.2 Photosynthetic pigments in cyanobacteria.....	18
2.2 <i>Fremyella diplosiphon</i> , a model of cyanobacterium.....	19
2.3 Cyanobacterial lipid production.....	20
2.3.1 Genetic transformation to enhance cyanobacterial lipid.....	22
2.4 Salinity stress induced lipid production.....	23
2.5 Cyanobacterial protein production.....	25
2.6 Biofuels: a renewable alternative to fossil fuels	26
2.6.1 Cyanobacterial lipid as biofuel agent.....	27
2.7 Steps in biofuel production from cyanobacteria	29

2.7.1 Total lipid extraction.....	29
2.7.2 Direct transesterification.....	29
2.8 Maximizing the potential of biofuel production by increasing lipid and fatty acid compositions	31
2.9 Using iron nanoparticles to enhance cyanobacterial total lipid content and fatty acid compositions	33
2.9.1 Iron- induced oxidative stress in cyanobacteria.....	33
CHAPTER III: EXPERIMENTAL.....	36
3.1 Materials and procedures	36
3.2 BG11 stock solutions for cyanobacterial growth.....	38
3.3 Instrumentation	40
3.4 Methods.....	42
3.4.1 Objective 1. Enhancement of lipids in <i>F. diplosiphon</i> using genetic Transformation	42
3.4.1.1 Overexpression of sterol desaturase and acyl-lipid desaturase genes in <i>F. diplosiphon</i> via electroporation-mediated genetic transformation	42
3.4.1.2 Comparison of total lipid content and fatty acid compositions in the WT and transformant by gravimetric analysis and GC-MS	52
3.4.1.3 Enhancement of total lipid content and essential fatty acid methyl esters by exposure to salinity stress	55
3.4.2 Enhancement of lipids and fatty acids in <i>F. diplosiphon</i> using iron Nanoparticles	59

3.4.2.1 Impact of iron nanoparticles (Nanofer 25 and Nanofer 25s) on growth and photosynthetic efficacy of two cyanobacteria strains (B481 and SF33)	59
3.4.2.2 The effect of iron nanoparticles on total lipid content and fatty acid composition of <i>F. diplosiphon</i> nano-treated cells determined using gravimetric analysis and GC-MS	60
CHAPTER IV: RESULTS AND DISCUSSION	63
4.1 Enhancement of lipid in <i>F. diplosiphon</i> using genetic transformation via. Electroporation	63
4.1.1 Overexpression of sterol desaturase and acyl-lipid desaturase genes in <i>F. diplosiphon</i> via electroporation-mediated genetic transformation.....	63
4.1.1.1 Identification of acyl-lipid desaturase and sterol desaturase homologues in <i>F. diplosiphon</i>	63
4.1.1.2 Cloning and transformation of acyl-lipid desaturase and sterol desaturase genes in <i>F. diplosiphon</i>	65
4.1.1.2.1 Comparison of growth and photosynthetic pigment accumulation in <i>F. diplosiphon</i> WT and B481-SD	69
4.1.2 Comparison of total lipid content and fatty acid compositions	74
in the WT and transformant by gravimetric analysis and GC-MS.	
4.1.2.1 Enhancement of total lipid content in transformant strain.....	74
4.1.2.2 Comparison of fatty acid methyl ester profile in WT and transformant via direct transesterification, GC-MS, and GC×GC-TOFMS	75

4.1.3 Enhancement of total lipid content and essential fatty acid methyl esters by exposure to salinity stress.....	83
4.1.3.1 Growth of <i>F. diplosiphon</i> WT and transformant (B481-SD) in media containing 40 g L ⁻¹	83
4.1.3.2 RT-qPCR analysis confirms overexpression of sterol desaturase gene in <i>F. diplosiphon</i> halotolerant transformant	84
4.1.3.3 Enhancement of total lipid content in halotolerant transformant strain	85
4.1.3.4 Comparison of fatty acid methyl ester profile in wild-type and halotolerant transformant via direct transesterification and GC-MS	86
4.1.3.5 Growth of wild-type and halotolerant transformant strains in sea water	93
4.1.3.6 Growth of wild-type and halotolerant transformant strains in sea water and brackish water amended with BG11 media	94
4.1.4 Proteomic comparison of <i>F. diplosiphon</i> B481-wild type, B481-SD, and B481-SDH	96
4.2 Enhancement of lipids and fatty acids in <i>F. diplosiphon</i> using iron nanoparticles...	99
4.2.1 Impact of iron nanoparticles (Nanofer 25 and Nanofer 25s) on growth and photosynthetic efficacy of two <i>F. diplosiphon</i> strains (B481 and SF33)	99
4.2.1.1 Effect of iron nanoparticles concentrations ranging from 1.5-600 mg L ⁻¹ on <i>F. diplosiphon</i> growth	99
4.2.1.2 Effect of iron nanoparticles concentrations ranging from 0.05-3.2 mg L ⁻¹ on <i>F. diplosiphon</i> growth	104
4.2.2 Effect of Nanofer 25s on <i>F. diplosiphon</i> photosynthetic efficacy	109
4.2.3 Enhancement of total lipid content in <i>F. diplosiphon</i> Nanofer 25s-treated cells...	113

4.2.4 Comparison of fatty acid methyl ester profile in <i>F. diplosiphon</i> wild-type and Nanofer 25s-treated cells via direct transesterification and GC-MS	115
4.2.5 Microscopy studies to visualize the presence of iron nanoparticle in <i>F. diplosiphon</i> cell	128
CHAPTER V	
CONCLUSIONS.....	131
5.1 Enhancement of lipid in <i>F. diplosiphon</i> using genetic transformation via electroporation	131
5.1.1 Overexpression of sterol desaturase and acyl-lipid desaturase genes in <i>F. diplosiphon</i> via electroporation-mediated genetic transformation.....	131
5.1.2 Comparison of total lipid content and fatty acid compositions in the WT and transformant by gravimetric analysis, GC-MS and GC-TOFMS	132
5.1.3 Enhancement of total lipid content and essential fatty acid methyl esters by exposure to salinity stress	132
5.1.4 Proteomic comparison of <i>F. diplosiphon</i> B481-wild type, B481-SD, and B481-SDH	133
5.2 Enhancement of lipids and fatty acids in <i>F. diplosiphon</i> using iron nanoparticles .	134
5.2.1 Impact of iron nanoparticles (Nanofer 25 and Nanofer 25s) on growth and photosynthetic efficacy of two <i>F. diplosiphon</i> strains (B481 and SF33)	134
5.2.2 Comparison of total lipid content, fatty acid methyl ester profile in <i>F. diplosiphon</i> wild-type and Nanofer 25s-treated cells using gravimetric analysis, direct transesterification and GC-MS	135

5.3 Perspectives and applications	136
5.4 Future work	137
REFERENCES.....	138

LIST OF FIGURES

Figure 1 Comprehensive flow chart demonstrating the research objectives.....	13
Figure 2 Outline of membranes and compartments in a cyanobacterial cell.....	15
Figure 3 Schematic representation of the intersecting photosynthetic and respiratory electron transport pathways in cyanobacterial thylakoid membranes.....	16
Figure 4 Main glycerolipid classes in cyanobacteria.....	21
Figure 5 Microwave-enhanced biofuel production process in cyanobacteria.....	30
Figure 6 (a) Gibb’s free energy differences in conventional and microwave heating methods and (b) activation energy reduction in microwave heating method.....	31
Figure 7 Iron is the final electron receptor in photosystem I of cyanobacterial thylakoid membrane.....	33
Figure 8 Reactive oxygen stress production and targets in cyanobacteria	34
Figure 9 Interaction of nZVI with cyanobacterial cells created oxidative stress resulting in lipid enhancement.....	35
Figure 10 Schematic diagram of pGEM-7Zf vector	47
Figure 11 Visualisation of iron nanoparticle (Nanofer 25s) using transmission electron microscopy (TEM).....	59
Figure 12 PCR amplification of acyl-lipid desaturase and sterol desaturase genes in <i>Fremyella diplosiphon</i>	64
Figure 13 Sequence alignments of (a) acyl-lipid desaturase and (b) sterol desaturases genes in <i>Fremyella diplosiphon</i>	65
Figure 14 PCR amplification of the acyl-lipid, and sterol desaturase genes, and pGEM- 7Zf (+) vector prior to digestion.....	66

Figure 15 Double digestion of acyl-lipid desaturase (insert 1), and sterol desaturase gene (insert 2) and triple digestion of pGEM-7Zf (+) vector.....	66
Figure 16 <i>Escherichia coli</i> containing plasmids grown in Luria-Bertani (LB) media amended with 80 mg L ⁻¹ ampicillin.....	67
Figure 17 Representative of sequenced extracted plasmid containing sterol desaturase gene.....	67
Figure 18 Relative quantification (RQ) of sterol desaturase transcript level in <i>Fremyella diplosiphon</i> wild type (WT) and transformant (B481-SD)	68
Figure 19 Growth of <i>Fremyella diplosiphon</i> wild type (WT-B481) and transformant (B481-SD) in BG11/HEPES medium over a ten day-period.....	69
Figure 20 Effect of overexpression of sterol desaturase (SD) gene on growth rate of <i>Fremyella diplosiphon</i> wild type (WT-B481) and transformant (B481-SD)	70
Figure 21 Impact of overexpression of sterol desaturase (SD) on chlorophyll <i>a</i> (chl <i>a</i>) accumulation in <i>Fremyella diplosiphon</i> wild type (WT-B481) and transformant strain (B481-SD)	71
Figure 22 Impact of overexpression of sterol desaturase (SD) on carotenoid accumulation in <i>Fremyella diplosiphon</i> wild type (WT-B481) and transformant strain (B481-SD)	72
Figure 23 Impact of overexpression of sterol desaturase (SD) gene on phycocyanin (PC) accumulation in <i>Fremyella diplosiphon</i> wild type (WT-B481) and transformant strain (B481-SD).....	72

Figure 24 Impact of overexpression of sterol desaturase (SD) gene on allophycocyanin (AP) accumulation in <i>Fremyella diplosiphon</i> wild type (WT-B481) and transformant strain (B481-SD)	73
Figure 25 Impact of sterol desaturase gene (SD) on phycoerythrin (PE) accumulation in <i>Fremyella diplosiphon</i> wild type (WT-B481) and transformant strain (B481-SD)	73
Figure 26 Comparison of total lipid content in wild type (WT) and transformant (B481-SD) <i>Fremyella diplosiphon</i>	74
Figure 27 Comparison of fatty acid methyl ester (FAME) composition of <i>Fremyella diplosiphon</i> wild type (WT) and transformant (B481-SD) total lipids subjected to direct transesterification.....	78
Figure 28 Representative one-dimensional gas chromatogram of <i>Fremyella diplosiphon</i> strains (a) wild type (WT-B481) and (b) transformant B481-SD total lipids subjected to direct transesterification.....	78
Figure 29 Representative of mass spectra of methyl palmitate (C16:0) which was detected as the most abundant fatty acid methyl ester (FAME) component in <i>Fremyella diplosiphon</i> transformant (B481-SD) extracted total lipids when subjected to direct transesterification.....	79
Figure 30 Theoretical biodiesel properties of <i>Fremyella diplosiphon</i> wild type (WT) and transformant (B481-SD) transesterified lipids.....	81
Figure 31 Fatty acid methyl ester (FAME) abundance in transesterified extractable lipids of wild type (WT) and transformant (B481-SD) <i>Fremyella diplosiphon</i> determined using GC×GC-TOFMS.....	82

Figure 32 Representative GC×GC-TOFMS chromatogram of <i>Fremyella diplosiphon</i> B481-SD fatty acid methyl esters (FAMES), alkanes, and other components.....	83
Figure 33 Effect of 0, 10, 20, 30, 40, and 50 g L ⁻¹ sodium chloride (NaCl) on <i>Fremyella diplosiphon</i> wild-type (B481-WT) and transformant (B481-SD) growth.....	84
Figure 34 Relative quantification (RQ) of transcript level in <i>Fremyella diplosiphon</i> wild type (WT) and halotolerant transformant (B481-SDH) using reverse transcription-quantitative PCR.....	85
Figure 35 Comparison of total lipid content in wild type (WT) and halotolerant transformant (B481-SDH) <i>Fremyella diplosiphon</i>	86
Figure 36 Comparison of fatty acid methyl ester (FAME) composition in <i>Fremyella diplosiphon</i> wild type (WT) and halotolerant transformant (B481-SDH) total lipids subjected to direct transesterification.....	89
Figure 37 Representative one-dimensional gas chromatogram of <i>Fremyella diplosiphon</i> strains (a) wild type (WT-B481) and (b) halotolerant transformant B481-SDH total lipids subjected to direct transesterification.....	90
Figure 38 Representative of mass spectra of methyl palmitate (C16:0) in <i>Fremyella diplosiphon</i> halotolerant transformant (B481-SDH) extracted total lipids when subjected to direct transesterification.....	90
Figure 39 Theoretical biodiesel properties of <i>Fremyella diplosiphon</i> wild type (WT) and halotolerant transformant (B481-SDH) transesterified lipids.....	93
Figure 40 Growth of WT and halotolerant transformant (B481-SDH) in sea water contained 37.1 g L ⁻¹ sodium chloride (NaCl).....	94

Figure 41 Growth of WT and halotolerant transformant (B481-SDH) in sea water which contained 37.1 g L ⁻¹ sodium chloride (NaCl) amended with 6% BG11 /HEPES media.....	95
Figure 42 Growth of WT and halotolerant transformant (B481-SDH) in brackish water which contained 9 g L ⁻¹ sodium chloride (NaCl) amended with 6% BG11 /HEPES media.....	95
Figure 43 Representative of growth of WT and halotolerant transformant (B481-SDH) in sea water (a, c respectively) and brackish water (b, d respectively) which contained 37.1 and 9 g L ⁻¹ NaCl amended with 6% BG11 /HEPES media.....	96
Figure 44 Protein expression in <i>Fremyella diplosiphon</i> wild type (B481-WT), transformant (B481-SD), and halotolerant transformant (B481-SDH)	97
Figure 45 Two-dimensional polyacrylamide gel electrophoresis of <i>Fremyella diplosiphon</i> wild type-B481 (A and D), B481-SD transformant (B and E), and halotolerant transformant (C and F)	98
Figure 46 Growth of <i>Fremyella diplosiphon</i> B481 strain in BG11/HEPES medium with different concentrations of Nanofer 25 over a period 18 days.....	100
Figure 47 Growth of <i>Fremyella diplosiphon</i> B481 strain in BG11/HEPES medium with different concentrations of Nanofer 25s over a period 18 days.....	101
Figure 48 Growth of <i>Fremyella diplosiphon</i> SF33 strain in BG11/HEPES medium with different concentrations of Nanofer 25 over a period 18 days.....	102
Figure 49 Growth of <i>Fremyella diplosiphon</i> SF33 strain in BG11/HEPES medium with different concentrations of Nanofer 25s over a period 18 days.....	103

Figure 50 Representative of <i>F. diplosiphon</i> growth in BG11 media amended with different concentrations of nZVIs.....	103
Figure 51 Growth of <i>Fremyella diplosiphon</i> SF33 strain in BG11/HEPES medium with different concentrations of Nanofer 25 over a period 15 days.....	104
Figure 52 Growth of <i>Fremyella diplosiphon</i> SF33 strain in BG11/HEPES medium with different concentrations of Nanofer 25s over a period 15 days.....	105
Figure 53 Growth of <i>Fremyella diplosiphon</i> B481 strain in BG11/HEPES medium with different concentrations of Nanofer 25 over a period 15 days.....	107
Figure 54 Growth of <i>Fremyella diplosiphon</i> B481 strain in BG11/HEPES medium with different concentrations of Nanofer 25s over a period 15 days.....	108
Figure 55 Representative of <i>F. diplosiphon</i> growth in BG11 media amended with different concentrations of nZVIs.....	109
Figure 56 Impact of different concentrations of Nanofer 25s on chlorophyll <i>a</i> (chl <i>a</i>) accumulation in <i>Fremyella diplosiphon</i> strains (SF33 and B481).....	110
Figure 57 Impact of different concentrations of Nanofer 25s on carotenoid accumulation in <i>Fremyella diplosiphon</i> strains (SF33 and B481).....	110
Figure 58 Impact of different concentrations of Nanofer 25s on phycocyanin (PC) accumulation in <i>Fremyella diplosiphon</i> strains (SF33 and B481).....	112
Figure 59 Impact of different concentrations of Nanofer 25s on allophycocyanin (AP) accumulation in <i>Fremyella diplosiphon</i> strains (SF33 and B481).....	112
Figure 60 Impact of different concentrations of Nanofer 25s on phycoerythrin (PE) accumulation in <i>Fremyella diplosiphon</i> strains (SF33 and B481).....	113

Figure 61 Comparison of total lipid content in <i>Fremyella diplosiphon</i> SF33 and B481 strains (control) and cultures amended with different concentrations of Nanofer 25s.....	115
Figure 62 Comparison of fatty acid methyl ester (FAME) composition of <i>Fremyella diplosiphon</i> SF33 strain total lipids subjected to direct transesterification.....	117
Figure 63 Comparison of fatty acid methyl ester (FAME) composition of <i>Fremyella diplosiphon</i> B481 strain total lipids subjected to direct transesterification.....	118
Figure 64 Representative one dimensional gas chromatogram of <i>Fremyella diplosiphon</i> strains SF33 (a) control, (b) nanotreated cells (1.6 mg L ⁻¹ Nanofer 25s) total lipid subjected to direct transesterification.....	119
Figure 65 Fatty acid methyl ester (FAME) abundance in transesterified extractable lipids of <i>Fremyella diplosiphon</i>	127
Figure 66 Fatty acid methyl ester (FAME) abundance in transesterified extractable lipids of <i>Fremyella diplosiphon</i> B481.....	128
Figure 67 Optical microscopy of <i>Fremyella diplosiphon</i> B481 exposed to Nanofer 25s stained with Prussian blue at (a) day 0 and (b) day 3.....	129
Figure 68 Transmission electron microscopy (TEM) micrographs (a) <i>Fremyella diplosiphon</i> B481 strain (b) <i>F. diplosiphon</i> treated with 1.6 mg L ⁻¹ Nanofer 25s.....	130

LIST OF TABLES

Table 1 Primers for acyl-lipid desaturase and sterol desaturase genes used for polymerase chain reaction (PCR).....	46
Table 2 Primers for acyl-lipid desaturase and sterol desaturase genes used for reverse transcription-quantitative PCR assay.....	49
Table 3 Breakdown of saturated and unsaturated fatty acid methyl ester (FAME) proportions in wild type (WT) and transformant (B481-SD) <i>Fremyella diplosiphon</i>	76
Table 4 Quantitative composition of fatty acid methyl ester in <i>Fremyella diplosiphon</i> wild type (WT-B481) and transformant (B481-SD) transesterified lipids.....	76
Table 5 Theoretical biodiesel properties of <i>Fremyella diplosiphon</i> wild type (WT) and transformant (B481-SD) transesterified lipids.....	80
Table 6 Breakdown of saturated and unsaturated fatty acid methyl ester (FAME) proportions in <i>Fremyella diplosiphon</i> wild type (WT) and halotolerant transformant (B481-SDH)	87
Table 7 Quantitative composition of fatty acid methyl ester in <i>Fremyella diplosiphon</i> wild type (WT-B481) and halotolerant transformant (B481-SDH) transesterified lipids.....	88
Table 8 Theoretical biodiesel properties of <i>Fremyella diplosiphon</i> wild type (WT) and halotolerant transformant (B481-SDH) transesterified lipids.....	92
Table 9 Breakdown of saturated and unsaturated fatty acid methyl ester (FAME) proportions in <i>Fremyella diplosiphon</i> SF33.....	120

Table 10 Breakdown of saturated and unsaturated fatty acid methyl ester (FAME) proportions in <i>Fremyella diplosiphon</i> B481	121
Table 11 Fatty acid methyl ester (FAME) composition in <i>Fremyella diplosiphon</i> SF33.....	122
Table 12 Fatty acid methyl ester (FAME) composition in <i>Fremyella diplosiphon</i> B481.....	123
Table 13 Theoretical biodiesel properties of <i>Fremyella diplosiphon</i> SF33.....	125
Table 14 Theoretical biodiesel properties of <i>Fremyella diplosiphon</i> B481	126

CHAPTER I

INTRODUCTION

Increasing industrialization has led to rising demand for energy consumption in recent years. Fossil fuels including coal, oil, and natural gas are primary sources of energy that provide about 85% of the worldwide energy needs (Afify et al., 2010; Quintana et al., 2011). Increasing petroleum costs and the environmental consequences of fossil fuel use such as pollution, greenhouse effects, and global warming have driven scientists to produce biofuel as a renewable source of energy (Griffiths et al., 2009; Modiri et al., 2015; Montgomery, 2016). Biofuels are currently receiving considerable attention due to its great potential as a sustainable and environmentally friendly alternative to petroleum-based fossil fuels (Mutanda et al., 2011). The first-generation biofuels from sugar, animal fats (Naik et al., 2010), and vegetable oil (Gabrielle, 2008), and second-generation biofuels from crops such as sunflower, wheat, sesame seeds, rapeseed, peanuts, and soybean are used to generate different types of energy (Naik et al., 2010; Sayre, 2010). However, one of the major limitations of first- and second-generation biofuels is competition for land, fresh water, human and animal food resources (Gabrielle, 2008; Sayre, 2010; Minhas et al., 2016). These feedstocks have low environmental impacts but could be invasive and disrupt the biological integrity of local ecosystems (Sayre, 2010; Radakovits et al., 2010; Machado et al., 2012; Minhas et al., 2016).

As a potential solution to these concerns, cyanobacteria which are photosynthetic prokaryotes, have been recognized as an ideal third generation substitute source of biofuel feedstock due to their rapid growth rate, simple nutritional requirements, ability to grow

under different light intensities, and lipid producing capability (Machado et al., 2012; Minhas et al., 2016). Cyanobacteria are conservative with negligible morphological change throughout the past two billion years (Blank and Sanchez-Baracaldo, 2010; Los and Mironov, 2015), and contain important lipids and fatty acids (FAs) in their thylakoid membrane. Thus, research on these organisms has mainly targeted their ability to produce lipids for biofuel production (Pate et al., 2011; Nozzi et al., 2013). The thylakoid membrane of cyanobacteria contains four major glycerolipids, including monogalactosyl diacylglycerol (MGDG), digalactosyl diacylglycerol (DGDG), sulfoquinovosyl diacylglycerol (SQDG), and phosphatidylglycerol (PG). The molecular action of these glycerolipids is generally determined by the amount and degree of unsaturated fatty acids which are esterified to the glycerol backbone (Los et al., 2013; Los and Mironov, 2015). Cyanobacteria typically accumulate more lipids in their stationary growth phase and under stress conditions such as nutrient deprivation, pH, and salinity (Quintana et al., 2011). Fatty acid composition of lipids is determined by the chain length (number of carbon atoms) and number of double bonds. Cyanobacterial fatty acid chain length usually ranges from C12 to C18 (Murata et al., 1992). The number of double bonds in the FA chains may vary from 0 to 4, which include fully saturated (with no double bonds), monoenoic (with 1 double bond), dienoic (with 2 double bonds), trienoic, and tetraenoic FAs (with 3 and 4 double bonds, respectively).

A unique system of classification of cyanobacteria is based on their fatty acid composition and was initially proposed by Kenyon et al., (1972) and modified by Murata et al., (1992). According to this classification, cyanobacterial strains are distributed into

four separate groups: in the first group, a single double bond is introduced at the $\Delta 9$ position (usually C16 or C18) of the FA esterified at the *sn-1* position of the glycerol moiety; cyanobacteria in the second group have the C18 (stearic acid) desaturated at the $\Delta 9$, $\Delta 12$, and $\Delta 15$ (Murata et al., 1992) positions, while the C16 (palmitic acid) is desaturated at the $\Delta 9$ and $\Delta 12$ positions, respectively; in the third group, the C18 is desaturated at the $\Delta 6$, $\Delta 9$, and $\Delta 12$ positions; and in the fourth group, FA is desaturated at the $\Delta 6$, $\Delta 9$, $\Delta 12$, and $\Delta 15$ positions (Kenyon et al., 1972; Murata et al., 1992).

Acyl-lipid desaturases and sterol desaturase are two types of desaturase enzymes which introduce double bonds in fatty acids chains. Acyl-lipid desaturases bound to acyl carrier protein (ACP) and fatty acids have been esterified to glycolipids in the cyanobacterial thylakoid membrane (Murata and Wada, 1995). The sterol desaturase represents a large super-family of enzymes which introduce double bonds into the sterol core and acts as a side chain. This super family presents a wide spectrum substrate, including steroids, alcohols, and sugars. Enzymes of this superfamily usually catalyze nicotinamide adenine dinucleotide phosphate (NADPH) which is a primary source of reactive oxygen species (ROS) resulting in lipid and fatty acid production (Kramm et al., 2012; Kamthan et al., 2017). The lipid including fatty acids, diglycerides, and phospholipids is analyzed using gas chromatography mass spectrometry (GC-MS). This method offers several advantages including, high ability to separate complex mixtures, quantify analytes, and identify trace levels of organic contamination (Bohin et al., 2005).

Fatty acid methyl esters (FAMES) are a type of fatty acid esters derived by transesterification of vegetable oils using methanol, and are identified as primary

molecules for biofuel. FAMEs are usually created by a catalyzed reaction between lipid and methanol in the presence of sodium hydroxide or potassium hydroxide (Lang et al., 2011; Shukla et al., 2012). FAMEs contain about 12-15 units higher cetane number than their unesterified components, which is an added benefit of using it as biofuel (Shukla et al., 2012). Of the various techniques that are used to convert metabolic products to biofuel, transesterification of lipids to form esters and glycerol is a main step (Vimalarasan et al., 2011). The transesterification process can be carried in the presence or absence of a catalyst. Non-catalytic transesterification with alcohol provides a new method for generating biofuel. Microwave and ultrasound treatments are known to assist in transesterification of lipids and can considerably reduce reaction times and improve product yields (Vimalarasan et al., 2011).

In recent years, engineered cyanobacteria have gained significant consideration as catalysts for the straight conversion of carbon dioxide into the biofuel (Seib et al., 2002; Chi et al., 2008). Genetic manipulation techniques such as transformation have been well-established in cyanobacteria, which have made this organism a highly tractable platform to build efficient biosynthetic pathways for biofuel production (Wada et al., 1990; Radakovits et al., 2010). Transformation techniques including methods to introduce foreign DNA into cells and effective promoters and expression vectors have been developed to increase total lipid content and reduce the cost of microalgal fuel production (Venegas-Calderón et al., 2010; Chen et al., 2014). In the transformation technique, promoters have significant roles in successful gene expression due to their ability to regulate expression of a transgene (Nazari et al., 2015). A number of transformation techniques such as electroporation,

artificial transposons, viruses, and *Agrobacterium*-mediated transformation have been established to introduce DNA in cyanobacterial cells (Gelvin, 2003; Nazari et al., 2015). Of the various transformation techniques, electroporation is known to be the best method to transfer foreign genes into a host cell. In this method, an electric current is applied across the cyanobacterial cell membrane resulting in temporary pore formation, which facilitates the uptake of DNA molecules thereby transforming the cell (Venegas-Calación et al., 2010). The use of electroporation offers several advantages such as reducing contamination and increasing efficiency of transformation since most cells can receive and take up the target DNA. In addition, this method requires small amount of DNA for the process of transformation (Bolhassani et al., 2014).

Cyanobacteria have developed constitutive and inducible mechanisms to adapt to a broad range of environmental stresses such as cold, heat, pH and salinity during their evolution. Of the various environmental stressors, salinity significantly affects photosynthesis and its productivity, ionic balance in cells protein profiles, and the functioning of cell membranes such as thylakoids, thus resulting in an effect on lipid yield as an interesting product for biofuel production (Pade and Hagemann, 2014). Increased salt concentrations have been reported to enhance the lipid content of microalgae *Dunaliella tertiolecta* (Takag and Yoshida, 2006) and *Nannochloropsis* sp. (Pal et al., 2011). In addition, high salinity has been reported to change the potassium-sodium ion gradient resulting in inactivation of photosystems I and II in the cyanobacterium *Synechococcus* PCC 7942 (Allakhverdiev et al., 2000). Thus, concerns on the increasing harmful effects of salinity have led to rising interest in generating halotolerant strains which are capable of

surviving in high concentrations of salt (up to 35 g L⁻¹) (Kanesaki et al., 2002; Tabatabai, 2017; Tabatabai et al., 2017-a). A recent study in our laboratory to enhance salt tolerance in *Fremyella diplosiphon* via overexpression of *mdh* and *hlyB* genes resulted in a transformant that thrives in 35 g L⁻¹ NaCl (Tabatabai, 2017; Tabatabai et al., 2017-b). These efforts have paved a way to maximize biofuel production in this organism. With freshwater constituting only about 2.5% of Earth's hydrosphere, enhancement of halotolerance to 35-40 g L⁻¹ NaCl, the average salinity of seawater, would be a desirable feature in order to grow the organism for biofuel production in naturally available salt water systems.

Proteins are another cyanobacterial constituent which make up a large fraction of cyanobacterial biomass. This macromolecule is one of the major factors involved in cyanobacterial photosystem I and II activities. It is known that cyanobacteria produce a wider range of proteins than most other bacteria (Pade and Hagemann, 2014). These photosynthetic organisms use protein regulatory systems to control cell behavior and gene expression in response to environmental changes (Pade and Hagemann, 2014). Protein regulatory systems typically contain two types of proteins, including histidine kinases and response regulators (Pade and Hagemann, 2014). Under stress conditions such as salinity, some proteins lose their activity and some others are induced (Xu et al., 2001). The genome and proteome analysis of cyanobacterial strains, *Synechocystis* sp., has revealed the expression of 20 different proteins under salinity stress (Xu et al., 2001).

In addition to salinity stress, physicochemical stress factors such as temperature, light intensity, and nitrates have been identified to promote lipid production. Of these, iron

is one of the most critical requirements for growth and lipid yield (Minhas et al., 2016). Additionally, iron is an essential element influencing several processes such as respiration, photosynthesis, oxygen transport, and cell proliferation in cyanobacterial and microalgal species (Huang et al., 2014). It also acts as a chelating agent and can scavenge hydroxyl radicals in the Fenton reaction used in the enzyme system of animals, microbes, and plants. Moreover, it serves as a restrictive factor under high salinity conditions (Huang et al., 2014; Minhas et al., 2016). In photosynthetic organisms, iron is one of the requirements for critical cellular functions such as haem-dependent oxygen transport, respiration, redox reactions, iron-dependent enzymatic reactions, RNA synthesis, and photosynthesis (Straus, 1994; Pattanaik et al., 2014). Iron-limitation/excess stress results in an elevated ROS concentration leading to increased oxidative stress in cyanobacterial cells. Oxidative stress negatively impacts cyanobacterial photosystem function, confirming that iron-limited growth is associated with oxidative stress (Pattanaik et al., 2014).

Iron is a requirement for the activity of photosystems and is functionally related to photosynthetic light-collecting complexes in microalgae and cyanobacteria. It is also a component of iron-sulfur (Fe-S) clusters which serves as cofactors in cyanobacterial photosynthetic protein complexes (Michel and Pistorius, 2004; Shcolnick and Keren, 2006). In cyanobacteria, the photosynthetic complexes require about 22-23 Fe atoms for photosystem I and II to act efficiently (Ferreira and Straus, 1994). In addition, iron is one of the major components for the synthesis of photosynthetic pigments, including phycobilisomes (PBSs) (Terry et al., 2002). Thus, the presence of iron is necessary for the regulation and function of cyanobacterial photosynthetic activities for all the

aforementioned advantages of this element. While iron is ubiquitous on Earth, it is often infrequently available in the environment due to its low solubility. Since iron is found mainly in its insoluble ferric form (Fe^{+3}), it is difficult for most organisms to uptake it from the environment. Therefore, iron can be one of the critical limiting factors for cyanobacterial growth (Ferreira and Straus, 1994; Terry et al., 2002; Pattanaik et al., 2014). The capabilities of the organisms to take up iron is significantly dependent on the bioavailability of the element and its chemical origin. Some organisms such as *Candida sp.* have developed enzymatic and non-enzymatic mechanisms to uptake iron (Fourie et al., 2018). Through these mechanisms, they can only uptake the ferrous ions and hence extracellular reduction of ferric iron is the limiting phase. In contrast, bioavailability of zero-valent iron nanoparticles (nZVIs), which are an ideal source of iron, supports its ready interaction with the cell membrane and facilitates penetration into the cell due to their small size (<100 nm). Iron nanoparticles can also penetrate into the cyanobacterial thylakoid membrane and act as electron acceptor in photosystem I, catalyzing a wide variety of reactions resulting in improved cell growth and photosynthetic efficacy (Padrova et al., 2015).

The freshwater cyanobacterium, *Fremyella diplosiphon* or *Tolypothrix sp.* PCC 7601, is a model cyanobacterial species which has great potential as a commercial biofuel agent due to its lipid production potential (Nozzi et al., 2013; Montgomery, 2016; Tabatabai et al., 2017-b). It has a light-dependent acclimation capability known as complementary chromatic adaptation (CCA), which increases the fitness of the organism to grow in minimal light intensities as low as $15 \mu\text{mol quanta m}^{-2}\text{s}^{-1}$ and at an optimal

temperature of 28 °C (Montgomery, 2016). In addition, the organism has a short generation time of 8-11 days, and its biofuel properties have also been characterized (Tabatabai et al., 2018).

1.1 OBJECTIVES

F. diplosiphon has been identified to have unique environmental applications due to its high lipid production, mainly present in its thylakoid membrane; however, achieving maximal lipid productivity is still a major concern which limits the feasibility of using the organism as a potential source for large scale commercial biofuel production. Thus, the aim of this dissertation was to enhance total lipid content and fatty acid composition of *F. diplosiphon* using genetic engineering and nanotechnological approaches. In addition, this study aimed to enhance the capability of the transformant strain to grow in saline waters by selection on 40 g L⁻¹ salt.

Objective 1. Enhancement of lipids in *F. diplosiphon* using genetic transformation via electroporation

Aim 1.1: Overexpression of sterol desaturase and acyl-lipid desaturase genes in *F. diplosiphon* via electroporation-mediated genetic transformation.

Lipid producing genes were overexpressed using electroporation-mediated transformation, and the transformants evaluated using reverse

transcription polymerase chain reaction (RT-qPCR). Protein expression in WT and transformants strains were evaluated using 1D- and 2D-PAGE. In addition, photosynthetic pigment accumulation in the wild type and transformant *F. diplosiphon* was compared.

Aim 1.2: Comparison of total lipid content and fatty acid compositions in the wild-type and transformant by gravimetric analysis and GC-MS.

Total lipid and fatty acids in wild-type and transformants were compared by using gravimetric analysis, direct transesterification, gas chromatography mass spectrometry (GC-MS), and two-dimensional gas chromatography with time-of-flight mass spectrometry (GC×GC-TOFMS).

Aim 1.3: Enhancement of total lipid content and essential fatty acid methyl esters by exposure to salinity stress.

The transformant was selected on media supplemented with 40g L⁻¹ sodium chloride and the effect of salinity stress on growth in BG-11 medium was assessed. Total lipid content and FAME composition was characterized using gravimetric analysis and GC-MS. Growth of the halotolerant transformant strain was tested in sea water and compared to the wild type.

Objective 2: Enhancement of lipids and fatty acids in *F. diplosiphon* using iron nanoparticles

Aim 2.1: Assess the impact of iron nanoparticles (Nanofer 25 and Nanofer 25s) on growth and photosynthetic efficacy of two cyanobacteria strains (B481 and SF33)

The effect of nanoparticle-mediated stress on *F. diplosiphon* growth was investigated by exposing the cells to 0.05 to 3.2 mg L⁻¹ Nanofer 25 and Nanofer 25s iron nanoparticles. In addition, photosynthetic pigment accumulation in *F. diplosiphon* nano-treated cells was compared to the control.

Aim 2.2: Determine the effect of iron nanoparticles on total lipid content and fatty acid composition of *F. diplosiphon* nano-treated cells using gravimetric analysis and GC-MS.

Total lipid and fatty acids in *F. diplosiphon* exposed to different concentrations of iron nanoparticles were compared to the control using gravimetric analysis, direct transesterification assay, GC-MS, and GC×GC-TOFMS. In addition, the presence of iron nanoparticle in *F. diplosiphon* cells was visualized using optical microscopy and transmission electron microscopy (TEM).

Efforts to enhance sterol desaturase gene in WT-B481 via electroporation mediated- transformation yielded a transformant with a 64-fold increase in transcript level

while maintaining pigment accumulation. Our results demonstrated that overexpression of lipid production genes did not negatively impact *F. diplosiphon* growth and growth rate kinetics. Selection on NaCl generated a halotolerant transformant with a 38-fold increase in transcript level, which is able to survive in 40 g L⁻¹ sodium chloride, the average salinity of sea-water. Total lipid content and key FAMES of the halotolerant transformant *F. diplosiphon* were higher when compared to the control. In addition, iron nanoparticles at specific concentrations (0.2-1.6 mg L⁻¹) enhanced growth, total lipid content, and fatty acid composition in *F. diplosiphon* with no negative effect on photosynthetic pigments.

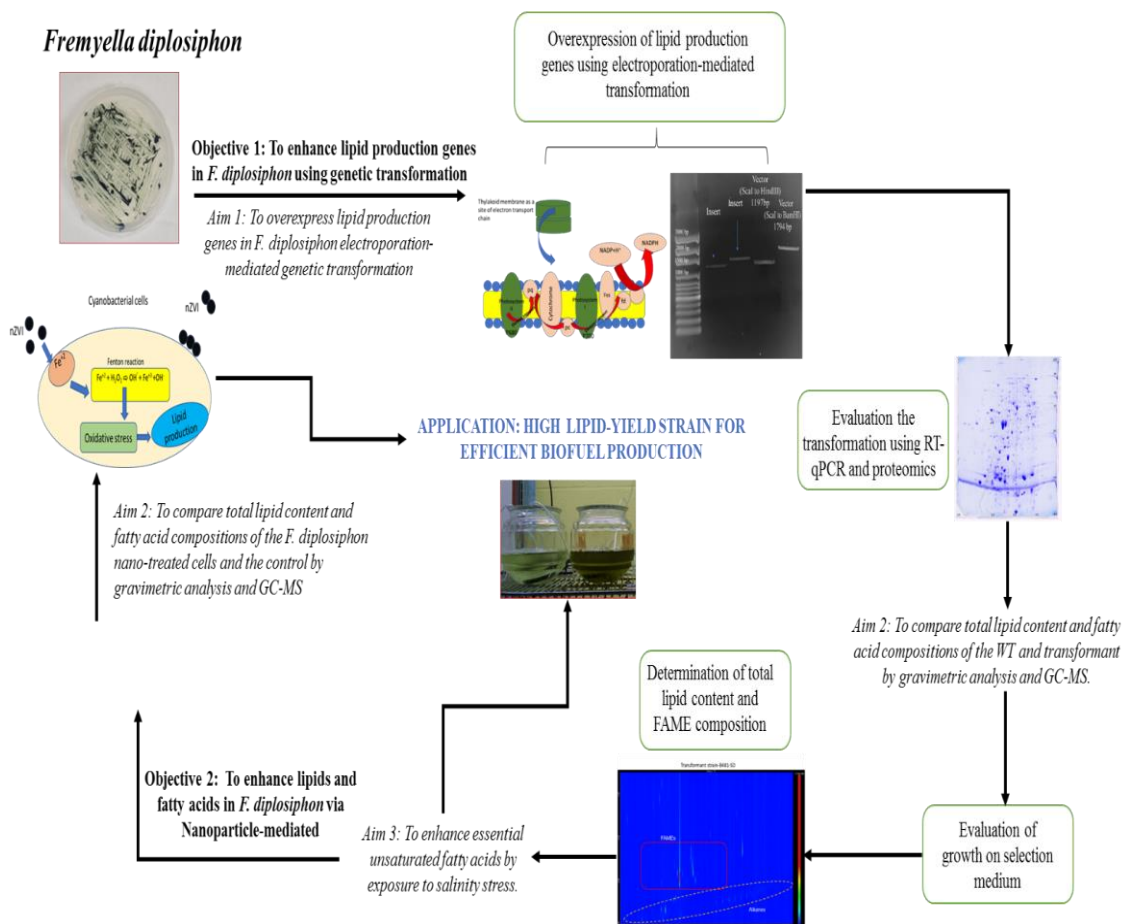


Figure 1 Comprehensive flow chart demonstrating the research objectives.

CHAPTER II

LITERATURE REVIEW

2.1 CYANOBACTERIA, A PHOTOSYNTHETIC PROKARYOTE

An ever-increasing energy demand and depletion of fossil fuels have (been) driven scientists to develop novel sources of renewable energy. Cyanobacteria, as photosynthetic prokaryotes have been identified as an alternative for biofuel production due to their ability to fix carbon dioxide (CO₂), their genetic tractability, and high lipid production capability (Machado and Atsumi, 2012; Nozzi et al., 2013). These organisms can survive at high temperatures ranging from 45 to 70 °C with optimal range of 25–35 °C, and pH levels higher than 4–5 with optimal range of 7.5–10 (Singh et al., 2016). Cyanobacteria acquire their required nitrogen through nitrogen fixation, thus producing bioactive compounds which can promote crop growth and improve soil nutrients. These organisms are also beneficial for wastewater treatment due to their ability to degrade the numerous toxic compounds such as pesticides (Singh et al., 2016). Cyanobacteria are able to directly fix CO₂ as their primary carbon source through exogenous metabolic pathways to produce chemicals needed for biofuel production (Zhang et al., 2017). Thus, these organisms are able to grow in water as they uptake higher concentrations of CO₂ compared to that of ambient air (Sheehan et al., 1998).

2.1.1 Cyanobacterial Photosynthetic Pathway

Effective metabolic pathways are the key reasons for the evolution of cyanobacteria (Vermaas, 2001). These organisms are capable of oxygenic photosynthesis and respiration simultaneously in the same compartment (Nozzi et al., 2013), which enable them to survive under a broad range of environmental conditions. Cyanobacterial photosynthesis and respiration systems require electron transport pathways which can be catalyzed by protein complexes in their cell membranes (thylakoid and cytoplasmic) (Nozzi et al., 2013). In cyanobacteria, thylakoid membrane is located between the cytoplasmic membrane and lumen (Figure 2) and contains both photosynthetic and respiratory electron transport chains that intersect and provide similar components to that in the thylakoid membrane. In most cyanobacterial strains such as *Synechocystis* sp. PCC 6803, the cytoplasmic membrane which contains the respiratory electron transport chain separates the cytoplasm from the periplasm (Vermaas, 2001).

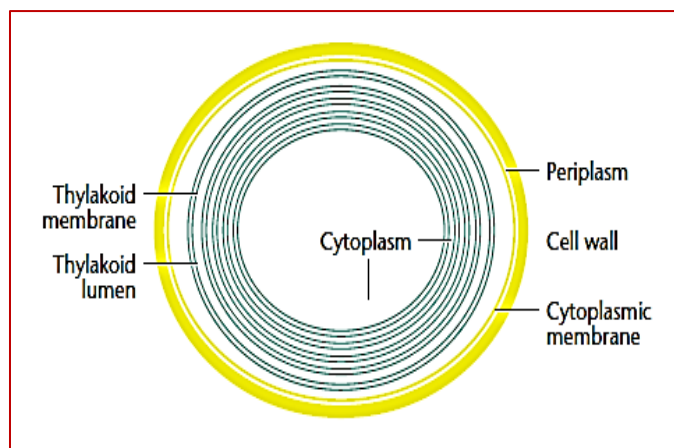


Figure 2 Outline of membranes and compartments in a cyanobacterial cell (Vermaas, 2001).

Hence, in this species, photosynthetic electron transport takes place only in the thylakoid membrane, while respiratory electron chain occurs in both thylakoid and cytoplasmic membranes (Figure 3). On the other hand, in Photosystem II, antenna complexes play an important role in light harvesting. While transfer of an electron to a quinone also stabilizes the primary light reaction in Photosystem II, the terminal electron acceptor is iron sulfur (Fe-S) cluster which causes ferredoxin reduction in Photosystem I (Vermaas, 2001; Lunde et al., 2003).

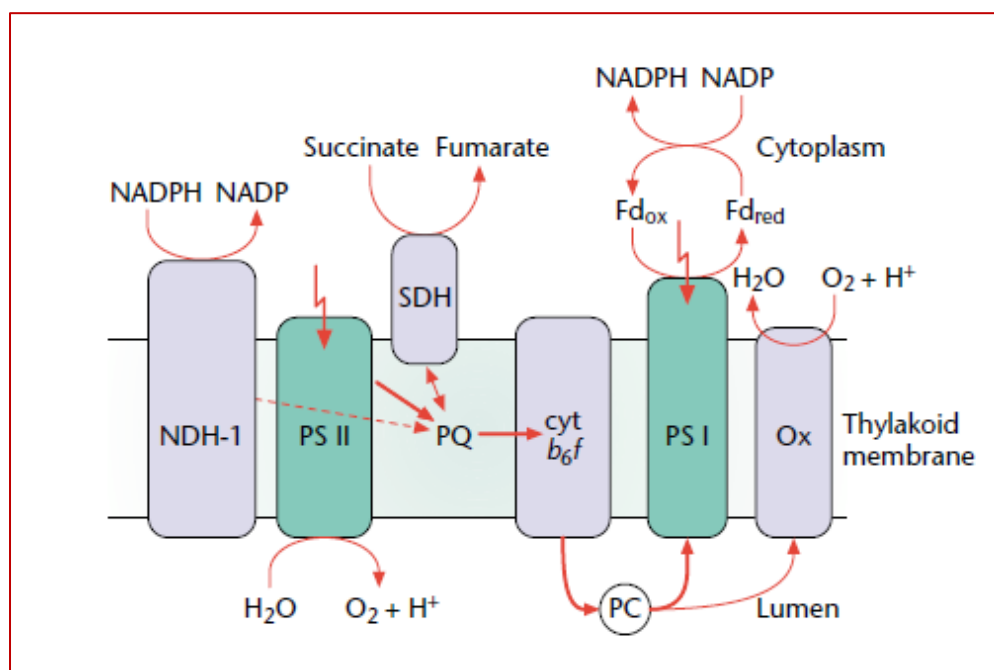


Figure 3 Schematic representation of the intersecting photosynthetic and respiratory electron transport pathways in cyanobacterial thylakoid membranes (Vermaas, 2001).

The photosystem I reaction center is a large multi-subunit complex which contains the core antenna and P_{700} that are linked to proteins PsaA and PsaB. In this photosystem, one of the electron acceptors is a complex of membrane-linked iron sulfur proteins bound to ferredoxins such as Fe-S_X, Fe-S_A, and Fe-S_B. In the next step, electrons are transferred across centers A and B and donated to ferredoxin (Fd), which is a small soluble protein (Lunde et al., 2003). In photosystem I, $NADP^+$ is reduced to NADPH by membrane-associated flavoprotein Fd–NADP reductase. The last reaction finalizes the noncyclic electron flow which starts with the oxidation of water (Lunde et al., 2003; Wada et al., 2013). In the thylakoid membrane, NADPH is the primary source of ROS such as superoxide anion radical ($O_2^{\cdot-}$), hydrogen peroxide (H_2O_2), and hydroxyl radical (OH^{\cdot}) which leads to oxidative stress (Wada et al., 2013). Cyanobacteria exhibit different responses to avoid over-production of ROS and its damage on biomolecules such as activation of the antioxidant system. These organisms protect themselves from light damage by mechanisms such as through sunscreen pigments and regulating photosynthetic electron transport to quench the ROS produced (Latifi et al., 2009). There is a maintained balance (redox balance) between oxidation induced by ROS and reduction created by antioxidants and their enzymes. However, this redox balance can be significantly interrupted by loss of antioxidant activities due to environmental stress. Once redox balance is disrupted irreversibly, homeostasis of cells can be destroyed leading to cell death (Wada et al., 2013).

2.1.2 Photosynthetic Pigments in Cyanobacteria

Pigments are chemical compounds which absorb specific wavelengths of light. Cyanobacterial pigments are altered by environmental light which is the result of change in phycobiliproteins (PBS) pigment-protein composition (Grossman et al., 2001). Cyanobacteria contain three major classes of pigments such as chlorophyll, carotenoids, and phycobilisomes (phycoerythrin and phycocyanin) (Wada et al., 2013; Montgomery, 2016). Chlorophyll *a*, which contains two different absorption bands at 430 nm and 660 nm in diethyl ether is the predominant photosynthetic pigment commonly identified in cyanobacteria (Wada et al., 2013). This difference in absorbance allows the adaptation to specific light in their locations. Carotenoids are another light-harvesting cyanobacterial pigment in photosynthesis that protect the cells against photo-oxidative damage. These pigments are hydrophobic isoprenoid compounds which are synthesized in cyanobacterial cell membranes (Blankenship, 2008; Latifi et al., 2009). Cyanobacterial phycobiliproteins which absorb specific wavelengths of light (470 and 650 nm) are unique light-harvesting complexes associated with photosystem II to transfer the light energy. The two main phycobiliproteins are allophycocyanin as a core and phycocyanin as a rod. In some cyanobacteria, phycobiliproteins contains phycoerythrin as an additional rod protein (Wada et al., 2013). The protein structure of this complex changes in response to the light and nutrition starvation or excess. For example, in low light intensity, synthesis of this pigment complex is promoted to extend rod structures. It has been also reported that phycoerythrin is sensitive to environmental stress factors such as salinity, pH, temperature, and light (Sinha, 2011).

2.2 FREMYELLA DIPLOSIPHON, A MODEL OF CYANOBACTERIUM

Fremyella diplosiphon belongs to the Domain Prokaryote, Kingdom Eubacteria, Group Terrabacteria, Phylum Cyanobacteria, Class Cyanophyceae, Order Nostocales, Family Rivulariaceae, Genus Microchaete, and Species diplosiphon. Of the approximately 125 species in this family, *Tolypothrix distorta*, *Spirirestis rafaensis*, and *Hassalia littoralis* are the most important species (The NCBI taxonomy database). The freshwater cyanobacterium, *F. diplosiphon* or *Tolypothrix sp.* PCC 7601 used in this study, has a great potential as a commercial biofuel agent due to its high FAME production (Tabatabai et al., 2018), available sequenced genome, and ability to grow in low light intensity (Montgomery, 2016). *F. diplosiphon* is a model cyanobacterial species well known for its complementary chromatic adaptation (CCA) (Federspiel and Grossman, 1990; Montgomery, 2016). Due to CCA, *F. diplosiphon* has been frequently used for biochemical and physiological studies to identify its response to their environment since it is able to harvest different wavelength of light, depending on the conditions (Federspiel and Grossman, 1990). PBS composition which is responsible for light harvesting by activating and repressing special operons is well regulated in *F. diplosiphon* (Montgomery, 2016). The two important operons, *cpeBA* and *cpeCD*, have been identified as coding for green-light harvesting proteins (Federspiel and Grossman, 1990; Pattanaik et al., 2011). PBSs are mainly contained phycobiliproteins (PBPs) such as phycoerythrin (PE; λ_{\max} ~565 nm), phycocyanin (PC; λ_{\max} ~620 nm) and allophycocyanin (AP; λ_{\max} ~650 nm) (Pattanaik et al., 2011; Montgomery, 2016). Cyanobacteria are able to alter the pigment and/or protein

composition of their PBSs in response to varying light wavelengths, which allows them to sustain photosynthesis and nitrogen fixation in prevailing light conditions (Montgomery, 2016).

2.3 CYANOBACTERIAL LIPID PRODUCTION

In cyanobacteria, lipids in the thylakoid membrane provide a matrix for both photosynthetic complexes to avoid diffusion of ions. This matrix is a requirement for the electrochemical potential alteration across the membrane which is essential to drive ATP synthase. Integral lipids bind specifically to the photosynthetic complexes, indicating that lipids are essential molecules for the structure and function of photosynthetic complexes (Kern et al., 2009, Montgomery, 2016).

Lipid composition of cyanobacterial thylakoid membrane is highly preserved among photosynthetic microorganisms and is composed of uncharged lipids including MGDG, DGDG, and anionic lipids such as SQDG and PG (Shimajima et al., 2009). While glycolipids including MGDG, DGDG, and SQDG are the major lipid components of the thylakoid membrane (Figure 4) (Siegenthaler, 1998; Shimajima et al., 2009; Boudiere et al., 2014), phospholipids are the major lipid components in cytoplasmic membrane. Lipids in the thylakoid membrane contain two acyl groups which esterifies at the positions of *sn*-1 and *sn*-2 of glycerol moiety, and a polar head group that is located at the *sn*-3 position and characterizes each specific class of lipids. MGDG contains β -galactose which is associated with the diacylglycerol, and DGDG has di-galactose that its second galactose bound to the first galactose of MGDG by an α 1-6 glycosidic linkage (Siegenthaler, 1998;

Shimajima et al., 2009). In cyanobacteria, MGDG and DGDG mainly operate as structural lipids known as bulk lipids due to their presence in considerable abundance (Sakamoto et al., 2009; Shimajima et al., 2009). In addition, DGDG has also been identified to have an important role in structure and function of photosystem II, specifically on the donor side (Crowe et al., 1998; Wada et al., 2013). PG is the only key phospholipid identified in thylakoid membranes (Tunnacliffe et al., 2003) and plays an important role in photosynthesis (Nozzi et al., 2013).

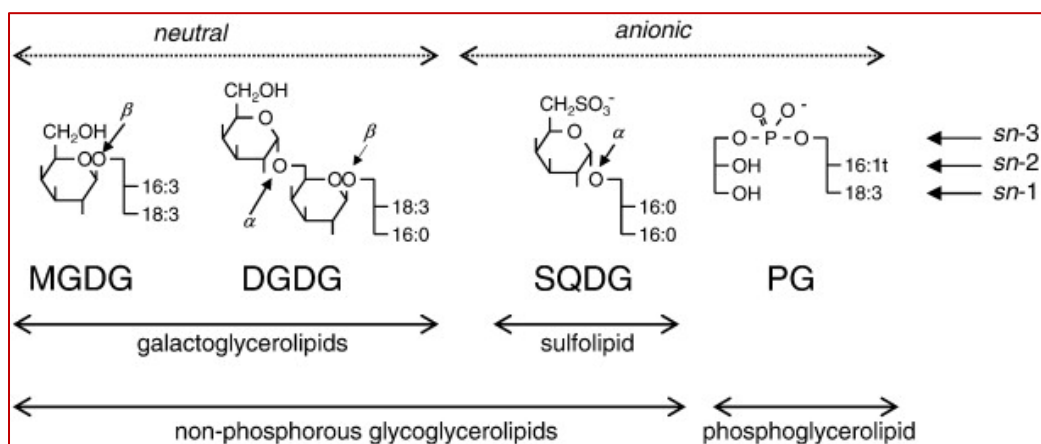


Figure 4 Main glycerolipid classes in cyanobacteria (Boudiere et al., 2014).

The function of the different lipid classes identified has been studied by biochemical and molecular and genetic approaches. The role of PG in photosynthesis has been identified by phospholipase treatment which is specific to phospholipids (Sakamoto et al., 2011; Wada et al., 2013). In addition, chemicals (acid or base) or enzyme (lipase) catalysis can be utilized to release fatty acids from triacylglycerols (TAG)/diacylglycerols (DAG) produced in algae/cyanobacteria lipid as the corresponding methyl or ethyl esters for biofuels production (Lu, 2010). Cyanobacteria are currently considered to be the

highest potential source of DAG due to their high lipid content and faster growth compared to microalgae and plants (Chisti, 2007).

2.3.1 GENETIC TRANSFORMATION TO ENHANCE CYANOBACTERIAL LIPID

Cyanobacteria exhibit a great tolerance to introduction of foreign genes through genetic manipulation and can be genetically modified to produce essential components for biofuel production (Machado and Atsumi, 2012). While *Synechocystis* sp. PCC6803 was the first strain to be sequenced (Kaneko et al., 1996), today the genomes of over thirty-five cyanobacterial species including *F. diplosiphon*, have been sequenced and their genetic and metabolic regulation pathways are well understood (Kaneko et al., 1996; Nozzi et al., 2013). This information has paved the way for genetic modification of this organism for biofuel production (Tabatabai et al., 2018). A study by Deng and Coleman (1999) has revealed that *Synechococcus elongatus* strain PCC7942, which was engineered using homologous transformation, over-produced ethanol in significant amounts. A yield of 54 nmol/optical density (OD₇₃₀) nm/unit liter/day in ethanol production was reported in this study. In another study, ethylene production in the cyanobacterium *Synechococcus* sp. PCC 7942 was enhanced about 52.9 nL/mL/OD₇₃₀/h using recombinant DNA technique (Sakai et al., 1997). With the focus on development of various types of biofuels, Dexter and Fu et al., (2009) reported over-production of bioethanol in *Synechocystis* sp. PCC6803 with a yield of 5.2 mmol OD₇₃₀ nm/unit liter/day. In addition, Lindberg et al., (2010) were able to genetically modify *Synechocystis* sp. PCC6803 for isoprene biosynthesis using

heterologous transformation. In cyanobacteria, genetic and metabolic engineering techniques can be applied to enhance total lipid content as well as FA compositions and reduce the cost of biofuel production (Lu, 2010; Liu et al., 2011; Chen et al., 2014). All these studies have outlined a promising approach to biofuel production based on the redirection of cyanobacterial intermediary metabolism.

Since polyunsaturated fatty acids (PUFAs) are vulnerable to oxidation, a higher percentage of unsaturated FAs in the feedstock oil has been beneficial for biofuel production with improved cold-flow properties (Lu, 2010; Liu et al., 2011). Hence, research aimed to improve PUFA especially unsaturated FAs, has a positive impact on biofuel production (Lu, 2010; Chen et al., 2014). Transformation of lipid production genes such as $\Delta 12$ desaturase, $\Delta 9$ desaturase and $\Delta 15$ desaturase has been reported to enhance the unsaturation FAs, thereby improving *Synechococcus sp.* PCC 7942 and *Synechocystis sp.* PCC6803 for biofuel production (Chen et al., 2014).

2.4 SALINITY STRESS INDUCED LIPID PRODUCTION

Increasing salinity of the hydrosphere caused by agricultural activities, long-term droughts, and rising seawater levels, have resulted in salt stress becoming a significant limitation for the survival of cyanobacteria due to the adverse effects of increased salinity on macromolecule metabolism, cellular morphology, and photosynthetic pigmentation (Tonk et al., 2007). Salinity, which has an adverse impact on 7% of the world's land area and 20% of agricultural land, is one of the major reasons for losing crop productivity (Zhang et al., 2005). Many studies have reported the physiological and molecular pathways

of osmotic and ionic tolerance to salinity (Zhang et al., 2005; Tonk et al., 2007; Hu et al., 2014). Increase in salinity affects cellular water potential resulting in loss of water, which leads to osmotic stress followed by cell death. In addition, Kanasaki et al., (2002) reported that cyanobacterium *Synechocystis* is capable of distinguishing salt and hyperosmotic stresses as separate stimuli. Cyanobacteria are naturally more tolerant to salt stress compared to microalgae and higher plants. Enhanced accumulation of Na⁺ ions in cyanobacterial cytoplasm is prevented by two mechanisms: first restricted uptake of sodium ions, and second its active efflux by Na⁺/H⁺ antiport proteins associated with H⁺-ATPase and respiratory cytochrome oxidase (Blumwald et al., 1984; Molitor et al., 1986). On the other hand, enhancement in Na⁺ toxicity is recompensed by (i) accumulating organic complexes to preserve the osmotic stress, and (ii) inducing antioxidative defense mechanism to detoxify the harmful effects of ROS (Bhagwat and Apte, 1989; Fulda et al., 2000). In a recent study, Tabatabai et al., (2017-b) enhanced salt tolerance in *F. diplosiphon* by overexpression of *mdh* and *hlyB* genes which led to a mutant that thrives in 35 g L⁻¹ NaCl. Significant changes in biomass and growth rate in cyanobacterium *Oscillatoria* sp. at salinities ranging from 10–35g L⁻¹ was reported by Khatoon et al., (2010). They also identified significant increase in protein and lipid levels of this organism when exposed to high salinity levels (30–35 g L⁻¹). In another study, Hu et al., (2014) reported that high salinity stress significantly decreased cyanobacterial *S. javanicum* growth, and inhibited Chlorophyll *a* yield per unit biomass.

2.5 CYANOBACTERIAL PROTEIN PRODUCTION

Cyanobacterial photosystem I contains 11–12 proteins, in which some are modified post-translationally. Genetic engineering techniques have been established to generate genotypes and phenotypes with high functionality (Xu et al., 2001). The cyanobacterial photosystem I proteins bind cofactors to provide different sites for electron transfer and contribute in tertiary and quaternary structures of this complex as well as protection of the electron transfer centers (Xu et al., 2001). Under various stress conditions, some proteins lose their activities, while others are enhanced or induced (Oren, 1999; Castielli et al., 2009). The proteome of numerous cyanobacterial species has been investigated during normal growth or adaptation to different types of stress (Muller and Oren, 2003). A study on the cyanobacterium *Anabaena* revealed that salinity-induced modification of protein synthesis is similar to plants and is critical for cyanobacterial osmotic properties (Apte and Bhagwat, 1989). In recent years, the proteome of *Synechocystis* exposed to salt stress has been extensively characterized. Six proteins were significantly overexpressed and three new proteins induced when these species were exposed to high salinity, and the most salt-enhanced proteins were enzymes involved in the modification of cell membrane structure (Fulda et al., 2000; Huang et al., 2006; Fulda et al., 2006). In another study, 55 soluble proteins with enhanced expression levels were reported in cultures exposed to long-term salt shock (37 proteins) (Fulda et al., 2006). However, there are limited studies on *F. diplosiphon* protein expression when exposed to various types environmental stresses. In a recent study in our laboratory, Tabatabai et al., (2017-a) reported an up-regulation in the proteins of *F. diplosiphon* heat mutant strain (Fd33) when exposed to 10 g L⁻¹ sodium

chloride. Similar results were reported by Singh et al., (2013) who identified a transcript encoding a protein similar to a glycine-betaine (GB) transport system in *F. diplosiphon* exposed to 200 mM sodium chloride. Marin et al., (2004) reported an increase in mRNA transcript level of cyanobacterium *Synechocystis* for the 18 short-term-induced proteins in cultures exposed to the salt stress.

2.6 BIOFUELS: A RENEWABLE ALTERNATIVE TO FOSSIL FUELS

Fossil fuels such as oil, coal and natural gas, provide about 85% of the global energy production; however, fossil fuels are a nonrenewable source of energy, and their over-consumption can lead to serious environmental problems including global warming and air pollution due to release of unwanted gases such as carbon dioxide, nitrogen dioxide, and sulfur dioxide (Bhattarai et al., 2011).

Since 1970, CO₂ emitted from fossil fuel combustion and industrial processes has increased by approximately 90%. The United States Environmental Protection Agency reported a 78% increase in greenhouse gas from 1970 to 2011 (United State Environmental Protection Agency, 2017). Thus, the increasing cost of petroleum products and environmental problems of fossil fuel have driven scientists to generate biofuel as an alternative renewable source of energy (Bhattarai et al., 2011; Nozzi et al., 2013). The development and consumption of biofuel provide significant benefits to the environment by augmentation of energy production and reduction in pollution (Nozzi et al., 2013).

First and second generation feedstock are currently the most common sources for biofuel production; however, their competition with agriculture land use for crop

production could lead to an increase in food prices (Sayre, 2010). The second generation biofuel feedstock such as *Miscanthus* and switchgrass has lower environmental impacts but can disrupt the integrity of ecosystems (Heaton et al., 2008). Cyanobacteria as a third generation of biofuel source are the potential solution to many of these concerns due to their ability to fix greenhouse gas and high lipid production capacity (Nozzi et al., 2013).

2.6.1 CYANOBACTERIAL LIPID AS BIOFUEL AGENT

Of the various microorganisms, cyanobacteria have great potential for use as an alternative for biofuel production (Nozzi et al., 2013). Cyanobacterial lipids can be processed through different techniques to generate biofuels such as biohydrogen, bioethanol, and biomethane (biogas). The development of large-scale production of cyanobacteria-derived biofuels requires an optimized process for biological uptake of inorganic carbon. Of the various methods for chromatographic determination of the lipid yield, transesterification is preferred (Meher et al., 2006; Nozzi et al., 2013). Biofuel is generally produced through transesterification of lipids via chemical conversion of triglycerides and diglycerides to methyl esters using solvent and catalyst (Meher et al., 2006). In the transesterification process, triglycerides react with a short-chain alcohol in the presence of catalysts such as acid, alkali, or lipase enzymes to create microalgal biofuel (Froehlich et al., 1990; Meher et al., 2006). Transesterification contains three phases where triglycerides are initially converted to diglycerides, then to monoglycerides, and finally to esters (biofuel), with glycerol as a by-product (Froehlich et al., 1990). Biofuel can be generated from high energy storage compounds such as TAGs synthesized by microalgae

in high abundance (Harwood and Guschina, 2009). TAGs are contained of long chain hydrocarbons (FAs) and a glycerol backbone. Available inorganic carbon of organism is an essential requirement for TAG synthesis. In cyanobacteria, a critical component of FA biosynthesis is acyl-acyl carrier protein (ACP) which is utilized by type II FA synthase complex. It has been identified that in this organism, the cellular ACP concentration is associated with the level of FA synthesis (Sabaitis and Powell, 1976). ACP thioesters particularly interact with the enzymes involved in FA synthesis and assist with the release of these fatty acids into the extracellular space (Harwood and Guschina, 2009). The mechanism for this procedure is hydrolysis reaction of the acyl-ACP thioester molecule by these thioesterases (Voelker et al., 1997). Therefore, cyanobacteria do not produce TAGs (Hu et al., 2014- a), which are required molecules in lipid transesterification. Thus, producing biofuel from cyanobacteria using traditional two-step extraction/transesterification is a major challenge (Wahlen et al., 2011). However, direct transesterification which is a single-step technique was invented to produce FAMES without a separate extraction step (Lepage and Roy, 1984). In this method, which is the combination of lipid extraction and biofuel conversion, biofuel is produced directly from extracted lipids (Lepage and Roy, 1984; Wahlen et al., 2011). In general, the process of generating biofuel from cyanobacteria has been mainly performed in two separate phases: lipid extraction and direct transesterification.

2.7 STEPS IN BIOFUEL PRODUCTION FROM CYANOBACTERIA

2.7.1 Total Lipid Extraction

Several organic solvents have been identified to selectively extract lipids from organisms. Of the various methods for cyanobacterial total lipid extraction, the Folch method is the best technique due to its simplicity and precision (Folch et al., 1957). This method is based on using chloroform–methanol (2:1 by volume) for lipid extraction from endogenous cells. In this technique, the homogenized cells are equilibrated with a saline solution and separated into two layers, with the lipids partitioned in the upper phase. A modified Folch method is performed for the estimation of cyanobacterial lipids spectrophotometrically (Wahlen et al., 2011). Rapid and easy production of large quantities of cells is the key advantage of this method.

2.7.2 Direct Transesterification

In direct transesterification, biofuel is created directly from cyanobacterial extracted lipids by blending cyanobacterial biomass, alcohol, and catalyst under high temperature (Lepage and Roy, 1986). In this process, lipids are not required to be separated in their extractive solvents which reduce the amount of energy consumed. In direct transesterification process, a heterogeneous catalyst can be more effective along with microwave heating (Lepage and Roy, 1986; Favretto, 2004). In this method, cyanobacterial cells react with methanol in the presence of a strong acid catalyst in a microwave, resulting in cell lysis and transesterification of FAs at the same time (Figure 5). In addition, polar molecules move continuously to align themselves via oscillating electric fields of the

microwaves, leading to fast heating of the liquid materials (Figure 6) (Favretto, 2004). In the next phase, transesterified lipids are extracted using chloroform: methanol phase separation. Using direct transesterification to produce biofuel from *Mucor circinelloides* has resulted in high FAME yields (Lewis et al., 2000). In another study, total lipid extracted from cyanobacteria *Synechocystis sp.* PCC 6803 and *Synechococcus elongatus* resulted in significant amounts of FAMES due to extraction of FAs from phospholipid bilayers (Wahlen et al., 2011).

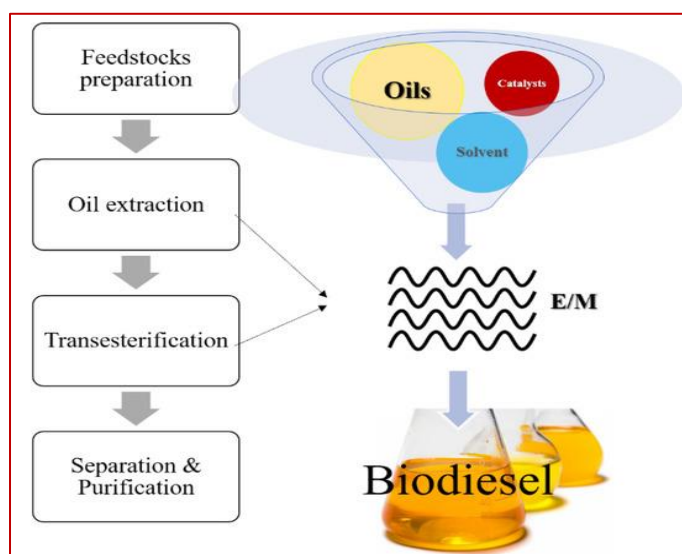


Figure 5 Microwave-enhanced biofuel production process in cyanobacteria (Nomanbhay and Ong, 2017).

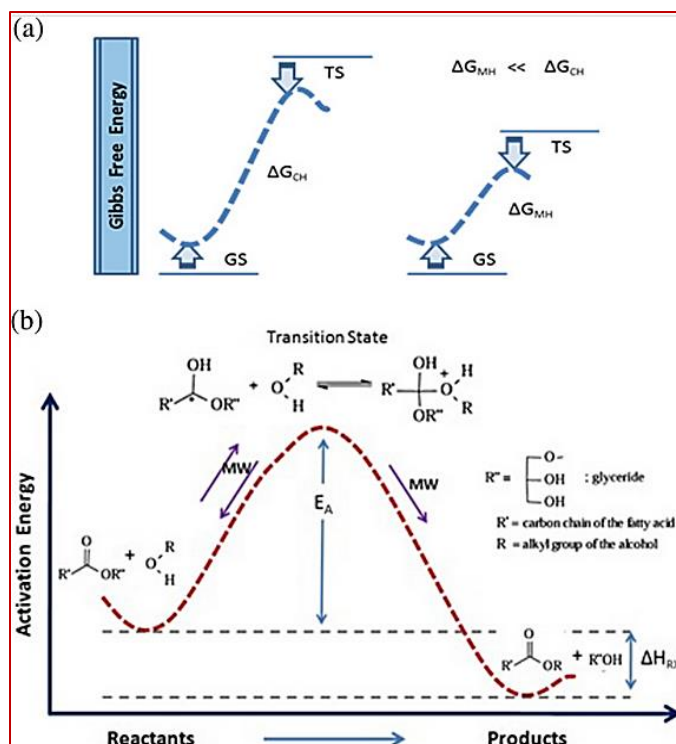


Figure 6: (a) Gibb's free energy differences in conventional and microwave heating methods and (b) activation energy reduction in microwave heating method (Gude et al., 2013).

2.8 MAXIMIZING THE POTENTIAL OF BIOFUEL PRODUCTION BY INCREASING LIPID AND FATTY ACID COMPOSITIONS

Lipids and FAs are the most effective source of energy and play a significant role as structural constituents of cyanobacterial membranes (Nozzi et al., 2013). They also have a critical role in cyanobacterial tolerance to environmental stress such as salinity (Pade and Hagemann, 2014). Enhancing fatty acid composition of cyanobacteria/ microalgae to increase biofuel yield of these organisms is one of the main concern of researchers. Exposure of organisms to different abiotic stresses such as salinity can result in a

significant effect on its total lipid content (Pade and Hagemann, 2014). A previous study reported 60% to 70% increases in total lipid content of microalgae *Dunaliella tertiolecta* ATCC 30929 when exposed to salt stress (Takagi and Yoshida, 2006). Another approach to improve the biofuel production can be a combination of multiple stress factors. In addition, Pal et al., (2011) reported a significant increase in total lipid content of the microalga *Nannochloropsis* sp. when exposed to high intensity light and salinity stresses simultaneously. In another study by Singh et al., (2002), exposure to salinity led to loss of saturation in the FAs located in membrane lipids as well as an increase in unsaturated FAs in multiple cyanobacterial species.

Genetic engineering techniques have also been applied to increase cyanobacterial total lipid content and FA compositions and make them suitable candidates for biofuel applications. It has been reported that genetic manipulation of the fatty acid desaturases genes, the enzymes that introduce double bonds in fatty acid chains, resulting in an increase in unsaturated FAs in the cyanobacteria *Synechocystis* and *Synechococcus* sp., (Tasaka et al., 1996; Allakhverdiev et al., 2000). In addition, Kaczmarzyk and Fulda, (2010) reported significant increases ($P \leq 0.05$) in free fatty acids of *Synechocystis* sp. PCC6803 and *Synechococcus* PCC7942 when the acyl-CoA synthetase gene was knocked out. A previous study on genetically engineered cyanobacterium *Synechocystis* sp. PCC6803 also revealed the successful overproduction and secretion of fatty acids with an efficiency of up to $133 \pm 12 \text{ mg L}^{-1} / \text{day}$ and a cell density of $0.23 \text{ g dry weight / liter}$ (Liu et al., 2011).

2.9 USING IRON NANOPARTICLES TO ENHANCE CYANOBACTERIAL TOTAL LIPID CONTENT AND FATTY ACID COMPOSITIONS

2.9.1 Iron- Induced Oxidative Stress in Cyanobacteria

Iron is one of the most critical metal requirements for growth and lipid yield in cyanobacterial species which influences several processes such as respiration, photosynthesis, electron transport, and cell proliferation (Figure 7). Iron serves as a final acceptor in electron transfer chain, providing the electrons needed to convert NADP to NADPH which is a primary source of ROS in photosystem I of cyanobacterial thylakoid membrane (Latifi et al., 2009; Padrova et al., 2015). Cyanobacterial ROS can be generated in their photosystem complexes via direct transfer of excitation energy (Figure 8).

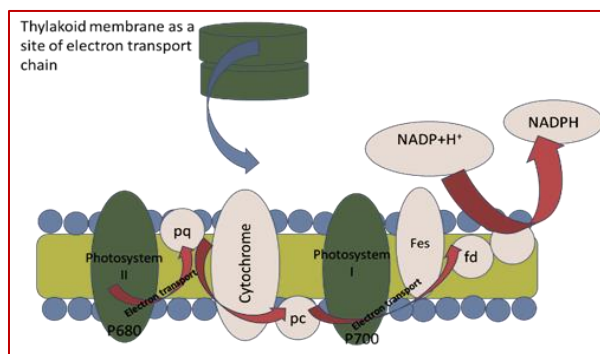


Figure 7 Iron is the final electron receptor in photosystem I of cyanobacterial thylakoid membrane.

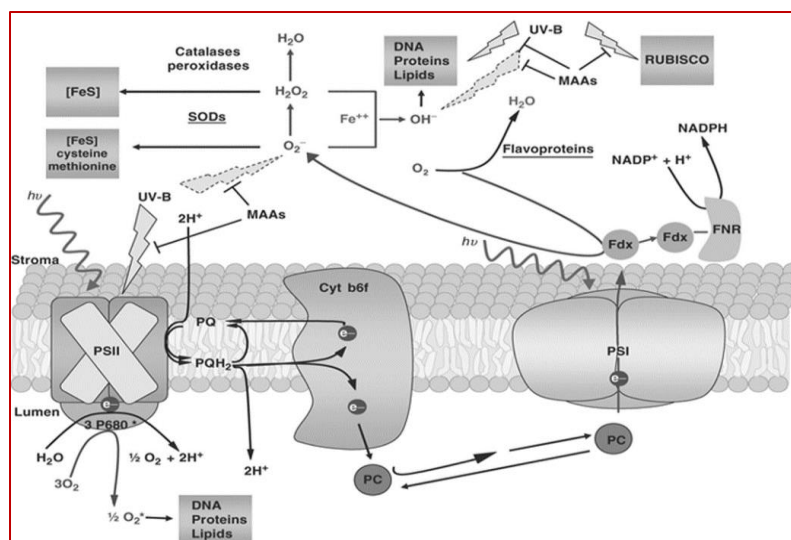


Figure 8 Reactive oxygen stress production and targets in cyanobacteria (Latifi et al., 2009).

In cyanobacterial photosystem complexes, the unreactive oxygen (O_2) leads to chemical generation of reactive species (Sevcu et al., 2011). In photosystem II, oxygen is created by energy from photosensitized chlorophyll. In photosystem I, reduction of oxygen using electrons from photosystem II generates superoxide anion radicals (O_2^-) which unequally transfer to H_2O_2 and O_2 by superoxide dismutase (SOD) (Sevcu et al., 2011; Wang et al., 2016). As a result of this process, H_2O_2 is reduced to water using catalases and peroxidases. In these organisms, the reduction of oxygen by A-type flavoproteins results in water production. However, the reduction of H_2O_2 through metal catalyzed Fenton reaction generates highly toxic hydrogen radicals (OH^\bullet) due to their inherent chemical characteristics (Sevcu et al., 2011; Latifi et al., 2009). In a recent study, the effects of iron on the lipid and carbohydrate production from *Dunaliella tertiolecta* were investigated by Rizwan et al., (2017). They reported that the lipid content was significantly increased ($P \leq 0.05$) in the presence of 0.65 mg L^{-1} ferric iron, while carbohydrate yield decreased.

In a study by El Baky et al., (2012), a 28.12% increase in transesterified lipids in the microalgae *Scenedesmus obliquus* exposed to $20 \text{ mg L}^{-1} \text{ Fe}^{+3}$ was identified. Transesterified lipids contained suitable fatty acid compositions for biofuel production with the most abundant compounds of oleic (32.19 –34.44%), palmitic (29.54 –25.12%) and stearic (12.26 –16.58% of total FAMES) acids having been reported.

Zero-valent iron nanoparticles (nZVI) is a novel approach to provide a suitable source of iron for cell growth and enhancement of FA yield. Oxidation of nZVI leads to the formation of ROS via the Fenton reaction ($\text{Fe}^{+2} + \text{H}_2\text{O}_2 \rightarrow \bullet\text{OH}^- + \text{OH}^-$) which increases oxidative stress in treated cells, and results in increased lipid content (Figure 9) (Sevcu et al., 2011; Padrova et al., 2015). Bioavailability of nZVI supports its interaction with the cell surface and penetration into the cytosol due to their small size (50 nm) (Sevcu et al., 2011). A recent study has reported a 24% increase in total lipid content of cyanobacterium *Arthrospira maxima* when exposed to 5.1 mg L^{-1} nZVI (Padrova et al., 2015). Another study reported a significant increase in rice growth, as well as a maximum activity in its root hydrolytic and antioxidant enzymes, when plants were exposed to 20 mg L^{-1} nZVI (Guha et al., 2018).

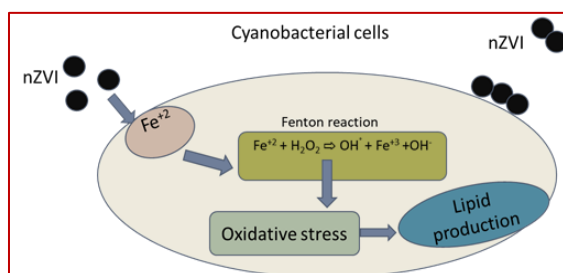


Figure 9 Interaction of nZVI with cyanobacterial cells created oxidative stress resulting in lipid enhancement.

CHAPTER III

EXPERIMENTAL

3.1 Materials and procedures

Specific reagents, chemicals, solutions, media, and instrumentation used in these studies include:

- Ethylenediaminetetraacetic acid disodium (EDTA) salt, citric acid ($C_6H_8O_7$), calcium chloride ($CaCl_2$), HEPES buffer (99%), potassium phosphate dibasic (K_2HPO_4), magnesium sulfate ($MgSO_4$), ferric ammonium citrate ($C_6H_{11}Fe(NO_7)_3$), BactoAgar, inoculating loops, methanol (LC/MS grade), Tris-HCl ($C_4H_{12}ClNO_3$), sodium chloride (NaCl), iron EDTA, Tris-acetate-EDTA (TAE) (50X), Tris-EDTA (TE) buffer, sodium carbonate ($NaCO_3$), boric acid (H_3BO_3), magnesium chloride ($MgCl_2$), zinc sulfate heptahydrate ($ZnSO_4 \cdot 7H_2O$), copper sulfate ($CuSO_4$), cobalt nitrate ($Co(NO_3)_2$), sodium molybdate (Na_2MoO_4), sodium nitrate ($NaNO_3$), sodium hydroxide (NaOH), hydrochloric acid (HCl), 3 different pH buffers (4.01, 7.0, 10.01), protein ladder, KOD Hot Start Master Mix, RNA loading and ladder, *Escherichia coli* FB5a competent cells, DNA ladder, GeneRuler 100 bp plus ladder, super optimal broth with catabolite repression media, and chloroform (HPLC grade) were obtained from Thermo Fisher Scientific (USA).
- 12% Bis-Tris gel was purchased from Invitrogen (USA).
- 3M vent tape was obtained from RS-Hughes Company (USA).

- *HindIII*, *BamHI* and *ScaI* restriction enzymes and pGEM-7Zf (+) vector were purchased from Promega (USA). T4 DNA ligase was bought from New England BioLabs (USA).
- Benzonase, liquid BG-11 50X concentrate, lysozyme, Bradford reagent, Prussian blue and protease inhibitors were purchased from Sigma-Aldrich (USA).
- Tissue culture flasks, pipette tips in three different sizes (10 uL, 100 uL and 1000 uL) and Petri plates were bought from Genesee Scientific (USA).
- GelRed nucleic acid stain was purchased from Phenix Research Products (USA) and TriReagent from Molecular Research Center, Inc. (USA). Ampicillin was bought from Gold Biotechnology, Inc.
- Custom oligonucleotide primers were designed in our laboratory and ordered from Integrated DNA Technologies (USA).
- β -mercaptoethanol (BME), 2X Laemmli sample buffer, 10% precast polyacrylamide gel and electroporation cuvettes (1 mm) were purchased from Bio-Rad Laboratories (USA). Sucrose, Luria-Bertani (LB) broth, and LB agar were obtained from PhytoTechnology Laboratories, Inc. (USA). SYBR green master mix was purchased from Applied Biosystems (USA).
- DNA Clean and Concentrator-5 kit, microcentrifuge tubes (0.6 and 1.5 mL), nuclease free water, ZR Fungal/Bacterial DNA Kit™, PCR tubes, and DNA Gel Recovery™ kit were bought from Zymo Research Corp. (USA). Protein sample buffer (4x) (loading dye), 3-(N-morpholino) propanesulfonic acid sodium dodecyl

sulfate (MOPS SDS) running buffer (20X) and high capacity RNA to cDNA kit were obtained from Life Technologies (USA).

- Iron nanoparticles (Nanofer 25 and Nanofer 25s) were purchased from Nano Iron Company (Rajhrad, Czech Republic).
- Green filters at λ_{max} of 530 nm and red filters at λ_{max} of 650 nm were purchased from Shop Wild Things, Inc. (USA).

3.2 BG11 stock solutions for cyanobacterial growth

Preparation of stock solution 1: 0.1 g $\text{Na}_2\text{Mg EDTA}$, 0.6 g ferric ammonium citrate, 0.6 g citric acid· $1\text{H}_2\text{O}$, and 3.6 g $\text{CaCl}_2\cdot 2\text{H}_2\text{O}$ were dissolved in 980 mL distilled H_2O and sterilized at 15 psi, for 25 min.

Preparation of stock solution 2: 7.5 g $\text{MgSO}_4\cdot 7\text{H}_2\text{O}$ were dissolved in 980 mL distilled H_2O and media transferred to a graduated cylinder. Distilled water was added to a final volume of 1000 mL. Media were autoclaved at 15 psi for 25 minutes.

Preparation of Stock solution 3: 4 g $\text{K}_2\text{HPO}_4\cdot 3\text{H}_2\text{O}$ was dissolved in 980 mL distilled H_2O and autoclaved at 15 psi for 25 minutes.

Preparation of Stock solution 4: 2 g Na_2CO_3 was dissolved in 980 mL distilled H_2O and autoclaved at 15 psi for 25 minutes.

Preparation of stock solution 5: 0.286 g H_3BO_3 , 0.181 g $\text{MnCl}_2\cdot 4\text{H}_2\text{O}$, 0.0222 g $\text{ZnSO}_4\cdot 7\text{H}_2\text{O}$, 0.0079 g $\text{CuSO}_4\cdot 5\text{H}_2\text{O}$, $\text{Co}(\text{NO}_3)_2\cdot 6\text{H}_2\text{O}$, and 0.039 g $\text{Na}_2\text{MoO}_4\cdot 2\text{H}_2\text{O}$ were dissolved in 90 mL distilled H_2O and autoclaved at 15 psi for 25 minutes.

1 M HEPES (pH 8.0)

For preparation of HEPES buffer, 119.15 g of HEPES were added to 350 mL distilled H₂O and stirred on magnetic stir plate until dissolved, then distilled H₂O was added to the final volume of 500 mL. In the next step, 6-12 g NaOH pellets (depends on the pH) were added to the media and dissolved to an approximate pH of 7.8 to 7.9 (2-3 pellets ~ +0.5 on pH scale). The pH was then adjusted to 8.0 with 10 M NaOH and HEPES solution, dispensed into glass bottles in aliquots of 125 mL, and autoclaved at 15 psi for 25 min.

BG-11 + HEPES Media (using 10X stock solutions above)

10 mL volumes from stock solutions 1-4 and 1 mL of stock solution 5 were added to 800 mL of distilled H₂O while stirring on magnetic stir plate. Then 1.5 g NaNO₃ was added to the solution and stirred until dissolved, and distilled water added to a final volume of 980 mL. To adjust the pH to 7.1, 1 M NaOH or 1 M HCl was added to the media. To prepare BG11 solid media, 15 g Bactoagar was added to 1L media and autoclaved at 15 psi for 25 min. The media was cooled to 55-60 °C in a shaker water bath with gentle swirling. In a laminar flow hood, 20 mL 1 M HEPES, pH 8.0, per liter of solution (10 mL of HEPES added to 500 mL of BG11 media) was added to the media using a sterile pipette.

For making BG11 liquid media supplemented with salt, 10 mL from stock solutions 1-4 and 1 mL of stock solution 5 were added to 800 mL of distilled H₂O while stirring on magnetic stir plate, followed by adding 1.5 g NaNO₃ and stirred until dissolved. In the next step, 40 g L⁻¹ NaCl was added to the solution and media prepared as described above.

Medium containing Bactoagar were poured on to 100 x 25 mm plates (approximately half full) or 100 x 20 mm plates (approximately two-thirds full). Plates were set in a hood with fan on until solidified, followed by storage at 4 °C.

3.3 Instrumentation

- Centrifuge 5417 R was purchased from Beckman-Coulter (Germany).
- Mini Protein Tetra Gel system was obtained from Bio-Rad (USA).
- Conviron model EF7 growth incubator which is from Adaptis (Canada)
- NUAIRE (USA) Sterile biosafety cabinet
- Benchmark Scientific model BSH5002 and Inc (USA) Dry block incubator which were obtained from Genesee Scientific (USA).
- Optical microscope BA210 was manufactured by Motic (USA).
- VersaDoc Gel Imager was purchased from Bio-Rad (USA).

-Sequencing was performed with an Applied Biosystems 3730xl DNA Analyzer at the Johns Hopkins University.

- LI-190SA quantum sensor connected to a LI-250 light meter was manufactured by Li-Cor (USA).
- Incubator shakers (Annova 44R) were from Eppendorf (USA).
- pH meter model A111 was purchased from Thermo Fisher Scientific (USA).
- Lyophilizer was purchased from Labconco (USA).

-Benchmark rocker shaker was obtained from Genesee Scientific (USA).

-Microcentrifuge model LX100 was purchased from Eppendorf (USA).

- NanoDrop spectrophotometer 2000 was obtained from Thermo- Fisher Scientific (USA).
- C1000 Thermal Cycler (PCR) was bought from Bio-Rad (USA).
- Gene Pulser Electroporator model GenePulser Xcell with CE module was obtained from Bio-Rad (USA).

-Two-dimensional polyacrylamide gel electrophoresis was performed at Kendrick Labs in Madison, WI (fee-for-service).

- CFX96 Quantitative real time PCR machine model C1000 Touch was purchased from Bio-Rad (USA).

-Multimode commercial scientific microwave was obtained from CEM Corporation (USA).

-Shimadzu GC17A/QP5050A GC/MS combination set with a low polarity (5% phenyl-, 95% methyl-siloxane) capillary column (30m length, 0.25mm ID, 0.25um film thickness, 10m length guard column) in the Mass Spectrometry Facility at the Krieger School of Arts and Sciences, Johns Hopkins University (Baltimore, MD).

-Transmission electron microscopy (TEM) was performed using the JEM-2100Plus TEM located in the Advanced Imaging and Microscopy Laboratory at University of Maryland (College Park, MD).

- Fluorescent microscopy was performed using Olympus BX51M.

3.4 Methods

3.4.1 Objective 1. Enhancement of lipids in *F. diplosiphon* using genetic transformation

3.4.1.1 Overexpression of sterol desaturase and acyl-lipid desaturase genes in *F. diplosiphon* via electroporation-mediated genetic transformation.

The filamentous *F. diplosiphon* strain (B481) was purchased from UTEX (USA) and used as the wild type, WT-B481. Cells were streaked on BG-11 solid medium containing 20 mM HEPES and grown at 28° C. To initiate liquid cultures, 5-day old early log phase *F. diplosiphon* cells were grown in BG11/HEPES under green, red, or white light with continuous shaking at 170 rpm and 28 °C for nine days. For growing cells under green and red light, filters with λ_{\max} of 530 nm and 650 nm, respectively were used. The light fluence rate was adjusted to 30 $\mu\text{mol m}^{-2} \text{s}^{-1}$ using a LI-190SA quantum sensor connected to a LI-250 light meter.

F. diplosiphon B481-WT strain adjusted to an initial optical density of 0.1 at 750 nm (OD_{750}) was grown in liquid BG-11/HEPES. Three replicates were maintained and growth was measured at OD_{750} every 24 h for nine days using a Cynmar 1105 spectrophotometer. *Escherichia coli* FB5 α competent cells were grown at 37 °C in Luria-Bertani (LB) broth and agar plates containing 80 mg L⁻¹ ampicillin as the selective antibiotic.

Total RNA was extracted from *F. diplosiphon*, B481 strain at optical density 0.6 using Tri Reagent according to the manufacturer's protocol with some modifications at the Hoffman/Koban laboratory (Morgan State University). At the specific optical density (0.6),

cells were collected by centrifugation for 8 minutes at 8000 rpm. Then 250 uL of cells were mixed with 5 mL Trizol and shaken vigorously for 1 minute. Samples were then incubated at room temperature for 5 minutes. In the next step, 0.7 mL of 1-bromo-3-chloropropane (BCP) was added to the samples and shaken vigorously for 30 s followed by incubation at room temperature for 15 minutes. Samples were centrifuged at 12000 g for 15 minutes at 4° C and the colorless supernatant was transferred to a fresh tube. In case the supernatant was not clear, centrifugation was repeated at 12000 g for 5 more minutes at 4° C. After transferring the colorless supernatant which contained RNA, 2.5 mL isopropanol was added to the samples and incubated at room temperature for 1 hour followed by centrifugation at 12000 g for 8 minutes at 4° C. The supernatant was removed and the RNA pellet washed with 80% cold ethanol, vortexed for 1 minute, and centrifuged at 7500 g for 5 minutes at 4° C. The supernatant was then removed and the RNA pellet washed with 90% cold ethanol, vortexed for 1 minute and centrifuged at 7500 g for 5 minutes at 4° C. Finally, the supernatant was removed and the RNA pellet washed with 100% cold ethanol, vortexed for 1 minute, and centrifuged at 7500 g for 5 minutes at 4° C. The supernatant was removed and the RNA pellet was dried by exposing to the air for 5 minutes. The pellet was dissolved in 30 uL RNase-DNase-free water and incubated for 10 minutes at 56° C in a heat block.

The quality and quantity of extracted RNA was verified using electrophoresis on 1.2% agarose gel stained with GelRed, and by A260/280 spectrophotometric ratio using the Nanodrop respectively. RNA was then aliquoted and stored at -80° C for further experiments.

Before running RNA on the gel, all glassware such as gel cassette and electrophoresis tank were washed with NaOH (20g NaOH pellets were dissolved in 500 mL diethyl pyrocarbonate (DEPC) water), waited 10 minutes, and rinsed twice with distilled water. Agarose gel was prepared by melting 0.5 g agarose in 36 mL DEPC water on a hot plate. Then 5 mL of 10X MOPS buffer was added to the melted gel and cooled to 60° C followed by adding 9 mL formaldehyde (37%), followed by addition of 5 mL GelRed, and the gel was poured into the cassette. Running buffer was prepared by adding 100 mL of 10X MOPS buffer to the 900 mL DEPC water. For loading RNA on the gel, 2000 ng of extracted RNA was mixed with the loading dye (up to 9ul depends on RNA concentration) and the mixture heated at 70° C for 10 minutes followed by chilling on ice. RNA ladder (5uL) was also spun down and heated at 70° C for 10 min and chilled on ice. RNA sample and ladder were run on the gel for 1 hour at 150 V and 100 mA.

Complementary DNA (cDNA) was reverse transcribed using high capacity RNA to cDNA kit (AB Applied Bio-system). Homologs of the lipid production genes sterol desaturase and acyl-lipid desaturase were identified in *F. diplosiphon* using polymerase chain reaction. PCR amplification was performed with 50 ng cDNA using a C1000 Touch Thermocycler. Primers for *F. diplosiphon* acyl-lipid desaturase and sterol desaturase genes were designed to amplify the genes containing a *HindIII* restriction site added to the 5' end and *BamHI* site at the 3' end (Table 1). Amplifications were performed at the following condition: 10 uL of 2X KOD Hot Start Master Mix (EMD Millipore) was mixed with each of 10 µM forward and reverse primers (specific for each gene), 50 ng template cDNA, and nuclease-free water up to 25 ul. Amplifications were performed under the

following conditions: 95 °C for 2 min; 40 cycles of 95 °C for 30 s, annealing temperature of 59 °C for 30s, followed by a final 45 s elongation step at 72 °C. Amplified products were electrophoresed on a 1.2% agarose gel, the expected band was excised under UV, and the cDNA bands extracted using the Gel Recovery kit (Zymo Research). Amplified fragments were sequenced at the Genetic Resources Core Facility at Johns Hopkins University using ABI 3130 XL Genetic Analyzer (Life Technologies) and chromatograms analyzed using Finch TV Version 1.4.0 (Geospiza Inc.). Basic Local Alignment Sequence Tool (BLAST) and BLASTx analysis were performed to confirm the homology of the genes. Sequences were compared to the NCBI nucleotide collection database to determine the percentage of identity relative to homologous genes in other submitted species at GenBank.

Gene	Acyl-lipid desaturase
Size (bp)	1122
Forward (5'-3')	GCGAAGCTTTATGACAACAGCACCCAGAGACAA GAG
Reverse (5'-3')	GCGGGAT CCT CTA ACT ATT CAC CAA AGC TGG AGTT

Gene	Sterol desaturase
Size (bp)	1314
Forward (5'-3')	ATCAAGCTTGATGTTGACTTTTGACTTCTTCAT AGCGGG
Reverse (5'-3')	GCGGGATCCGTTA GTT CAA AGA TTG AACCTTTTAA

Table 1: Primers for acyl-lipid desaturase and sterol desaturase genes used for polymerase chain reaction (PCR).

Expression plasmids pGEM-7Zf (+)- acyl-lipid desaturase and pGEM-7Zf (+)-sterol desaturase with promoters (Sp6 and T7) were constructed to overexpress these genes. The amplified cDNA gene products were double digested with *HindIII* and *BamHI*. The pGEM-7Zf (+) vector (Figure 10) was also triple-digested with *HindIII*, *BamHI* and *ScaI* restriction enzymes, and the digested products were extracted as previously described. Purified inserts were ligated into the vector with T4 DNA ligase by adding 2 uL 10 x ligase buffer to 3 uL insert, 2 uL digested vector, and 0.5 uL bovine serum albumin (BSA). Recombinant plasmids containing the lipid production genes were transformed into *E. coli* FB5 α competent cells via heat shock at 42 °C for 20 s, followed by incubation in optimal broth with catabolite repression media at 37 °C for 1 hour. The transformed cells were then plated on LB agar media supplemented with 80 mg L⁻¹ ampicillin and incubated for 16 hours at 37 °C. Ampicillin-resistant single colonies were selected and grown in liquid LB

medium containing 80 mg L⁻¹ ampicillin overnight. Plasmids were extracted from transformed cells using the Zyppy Plasmid Miniprep kit according to the manufacturer's protocol and checked for the presence of the inserts by PCR under conditions mentioned above. Presence of the inserts is further confirmed by DNA sequence analysis.

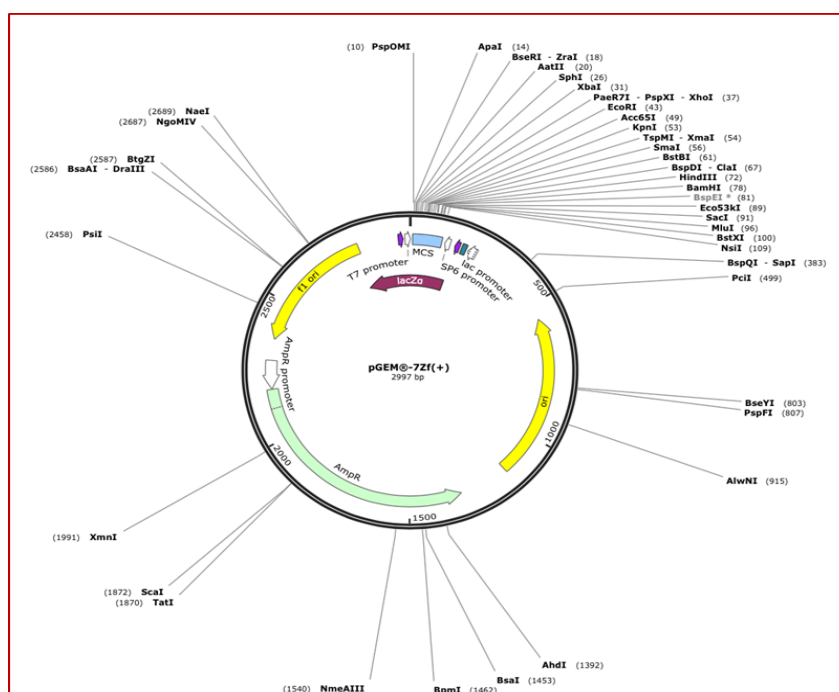


Figure 10 Schematic diagram of pGEM-7Zf vector.

Expression plasmids containing acyl-lipid desaturase and sterol desaturase genes were transformed into wild type *F. diplosiphon* B481 using electroporation as described by Kehoe and Grossman (1998). Cultures were grown in BG-11/HEPES to an optical density at 750 nm (OD₇₅₀) of 0.5 under continuous white light at 15 μmol m⁻² s⁻¹ followed by 72 hours in dark at 170 rpm. In the next step, cultures were centrifuged at 3450 × g for 10 min and the pellet washed three times with autoclaved distilled water and the

supernatant removed. Concentrated cells (40 μ l) were mixed with 6 μ g purified plasmid DNA in ice and electroporated using a GenePulser Xcell at 200 Ω resistance, 1.0 kV, and 25 μ F capacitance. After incubation in ice for 20 min, cells were grown in 10 mL BG11/HEPES liquid media for 16 h and transferred to BG-11/HEPES solid plates containing 80 mg L⁻¹ ampicillin.

To verify the insertion of acyl-lipid desaturase and sterol desaturase genes, PCR was performed with gene specific primers (Table 1). Amplifications were performed by mixing 2X KOD Hot Start Master Mix, forward and reverse primers (10 μ M of each), 50 ng template cDNA, and nuclease-free water as described above and products visualized on a 1.2% agarose gel with a GeneRuler 100 bp plus ladder.

Total RNA in B481-WT and transformants were extracted and cDNA synthesized according to the manufacturer's protocol as described before. Reverse transcriptase-quantitative PCR (RT-qPCR) was used to quantify gene overexpression in the transformants. Primers were designed for acyl-lipid desaturase and sterol desaturase genes (Table 2) and real-time amplifications performed using SYBR Green master mix (Applied Biosystems). A Thermal Cycler CFX96 Real-Time machine was used to perform RT-qPCR. The reactions were performed in 20 μ l volume containing 10 μ l SYBR green Master Mix and 10 ng cDNA template. Amplifications were performed under the following conditions: 95 $^{\circ}$ C for 20s; 95 $^{\circ}$ C for 20s; and 40 cycles of 50.9 $^{\circ}$ C for 30 s. Four replicates were maintained for each treatment type. Relative quantification (RQ) data of the wild type and transformants were analyzed using the Δ Ct method with CFX Manager 3.1 (Bio-Rad)

with WT serving as the calibrator (RQ set to 1). Based on the gene expression level, sterol desaturase (SD) gene was selected for further experiments.

Gene	Acyl-lipid desaturase
Forward (5'-3')	TGACAACAGCACCCAGAGACA
Reverse (5'-3')	ACTTTCAGCCAGATTTGCGG
Gene	Sterol desaturase
Forward (5'-3')	CGGGACTAGCGCTGATAAAA
Reverse (5'-3')	TTACCAAGCGAGGGGACAT

Table 2: Primers for acyl-lipid desaturase and sterol desaturase genes used for reverse transcription-quantitative PCR assay.

To confirm stability of the transformant (B481-SD), the strain was cultured in liquid BG-11/HEPES media containing 80 mg L⁻¹ ampicillin over a nine day-period under conditions described before. *F. diplosiphon* B481-WT grown in the absence of ampicillin served as control. Culture conditions were maintained as described above, and growth (OD₇₅₀) measured every 24 h. Stability of the transformant in BG11/HEPES media containing 80 mg L⁻¹ ampicillin was monitored for 28 generations.

Growth of the transformant was compared to WT in order to determine the effect of overexpression of the inserted gene on *F. diplosiphon* growth. Culture conditions were maintained as mentioned above with three biological replicates and mean growth and growth rate calculated. Statistical significance was determined using one-way analysis of variance (ANOVA) and Tukey's honest significant differences post-hoc test at 95% confidence intervals ($P \leq 0.05$). The single factor, fixed-effect ANOVA model, $Y_{ij} = \mu + \alpha G_i + \epsilon_{ij}$, was used where Y is the growth (OD_{750} or growth rate) in strain i and biological replicate j . The μ represents mean growth with adjustments from the effects of strain (αS), and ϵ_{ij} is the experimental error from strain i and biological replicate j . Growth rate was calculated as doublings per day and average growth analyzed (\pm standard error) using ANOVA and Tukey's Honest Significant Differences tests with a level of significance set at $P \leq 0.05$.

The impact of SD overexpression on *F. diplosiphon* photosynthetic pigmentation was quantified according to a method described by Tandeau de Marsac and Houmard (1988) and Kahn et al., (1997), and phycobiliproteins reported as $\mu\text{g}/\mu\text{g}$ *chl a* (Whitaker et al., 2009). *F. diplosiphon* WT and transformant were grown in BG-11/HEPES to an OD_{750} of ~ 0.6 under fluorescent white light as explained above. From each culture, 1 mL samples were aliquoted in new microcentrifuge tubes followed by incubation in ice for 1 hour. Samples were then centrifuged at $13,000 \times g$ for 5 min and the supernatant removed. The pellet was immediately flash-frozen in liquid nitrogen and thawed at room temperature.

For *chl a* and carotenoid extraction, *F. diplosiphon* pellet was resuspended in 500 μl of 90% methanol followed by incubation in dark at 4°C for 1 hour on a rocking shaker.

Samples were centrifuged at 10,000 g for 10 min, and the supernatant transferred into pre-weighed microcentrifuge tubes. This step was repeated once, and the supernatant transferred into the same microcentrifuge tubes. The weight of each sample was noted followed by measurement of carotenoids and *chl a* at A_{470} and A_{665} , respectively. In the next step, sample weight and absorbance values were inserted in the following equations to determine *chl a* and carotenoids quantities:

$$(1) \quad \text{Chlorophyll } a \text{ (Chl } a\text{)} \text{ (mg mL}^{-1}\text{)} = ((A_{665} \times 13.9 \times (\text{weight}/0.8)/1.5))/1000$$

$$(2) \quad \text{Carotenoids (mg mL}^{-1}\text{)} = ((1000 \times A_{470}) - (1.91 \times \text{Chl } a))/225$$

The phycobiliproteins phycoerythrin (PE), phycocyanin (PC), and allophycocyanin (AP) were extracted as follows: pellets were resuspended in 1 ml of cold STES buffer containing lysozyme and incubated at room temperature (in the dark) for 30 min while samples were rocking on the shaker. Cells were then centrifuged at 13,000 g for 5 min at room temperature, followed by measurement of optical density of the supernatant at OD_{565} , OD_{620} and OD_{650} . These absorbance values were used to quantify different pigment concentrations using the following equations:

$$(3) \quad \text{Phycocyanin (PC) (mg mL}^{-1}\text{)} = ((A_{620} - (0.7 \times A_{650}))/7.38$$

$$(4) \quad \text{Allophycocyanin (AP) (mg mL}^{-1}\text{)} = ((A_{650} - (0.19 \times A_{620}))/5.65$$

$$(5) \quad \text{Phycoerythrin (PE) (mg mL}^{-1}\text{)} = ((A_{565} - (2.8 \times \text{PC}) - (1.34 \times \text{AP}))/12.7$$

$$(6) \quad \text{Standard deviations: } SD = \sqrt{\left(\frac{SDX}{avgX}\right)^2 + \left(\frac{SDY}{avgY}\right)^2}$$

3.4.1.2 Comparison of total lipid content and fatty acid compositions in the WT and transformant by gravimetric analysis and GC-MS.

Total lipid content in *F. diplosiphon* B481-WT and transformant was determined using a chloroform: methanol extraction method based on Folch et al., (1957) reported in Wahlen et al., (2011). About 80-100 mg of dried samples were sonicated in 5 mL of chloroform: methanol (2:1 by volume) for 30 s followed by centrifugation at 6000 rpm at temperature room. Samples were washed with 1 mL distilled water and centrifuged again at 2000 rpm for 5 minutes to simplify phase separation. Methanol and sulfuric acid which were partitioned with water were placed in the upper phase, while lipids separated with chloroform in the lower phase. In the next step, the organic phase was transferred into a new tube and extraction was repeated twice to collect residual lipids. The organic phase was transferred into flasks which were pre-weighed and then dried in a rotary evaporator machine followed by weighing to determine lipid content of each sample. For each sample, three biological replicates were maintained and the experiment repeated once. Significance among cumulative treatment means was determined using ANOVA and Tukey's honest significant differences post hoc test at 95% confidence intervals ($P < 0.05$). The single factor, fixed-effect ANOVA model, $Y_{ij} = \mu + \alpha S_i + \epsilon_{ij}$, was used where Y is the total lipid yield content in strain i and biological replicate j . The μ represents overall total lipid content mean with adjustments from the effects of strain (αS), and ϵ_{ij} is the experimental error from genotype i and biological replicate j .

F. diplosiphon WT and transformant extracted lipids were converted to FAMES via direct transesterification which combines extraction and in situ biofuel production. About

80-100 mg of *F. diplosiphon* WT and transformant lyophilized cells were dissolved in 4 mL methanol containing 1.8% (v/v) sulfuric acid and the reaction was performed in a commercial multimode scientific microwave at 80 °C and 1378.95 kPa for 20 min with a maximum power output set at 25 W per each sample. The reaction was stopped with 8 mL chloroform (2:1 by volume) and the mixture washed with 5 mL distilled water followed by centrifugation at 2000 rpm for phase separation. The organic phase which contained chloroform was transferred to a new flask and the remaining biomass washed twice with 2 mL chloroform.

FAME composition of transesterified lipids from *F. diplosiphon* WT and transformant was determined using a Shimadzu GC17A/QP5050A GC-MS combination at the Mass Spectrometry Facility at Johns Hopkins University (Baltimore, MD). The GC17A contains a low-polarity (5% phenyl-, 95% methyl-siloxane) capillary column (30 m length, 0.25 mm ID, 0.25 µm film thickness, and 10 m length guard column). After dissolving in chloroform, 1 µl of each sample was transferred to the machine using an autosampler. The temperature of the injector was maintained at 280° C. However, the oven temperature was maintained at 130 °C for 10 min at the beginning and then ramped to 160° C (hold for 7 min); from 160 to 190 °C (hold for 7 min), 190 to 220 °C (hold for 22 min), and 220 to 250 °C (hold for 17 min) at a rate of 10 °C min⁻¹ for each step. The mass scan of QP5050A EI quadrupole was in the range of m/z 40 to 900 and its electron-impact ionization was at 70 eV. In the next step, peaks were identified by comparing mass spectra to the American Oil Chemists Society Lipid Library Spectra of FAME. For each sample three biological replicates were maintained, data were analyzed, and the experiment repeated once. In

addition, chemical and physical properties of the transesterified lipids from FAME composition (w%) were calculated using BiodieselAnalyzer© software Version 2.2 (Talebi et al., 2014).

For identification of FAMES from the WT and transformant strain, a high-resolution GC × GC-TOFMS from LECO (USA) was used. *F. diplosiphon* WT and transformant total lipids were extracted and subjected to direct transesterification as explained above. Total lipids were then dried under nitrogen (N₂) and reconstituted in 2 mL dichloromethane with 50 µg mL⁻¹ cholestane spiked as an internal standard. For each sample, 1 µL transesterified lipid was injected splitless. The first dimension column was a BP-1 (60 m × 0.25 mm ID, 0.25 µm film thickness, 100% polysiloxane, SGE Inc.), and the second was a BPX50 (1.5 m × 0.1 mm ID, 0.1 µm film thickness, 50% Phenyl, SGE, Inc.). The temperature GC inlet was 300 °C and helium was operated as transporter gas with the flow rate of 1 mL min⁻¹. The temperature of GC oven was initially held at 40 °C for 0.5 min, then ramped at 2 °C min⁻¹ to 340 °C and maintained at a final temperature for 10 min. In addition, the modulator had an offset of + 10 °C with a modulation period of 6 s and hot pulse of 0.8 s. Electron-impact ionization at 70 eV was used with the ion source set at 225 °C and the transfer line at 280 °C. MS data were collected with an acquisition rate of 100 spectra/s and mass range from m/z 40 to 550.

3.4.1.3 Enhancement of total lipid content and essential fatty acid methyl esters by exposure to salinity stress

F. diplosiphon B481-WT and transformant were grown in BG11/HEPES containing 0, 10, 20, 30, 40, and 50 mg L⁻¹ NaCl. For each sample, three replicates were maintained. Cultures were grown for 10 days under constant shaking at 28 °C and 170 rpm with an initial optical density of 0.1. Statistical significance was determined using one-way analysis of variance (ANOVA) and Tukey's honest significant differences post-hoc test at 95% confidence intervals ($P \leq 0.05$) as mentioned in section 3.4.1.1. According to the growth data, *F. diplosiphon* transformant grown in 40 g L⁻¹ NaCl was selected as a halotolerant strain for the further experiments.

Total RNA in WT and halotolerant transformant was extracted and cDNA synthesized according to the manufacturer's protocol as mentioned at section 3.4.1.1. RT-qPCR was used to quantify gene expression in the halotolerant transformant. Primers were designed as mentioned in Table 2 and real-time amplifications performed using SYBR green master mix as described above. Four replicates were maintained for each treatment type. Relative quantification (RQ) data of the wild type and halotolerant transformants were analyzed using the ΔC_t method with CFX Manager 3.1 (Bio-Rad) with WT serving as the calibrator (RQ set to 1). Total lipid content in *F. diplosiphon* WT and halotolerant transformant was determined using a chloroform: methanol extraction method based on Folch et al., (1957) reported in Wahlen et al., (2011) as described at section 3.4.1.2. For each sample three biological replicates were maintained, and the experiment repeated once. Significance among cumulative treatment means was determined using ANOVA and

Tukey's honest significant differences post hoc test at 95% confidence intervals ($P < 0.05$) as mentioned above.

F. diplosiphon WT and halotolerant transformant extracted lipids were converted to FAMES via direct transesterification as mentioned at section 3.4.1.2. FAME composition of transesterified material from *F. diplosiphon* WT and halotolerant transformant was determined using a Shimadzu GC17A/QP5050A GC-MS combination at the Mass Spectrometry facility as described at section 3.4.1.2. In the next step, peaks were identified by comparing mass spectra to The Lipid Web Archive of FAME Mass Spectra. For each sample three biological replicates were maintained, data were analyzed, and the experiment repeated once. In addition, theoretical chemical and physical properties of the transesterified lipids from FAME composition (w%) were calculated using BiodieselAnalyzer© software Version 2.2 (Talebi et al., 2014).

F. diplosiphon WT and halotolerant transformant were grown in sea water which contained 37.1 g L^{-1} NaCl for 10 days under constant shaking at 28°C and 170 rpm, with an initial optical density of 0.1 at 750 nm. Statistical significance was determined using one-way analysis of variance (ANOVA) and Tukey's honest significant differences post-hoc test at 95% confidence intervals ($P \leq 0.05$) as mentioned at section 3.4.1.1.

F. diplosiphon WT and halotolerant transformant were grown in sea water which contained 37.1 g L^{-1} NaCl and brackish water amended with 6% BG11 /HEPES media for 10 days under constant shaking at 28°C and 170 rpm, with an initial optical density of 0.1 at 750 nm. Statistical significance was determined using one-way analysis of variance

(ANOVA) and Tukey's honest significant differences post-hoc test at 95% confidence intervals ($P \leq 0.05$) as described at sections 3.4.1.1 and 3.4.1.2.

One dimensional polyacrylamide gel electrophoresis (1D-PAGE) was used to determine protein expression in the B481-WT, B481-SD and B481-SDH strains. To extract total protein, *F. diplosiphon* WT and B481-SD were grown in BG11 media/HEPES and B481-SDH grown in BG11 media/HEPES amended with 40 g L^{-1} NaCl as explained at section 3.4.1.1. After nine days, cells were centrifuged at 8000 rpm for 15 minutes at 4°C to harvest the pellet. For each sample, two protease inhibitor tablets were dissolved in 30 mL of binding buffer which contained $50 \mu\text{M}$ tris and $500 \mu\text{M}$ NaCl. Then 0.03 g lysozyme which melted in 3 mL binding buffer was added to each sample and incubated in ice for 1 hour. The pellet was sonicated at 100% ampere for 10 seconds in ice. Each sample was sonicated for 10 s with 1 minute intervals, and this process was repeated nine times. Cells were then spun down at 10,000 rpm for 15 minutes at 4°C . Supernatant was separated and transferred to new tubes. Next, 1 μL of Bradford reagent (Sigma) was mixed with 1 μL of each sample and those samples which turned blue were selected to run on the gel. In the next step, 30 μL of each sample was mixed with 10 μL of 4x protein sample buffer and mixtures were heated at 98°C for 5 minutes. Then, 15 μL of each mixture was run on 12% Bis-Tris gel in a Mini-Protean Tetra Gel system at 200 V for 60 min and 1X MOPS SDS used as the running buffer.

The gel was washed thrice with distilled water to remove excess buffer and stained by staining solution (0.25 g Coomassie Brilliant Blue, 450 mL methanol, 450 mL distilled water, and 100 mL glacial acetic acid) for 1 hour. The gel was de-stained using de-staining

solution (450 mL methanol, 450 mL distilled water, and 100 mL glacial acetic acid) for additional 1 hour and left in distilled water overnight.

Two-dimensional electrophoresis was performed according to the carrier ampholine method (O'Farrell, 1975; Burgess-Cassler, 1989) by Kendrick Labs, Inc. (Madison, WI). Isoelectric focusing was carried out in a glass tube of inner diameter 3.0 mm using 2.0% pH 4-8 mix ampholines (Serva, Heidelberg) at 20,000 V. In the next step, 1 μ g tropomyosin was added to the sample and used as an internal standard. The lower polypeptide spot of tropomyosin which is located at MW 33,000 Da and Isoelectric point (pI) 5.2 migrated as a doublet. The pH gradient plot for ampholines was determined with a surface pH electrode. After equilibration for 10 min in buffer "O" (10% glycerol, 50 mM dithiothreitol, 2.3% SDS, and 0.0625 M tris, pH 6.8), the tube gel was sealed to the top of a stacking gel that overlaid on a 10% acrylamide slab gel (1.0 mm thick) followed by electrophoresis at 25 mA/gel for 5 hours.

Myosin (220,000), phosphorylase A (94,000), catalase (60,000), actin (43,000) carbonic anhydrase (29,000), and lysozyme (14,000) were used as standard proteins. The Coomassie blue-stained gels were scanned wet and dried between sheets of cellophane with the acid edge to the left.

3.4.2 Enhancement of lipids and fatty acids in *F. diplosiphon* using iron nanoparticles

3.4.2.1 Impact of iron nanoparticles (Nanofer 25 and Nanofer 25s) on growth and photosynthetic efficacy of two cyanobacteria strains (B481 and SF33)

Two different types of Zero-valent iron nanoparticles (nZVI), Nanofer 25 and Nanofer 25s, used in this experiment were purchased from Nano iron company (Rajhrad, Czech Republic) (Figure 11). Both Nanofer 25 and 25s exhibited an average size of 50 nm, an average surface area of 20-25 m²g⁻¹ and a high content of iron (20 mg nZVI /100 ml water), making them ideal candidate particles for cellular entry.

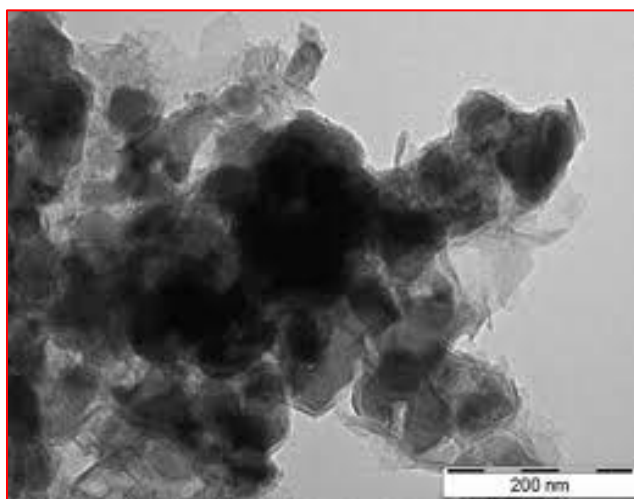


Figure 11 Visualization of iron nanoparticle (Nanofer 25s) using transmission electron microscopy (TEM).

F. diplosiphon B481 and SF33 strains were grown in BG11/HEPES containing 1.5, 5, 15, 50, 150, 200, 300, 400, 500 and 600 mg L⁻¹ of Nanofer 25 and 25s. Cultures containing Fe-EDTA (0.5 mg L⁻¹ Fe) served as control. Three replicated treatments were maintained and cultures grown for 18 days under constant shaking at 28 °C and 70 rpm,

with an initial optical density of 0.1. Statistical significance was determined using one-way analysis of variance (ANOVA) and Tukey's honest significant differences post-hoc test at 95% confidence intervals ($P \leq 0.05$) as mentioned at section 3.4.1.1.

In the next set, *F. diplosiphon* B481 and SF33 strains were grown in BG11/HEPES containing 0.05, 0.1, 0.2, 0.4, 0.8, 1.6 and 3.2 mg L⁻¹ of Nanofer 25 and 25s for 15 days under condition mentioned above. Three replicated treatments were maintained and statistical significance determined using one-way analysis of variance (ANOVA) and Tukey's honest significant differences post-hoc test at 95% confidence intervals ($P \leq 0.05$) as described at section 3.4.1.1.

Chlorophyll *a* (chl*a*), carotenoids, and phycobiliproteins were extracted and quantified as described at section 3.4.1.1 to test the impact of Nanofer 25 and 25s on photosynthetic efficiency.

3.4.2.2 The effect of iron nanoparticles on total lipid content and fatty acid composition of *F. diplosiphon* nano-treated cells determined using gravimetric analysis and GC-MS.

Total lipid content in *F. diplosiphon* B481 and SF33 strains (control) and nano-treated cells was determined using a chloroform: methanol extraction method based on Folch et al., (1957) and reported in Wahlen et al., (2011) as described at section 3.4.1.2. For each sample three biological replicates were maintained and the experiment repeated once. Significance among cumulative treatment means was determined using ANOVA and

Tukey's honest significant differences post hoc test at 95% confidence intervals ($P < 0.05$) as mentioned at section 3.4.1.1.

F. diplosiphon control and nano-treated cells extracted lipids were converted to FAMES via direct transesterification as mentioned at section 3.4.1.2. FAME composition of transesterified material from *F. diplosiphon* control and nano-treated cells was determined using a Shimadzu GC17A/QP5050A GC-MS combination at the Mass Spectrometry as described above. In the next step, peaks were identified by comparing mass spectra to the American Oil Chemists Society Lipid Library Spectra of FAME. For each sample, three biological replicates were maintained. Data was analyzed and the experiment repeated once. In addition, theoretical chemical and physical properties of the transesterified lipids from FAME composition (w%) were calculated using BiodieselAnalyzer© software Version 2.2 (Talebi et al., 2014).

High-resolution GC × GC-TOFMS from LECO was used to identify FAMES from the *F. diplosiphon* control and nano-treated cells as described at section 3.4.1.2.

Growth, photosynthetic pigment accumulation, and FAME studies were performed in three biological replicates and the experiments repeated once. Results were reported as cumulative treatment mean ± standard error. Statistical significance was determined using one-way analysis of variance and Tukey's Honest Significant Differences post-hoc test at 95% confidence intervals ($P < 0.05$) as mentioned at section 3.4.1.1.

F. diplosiphon nano-treated cells were stained with Prussian blue and visualized using Olympus BX51M fluorescent microscopy.

TEM was performed using the JEM-2100Plus microscope located in the Advanced Imaging and Microscopy Laboratory at University of Maryland (College Park, MD) to visualize the presence of iron nanoparticle in *F. diplosiphon* cells.

CHAPTER IV

RESULTS AND DISCUSSION

4.1 ENHANCEMENT OF LIPID IN *F. DIPLOSIPHON* USING GENETIC TRANSFORMATION VIA. ELECTROPORATION

4.1.1 Overexpression of sterol desaturase and acyl-lipid desaturase genes in *F. diplosiphon* via electroporation-mediated genetic transformation.

4.1.1.1 Identification of acyl-lipid desaturase and sterol desaturase homologues in *F. diplosiphon*

In cyanobacteria, genetic engineering approaches can be applied to enhance total lipid content as well as fatty acid compositions and reduce the cost of biofuel production (Lu, 2010; Liu et al., 2011; Chen et al., 2014). In this study, identification of lipid producing genes in *F. diplosiphon* was the first and major step for genetic engineering of this organism. PCR amplification of acyl-lipid desaturase and sterol desaturase genes revealed a single discrete band at the expected sizes of 1122 and 1314 basepairs (bp) respectively (Figure 12). NCBI BLAST analysis confirmed that these sequences matched with the lipid production genes, acyl-lipid desaturase and sterol desaturase and their predicted amino acid sequence. Our results revealed open reading frames of 1122 and 1314 base pairs encoding 373 amino acids for acyl-lipid desaturase and 437 for sterol desaturase. Further sequence alignment analysis revealed a 99% match to acyl-lipid desaturase and 94% to sterol desaturase in *F. diplosiphon*, thus confirming the identity of the genes (Figure 13). The amino acid sequence of acyl-lipid desaturase showed 95%, 94%, 93% and 72% match to *Nostoc carneum* NIES-2107, *Calothrix brevissima* NIES-22, *Calothrix sp.* NIES-2100, and

Nodularia spumigena respectively. The sterol desaturase amino acid sequence revealed 93%, 86%, 77%, and 77% similarities to *Nostoc carneum* NIES-2107, *Calothrix sp.* NIES-2100, *Nodularia sp.* NIES-3585, and *Fortiea contorta* respectively. These findings indicate high similarities to the published sequences of these proteins in various cyanobacteria, confirming their functional importance in lipid biosynthesis pathways. In a previous study, 15 proteins that resemble acyl-lipid desaturase enzyme (BLAST scores from 75 to 123) have been identified in *Arabidopsis* (Beisson et al., 2013). The acyl-lipid desaturase and sterol desaturase sequences were deposited at NCBI Genbank with the accession numbers MH329182 and MH329183 respectively.

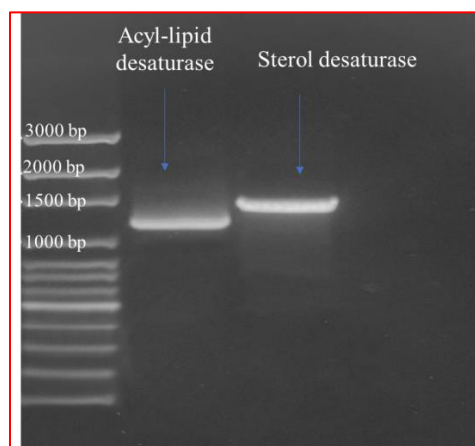


Figure 12 PCR amplification of acyl-lipid desaturase and sterol desaturase genes in *Fremyella diplosiphon*.

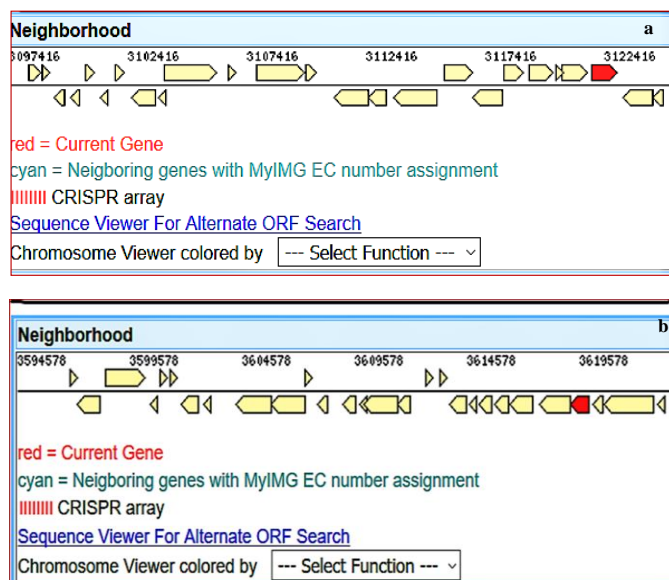


Figure 13 Sequence alignments of (a) acyl-lipid desaturase and (b) sterol desaturases genes in *Fremyella diplosiphon*.

4.1.1.2 Cloning and transformation of acyl-lipid desaturase and sterol desaturase genes in *F. diplosiphon*

Homologous transformation techniques using effective promoters and expression vectors have been developed to increase total lipid content and reduce the cost of microalgal fuel production (Venegas-Calderón et al., 2010; Chen et al., 2014). In our study, PCR products of acyl-lipid desaturase and sterol desaturase genes were double digested using *HindIII* and *BamHI*. The pGEM-7Zf (+) vector was triple digested using *ScaI*, *HindIII*, and *BamHI* (Figures 14 and 15) followed by ligation of purified inserts into the vector at the corresponding restriction sites. pGem-7Zf plasmids containing acyl-lipid desaturase and sterol desaturase genes were constructed and cloned in *E. coli* FB5 α strain (Figure 16) to significantly overexpress lipid production genes. Recombinant plasmids containing lipid producing genes were transformed into WT-B481 using electroporation-

mediated transformation which has proven successful in introducing genes related to fatty acid desaturase synthesis. This vector has been used in the past studies for homologous overexpression in bacterial systems (Chen et al., 2008; Goda et al., 2004). In a previous effort in our laboratory, plasmids pGEM-7Zf-HlyB and pGEM-7Zf-MDH were successfully constructed and delivered into *F. diplosiphon* WT-Fd33 using electroporation-mediated transformation to increase halotolerance of the strain (Tabatabai et al., 2017-b).

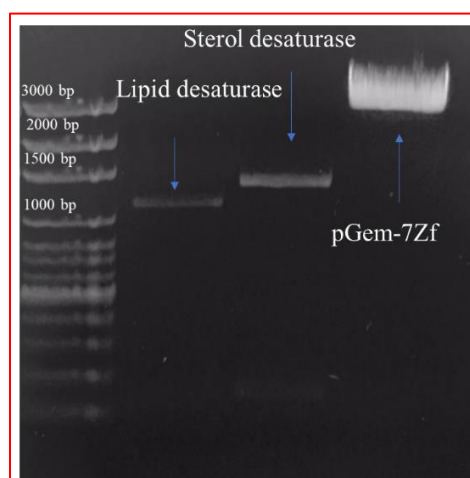


Figure 14 PCR amplification of the acyl-lipid desaturase and sterol desaturase genes, and pGEM-7Zf (+) vector prior to digestion.

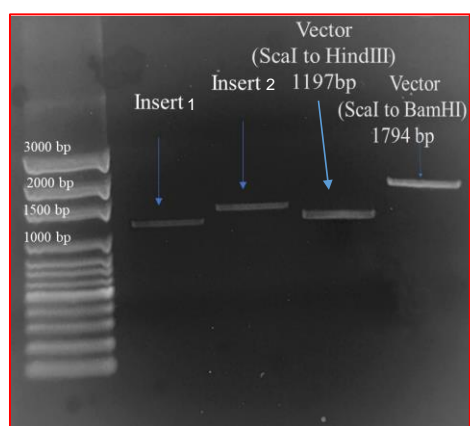


Figure 15 Double digestion of acyl-lipid desaturase (insert 1) and sterol desaturase gene (insert 2), and triple digestion of pGEM-7Zf (+) vector.



Figure 16 *Escherichia coli* containing plasmids grown in Luria-Bertani (LB) media amended with 80 mg L⁻¹ ampicillin.

Insertion of the acyl-lipid desaturase and sterol desaturase genes was confirmed by PCR and Sanger sequencing indicating successful cloning of the genes in the plasmid (Figure 17). The sterol desaturase gene was reported to be successfully overexpressed in the yeast, *Saccharomyces cerevisiae*, to produce ergosterol which is responsible for structural membrane features such as fluidity and permeability (Cai et al., 2007).

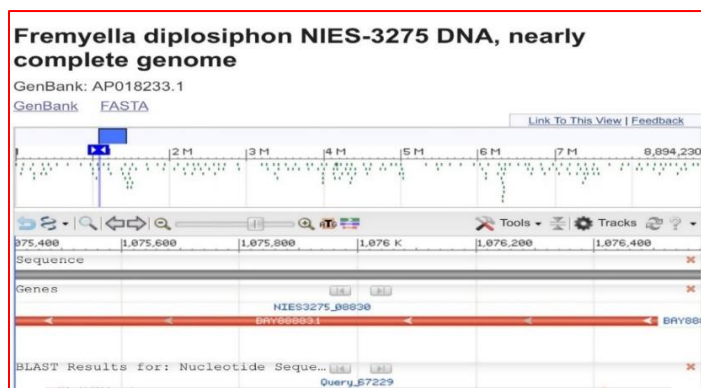


Figure 17 Representative of sequenced extracted plasmid containing sterol desaturase gene.

Results of RT-qPCR revealed a 64-fold increase in sterol desaturase transcript abundance in B481-SD relative to that in the WT (Figure 18). However, no difference was observed in acyl-lipid desaturase transcript abundance of the transformant compared to WT.

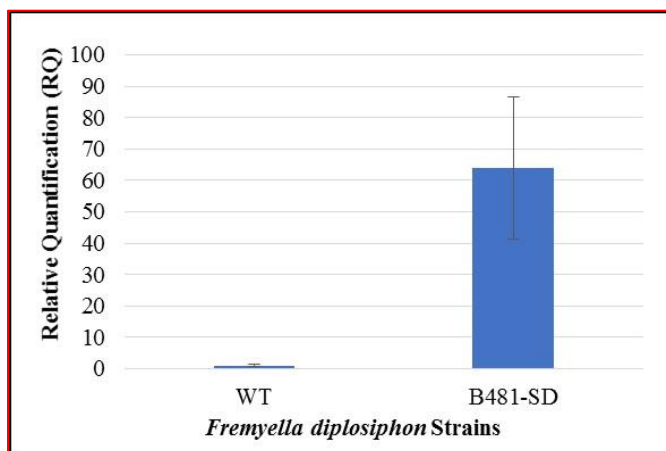


Figure 18 Relative quantification (RQ) of sterol desaturase transcript level in *Fremyella diplosiphon* wild type (WT) and transformant (B481-SD).

The sterol desaturase-overexpressing *F. diplosiphon* strain was designated as B481-SD. We identified a 64-fold increase in sterol desaturase mRNA transcript level indicating successful integration of the pGEM-7Zf-SD plasmid in *F. diplosiphon*. Results of this study suggest that the use of cDNA as a template for overexpression could result in more robust increase in gene regulation. Similar results have been reported by other researchers as well. Using cDNA as a template, a 73-fold increase in sterol desaturase mRNA transcript level was reported in the yeast *Xanthophyllomyces dendrorhous* (Loto et al., 2012). Our findings indicate an increase in mRNA transcript abundance, thereby enhancing the robustness of the organism to produce lipids. Based on these results, the sterol desaturase gene was selected for further experiments.

4.1.1.2.1 Comparison of growth and photosynthetic pigment accumulation in *F. diplosiphon* WT and B481-SD

To identify the effect of overexpression on growth of *F. diplosiphon* B481-SD, cultures were grown in BG-11 medium supplemented with 80 mg L⁻¹ ampicillin. No significant difference in growth or growth rate of B481-SD in liquid BG-11/HEPES medium containing 80 mg L⁻¹ ampicillin compared to WT (Figures 19 and 20) was observed. These findings indicate that sterol desaturase gene overexpression had no negative effect on *F. diplosiphon* growth. B481-SD was persistently grown in BG11/HEPES media containing 80 mg L⁻¹ ampicillin for 28 generations.

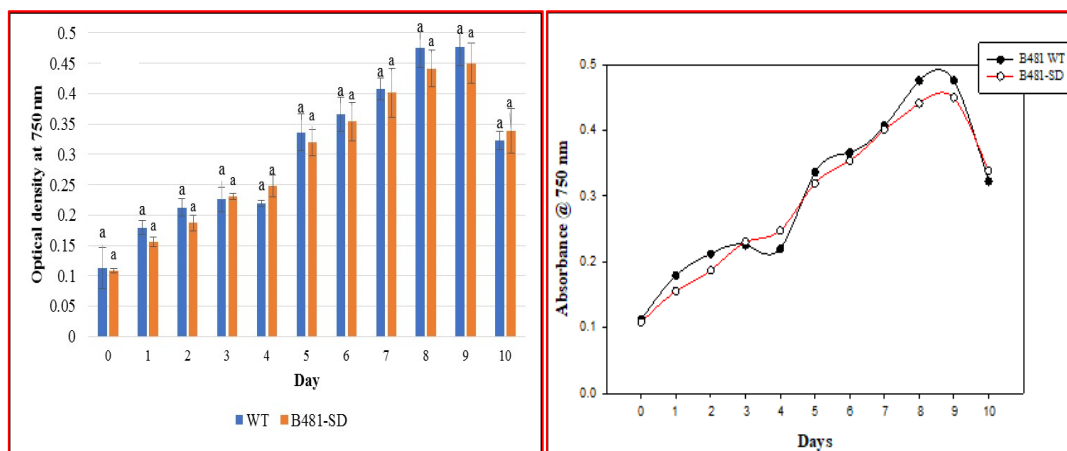


Figure 19 Growth of *Fremyella diplosiphon* wild type (WT-B481) and transformant (B481-SD) in BG11/HEPES medium over a ten day-period.

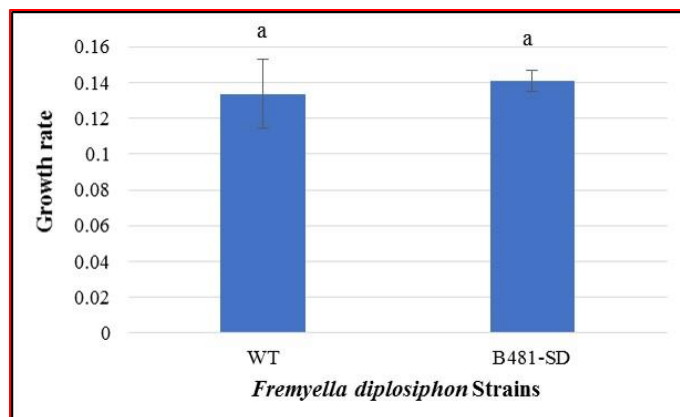


Figure 20 Effect of overexpression of sterol desaturase (SD) gene on growth rate of *Fremyella diplosiphon* wild type (WT-B481) and transformant (B481-SD).

Cyanobacteria have a significant advantage for use in biofuel production due to its high photosynthetic capacity (up to 10%) compared to higher plants which convert just 1% of the sun's energy into biomass (Parmar et al., 2011). In cyanobacteria, synthesis of metabolic products such as fatty acids is mediated by photosynthetic carbon (Lindberg et al., 2010). Thus, in this study, photosynthetic pigments and phycobiliproteins in the wild type *F. diplosiphon* (WT-B481) were compared to the transformant (B481-SD) strain to determine the effect of overexpression on photosynthetic capacity. Quantification of photosynthetic pigments revealed no significant differences between WT and B481-SD indicating that the photosynthetic activity of the transformant was unaltered by overexpression (Figures 21-25). However, a 13.6% increase in phycobiliprotein levels suggests that enhanced pigment accumulation in B481-SD are linked to enhanced lipid production. FAME synthesis is significantly impacted by cellular photosynthetic pathways, indicating a direct correlation between cyanobacterial lipid and their photosynthetic

pigments (Liu et al., 2011). Thus, any loss in photosynthetic pigments could have negative impact on lipid production and fatty acid composition. It is possible that antioxidative properties of photosynthetic pigments could contribute to a cellular response against oxidative stress induced by overexpression (Riss et al., 2007; Los and Mironov, 2015). This defense mechanism has been reported by Riss et al., (2007) in the cyanobacterium *Spirulina platensis*, where phycobiliproteins such as phycocyanin reduced reactive oxidative enzyme activity up to 82% indicating cellular defense response against oxidative stress.

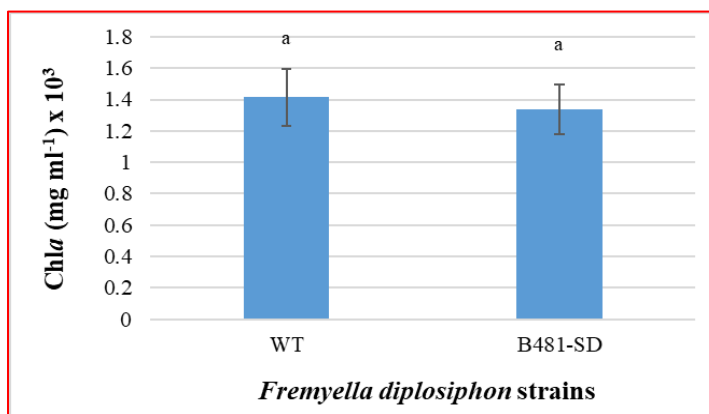


Figure 21 Impact of overexpression of sterol desaturase (SD) on chlorophyll *a* (*chl a*) accumulation in *Fremyella diplosiphon* wild type (WT-B481) and transformant strain (B481-SD).

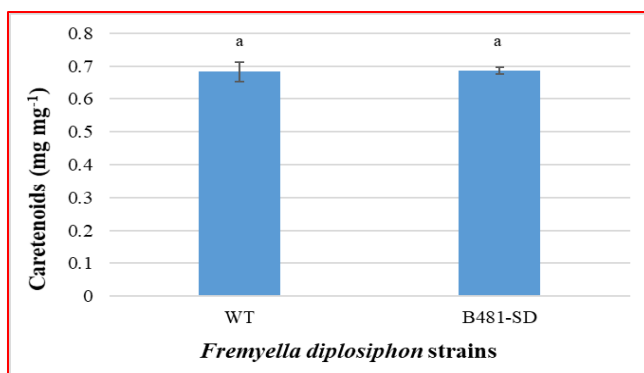


Figure 22 Impact of overexpression of sterol desaturase (SD) on carotenoid accumulation in *Fremyella diplosiphon* wild type (WT-B481) and transformant strain (B481-SD).

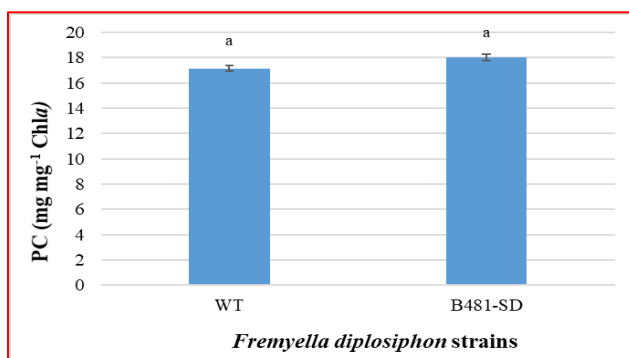


Figure 23 Impact of overexpression of sterol desaturase (SD) gene on phycocyanin (PC) accumulation in *Fremyella diplosiphon* wild type (WT-B481) and transformant strain (B481-SD).

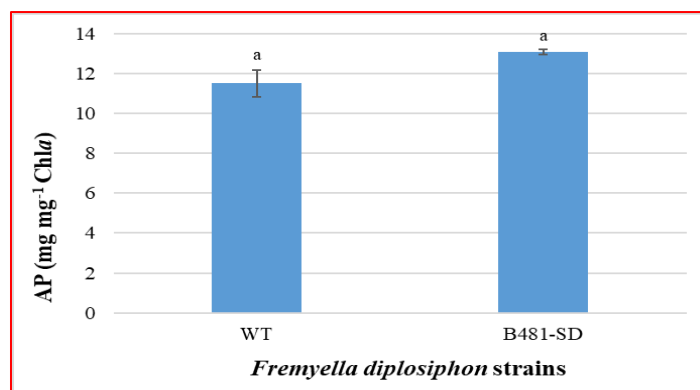


Figure 24 Impact of overexpression of sterol desaturase (SD) gene on allophycocyanin (AP) accumulation in *Fremyella diplosiphon* wild type (WT-B481) and transformant strain (B481-SD).

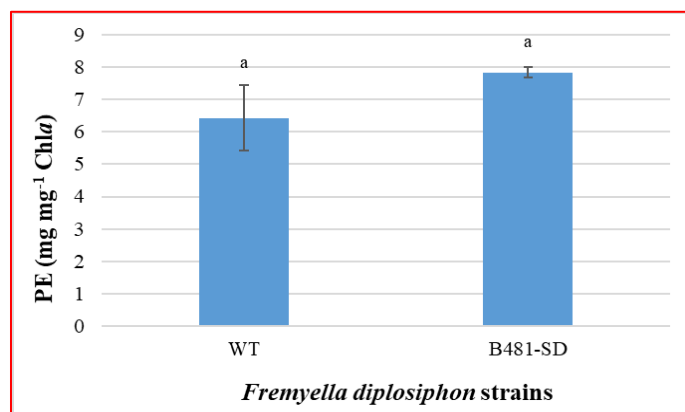


Figure 25 Impact of sterol desaturase gene (SD) on phycoerythrin (PE) accumulation in *Fremyella diplosiphon* wild type (WT-B481) and transformant strain (B481-SD).

4.1.2 Comparison of total lipid content and fatty acid compositions in the WT and transformant by gravimetric analysis and GC-MS.

4.1.2.1 Enhancement of total lipid content in transformant strain

Quantification of total lipid content of cyanobacteria is a major step for biofuel production. Of the various methods for determination of total lipid yield such as high-performance liquid chromatography and Fourier-transform infrared spectroscopy, gravimetric analysis is preferred method due to its simplicity and precision (Wahlen et al., 2011). In this study, efforts to determine lipid using gravimetric analysis indicated a significant increase ($P \leq 0.05$) in B481-SD total lipid yield compared to the WT-B481 (Figure 26). While 17% total lipid content of cellular dry weight was detected in the wild type, 23% lipid yield recovered in the transformant (B481-SD). A 27% increase in total lipid content was observed in *F. diplosiphon* B481-SD relative to WT.

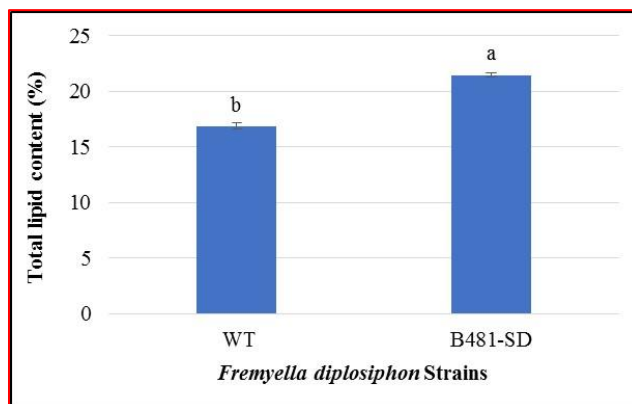


Figure 26 Comparison of total lipid content in wild type (WT) and transformant (B481-SD) *Fremyella diplosiphon*.

In cyanobacteria, sterol desaturase enzymes contribute to biochemical processes such as photosynthesis, respiration, and lipid metabolism (Kramm et al., 2012). The

enzymes of this superfamily typically reduce NADP^+ to NADPH which is a primary source of ROS resulting in oxidative stress in cyanobacterial cells. In response to oxidative stress, cyanobacterial lipid biosynthesis pathways are activated, generating storage lipids particularly unsaturated fatty acids (Kramm et al., 2012; Nozzi et al., 2013). These findings indicate that enhanced total lipid content is induced by catalyzed NADP(H)-dependent reactions which are the primary source of ROS in the transformed strain.

4.1.2.2 Comparison of fatty acid methyl ester profile in WT and transformant via direct transesterification, GC-MS, and GC×GC-TOFMS.

Fatty acid methyl esters derived by transesterification of lipids using a catalyzed reaction and methanol in the presence of strong acids and bases such as sodium hydroxide, potassium hydroxide, and sulfuric acids have been identified as primary molecules for biofuel (Lang et al., 2011; Wahlen et al., 2011; Shukla et al., 2012). Another advantage of using FAMES as a source of biofuel production rather than unesterified components is the higher cetane number (about 12-15) of the resultant fuel (Shukla et al., 2012). Various techniques such as GC-MS and GC×GC-TOFMS offer several advantages including the ability to separate complex mixtures, quantify analytes, and identify trace levels of organic contamination (Bohin et al., 2005). In this study, we identified methyl palmitate, the methyl ester of hexadecanoic acid (C16:0), to be the most abundant FAME. This component accounted for 76.35% and 65.93% of total FAMES produced from WT and B481-SD total transesterified lipids respectively. In addition, saturated FAMES proportion produced from WT and B481-SD total transesterified lipids accounted for 80.99% and 76.62%

respectively (Table 3). Other FAME components such as methyl tetradecanoate (C14:1), methyl hexadecanoate (C16:1), methyl octadecanoate (C18:0), methyl octadecenoate (C18:1), and methyl octadecadienoate (C18:2) were also identified (Table 4).

Strain	FAME Type (%)		Ratio FAME
	Saturated	Unsaturated	Saturated/ Unsaturated
WT	80.99	19.01	4.26
B481-SD	76.62	23.38	3.27

Table 3 Breakdown of saturated and unsaturated fatty acid methyl ester (FAME) proportions in wild type (WT) and transformant (B481-SD) *Fremyella diplosiphon*.

	WT				B481-SD			
	:0 ^b	:1	:2	SUM	:0	:1	:2	SUM
C14^a	-	3.07	-	3.07	-	3.21	-	3.21
C16	72.39	11.66	-	84.05	65.67	7.67	-	73.34
C18	8.60	1.79	2.49	12.88	10.95	5.16	7.34	23.45
SUM	80.99	16.52	2.49	100	76.62	16.04	7.34	100

^a Column represents length of the carbon chain.

^b Row represents degree of saturation (number of double bonds in chain).

Table 4 Quantitative composition of fatty acid methyl ester in *Fremyella diplosiphon* wild type (WT-B481) and transformant (B481-SD) transesterified lipids.

Analysis of FAMES revealed significant increases ($P \leq 0.05$) in methyl octadecenoate (C18:1) and methyl octadecadienoate (C18:2) abundance in B481-SD transesterified lipids. This suggests that sterol desaturase gene overexpression enhances desaturated FAME levels, which are primary components in biofuel production. These components could impact the cloud point, lubricity, and stability caused by oxidative degradation. Thus, high amounts of unsaturated FAs particularly oleic acid (C18:1) and lower quantities of saturated fatty acids such as palmitic acid (C16:0) and stearic acid (C18:0) are considered to be beneficial for biofuel production (Biswas et al., 2011). In previous studies, overexpression of sterol desaturase gene in the yeast *Saccharomyces cerevisiae* and tobacco BY-2 cells resulted in a significant increase ($P \leq 0.05$) in desaturated FAs particularly oleic acid (C18:1) (Zhang et al., 2005; Kamthan et al., 2017). We did not observe significant differences ($P > 0.05$) in other desaturated FAME components (methyl tetradecanoate (C14:1) and methyl hexadecenoate (C16:1)), or saturated FAs (palmitic acid (C16:0) and octadecanoic acid (C18:0)) in B481-SD compared to WT (Figure 27-29). However, we observed 8% and 65% decreases in the saturated components of the transesterified lipids from B481-SD suggesting that overexpression of sterol desaturase gene could be attributed to desaturation of fatty acids by introducing double bond(s) to their carbon chain by removing two hydrogen atoms from a FA followed by insertion of a carbon/carbon double bond (Aguilar et al., 2006; Mansilla et al., 2008).

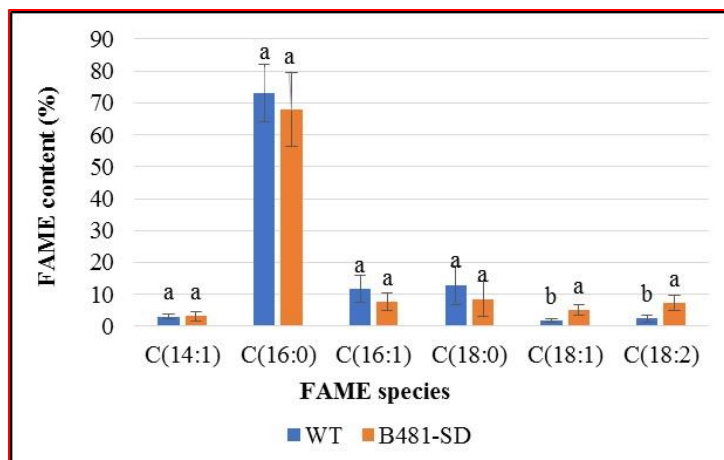


Figure 27 Comparison of fatty acid methyl ester (FAME) composition of *Fremyella diplosiphon* wild type (WT) and transformant (B481-SD) total lipids subjected to direct transesterification.

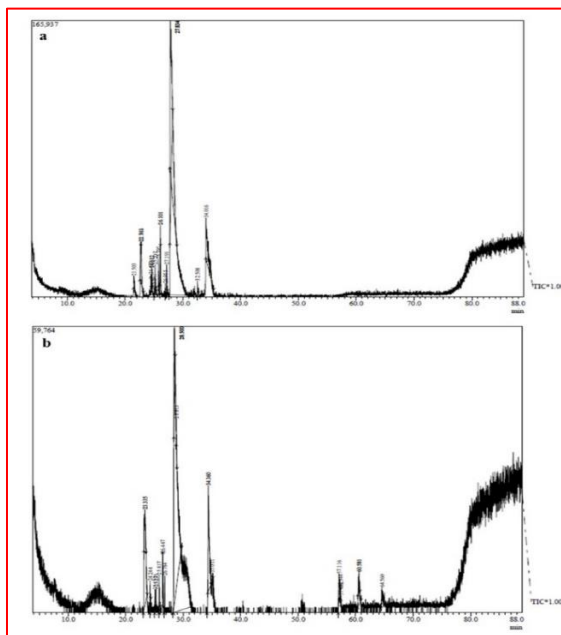


Figure 28 Representative one-dimensional gas chromatogram of *Fremyella diplosiphon* strains (a) wild type (WT-B481) and (b) transformant B481-SD total lipids subjected to direct transesterification.

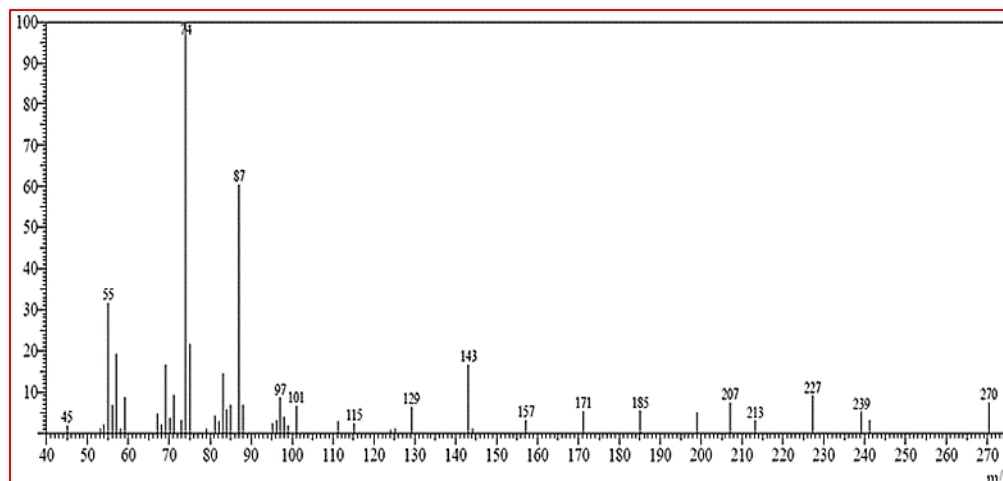


Figure 29 Representative mass spectra of methyl palmitate (C16:0) which was detected as the most abundant fatty acid methyl ester (FAME) component in *Fremyella diplosiphon* transformant (B481-SD) extracted total lipids when subjected to direct transesterification.

Based on FAME composition of transesterified lipids, different theoretical chemical and physical properties were identified to evaluate the potential of the B481-SD strain as an ideal biofuel agent. Calculation of theoretical chemical and physical biofuel properties revealed a product with high cetane number (65.97–67.49) and oxidative stability (50.49–18.67 h). In addition, other values such as density (0.867–0.868 g/cm³), viscosity (3.781–3.817 mm²/s), and iodine content (17.723–25.590 g I₂/100 g) were identified (Table 5 and Figure 30). These findings indicate that the chemical and physical properties of WT and B481-SD-derived biofuel are significantly higher than minimum acceptable fuel standards for cetane number which is 47 and 51 respectively. In addition, these properties were also higher than the fuel standards for oxidative stability which is 3h and 6 h respectively (Masera and Hossain, 2017). Other biofuel properties such as iodine value, density, and

viscosity were also within standard range for commercial fuels. However, temperature-based properties such as pour and cloud points were much higher than ideal levels for current fuels. These findings suggest that mixing *F. diplosiphon*-derived fuels with conventional fuels or including additives will be efficient.

Biodiesel Properties	WT	B481-SD
Saponification Value (mg KOH/g fat)	216.743	214.627
Iodine Value (g I ₂ /100 g)	17.723	25.590
Cetane number	67.494	65.972
Long Chain Saturated Factor	11.540	12.044
Cold Filter Plugging Point (°C)	19.771	21.361
Cloud Point (°C)	33.087	29.550
Pour Point (°C)	29.097	25.258
Allylic Position Equivalent	6.722	19.836
Bis-Allylic Position Equivalent	2.462	7.336
Oxidation Stability (h)	50.493	18.666
Higher Heating Value (mJ/kg)	39.208	39.259
Kinematic Viscosity (mm ² /s)	3.781	3.817
Density (g/cm ³)	0.867	0.868

Table 5 Theoretical biodiesel properties of *Fremyella diplosiphon* wild type (WT) and transformant (B481-SD) transesterified lipids.

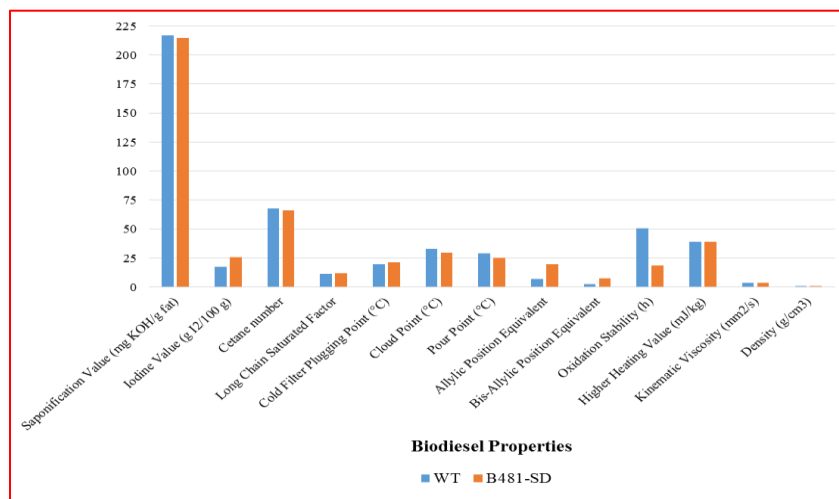


Figure 30 Theoretical biodiesel properties of *Fremyella diplosiphon* wild type (WT) and transformant (B481-SD) transesterified lipids.

GC×GC-TOFMS is a more robust for comprehensive FAME characterization than conventional GC-MS, which is constrained by resolving power that is less effective in detecting trace and co-eluted components (Frysjnger et al., 2003). Unlike GC-MS, high-resolution GC×GC-TOFMS separates compounds by properties of volatility and polarity. While volatility is determined according to their molecular weight (carbon number) on the first dimension, polarity correlates to the degree of unsaturation (number of double bonds) on the second dimension (Lea-Smith et al., 2015; Valentine and Reddy, 2015). In our study, GC×GC-TOFMS analysis revealed the presence of FAMES with carbon number from 12-18, as well as alkanes from C11 to C34. However, in the transformant strain, FAME abundance (80.92% TL) was significantly higher than that of the WT (77.92% TL) (Figures 31 and 32). FAME compounds such as C12:0 C15:0, C18:3, and C18:4 as well as alkanes which were not detected in 1D GC-MS were identified by GC×GC-TOFMS. These

findings suggest additional benefits of *F. diplosiphon*-derived biodiesel. Abundant hydrocarbons in the cyanobacteria, *Prochlorococcus* sp. and *Synechococcus* sp., have been identified using GC×GC-TOFMS (Lea-Smith et al., 2015; Valentine and Reddy, 2015). Higher FAME abundance in B481-SD as observed in this study indicates that overexpression of sterol desaturase gene enhances FA yield paving the way for its potential application as a more efficient strain for production-level biofuel agent. These findings suggest that overexpression of the SD gene enhances lipid yield and essential FA abundance in cyanobacteria. This is the first report of sterol desaturase overexpression resulting in enhanced total lipid content and essential unsaturated fatty acid compositions in *F. diplosiphon*, suggesting this gene is an ideal candidate for augmenting biodiesel production capacity. A Non provisional patent application (US Patent Application No.: 16/123,484; September 6, 2018) describing this genetic engineering-based approach to augment total lipid content and essential FAs has been filed (Sitther and Gharaie Fathabad, 2018).

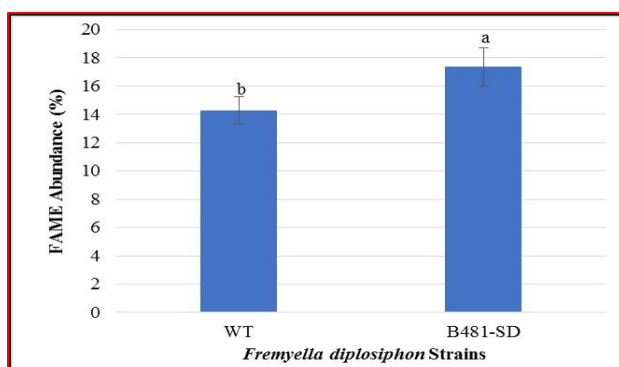


Figure 31 Fatty acid methyl ester (FAME) abundance in transesterified extractable lipids of wild type (WT) and transformant (B481-SD) *Fremyella diplosiphon* determined using GC×GC-TOFMS.

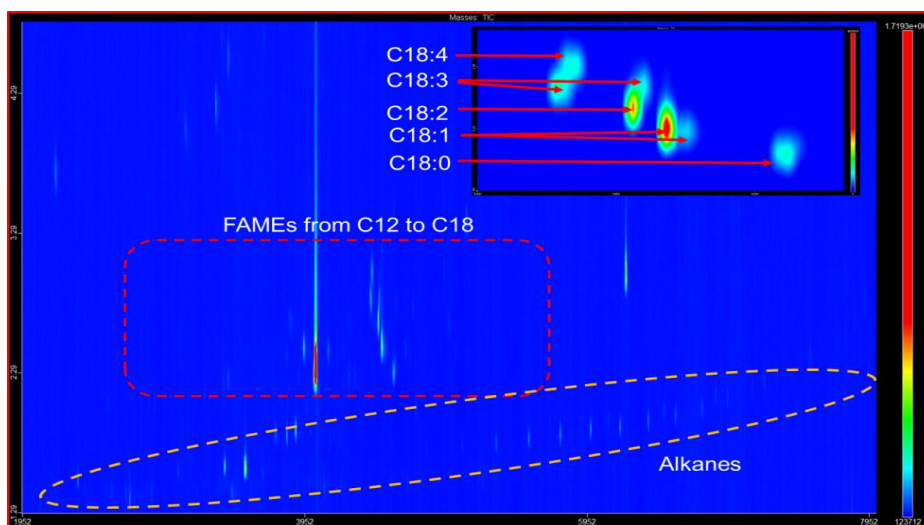


Figure 32 Representative GCxGC-TOFMS chromatogram of *Fremyella diplosiphon* B481-SD fatty acid methyl esters (FAMEs), alkanes, and other components.

4.1.3 Enhancement of total lipid content and essential fatty acid methyl esters by exposure to salinity stress.

4.1.3.1 Growth of *F. diplosiphon* WT and transformant (B481-SD) in media containing 40 g L⁻¹

To establish the halotolerance level of *F. diplosiphon* B481-SD, cells were grown in BG11 media supplemented with different concentrations of NaCl ranging from 0 to 50 g L⁻¹ was compared to the WT strain grown under identical conditions. Results of the study revealed significantly higher ($P \leq 0.05$) growth of WT and transformant grown in the absence of NaCl relative to the cultures exposed to salinity conditions. No significant difference ($P > 0.05$) between WT-B481 and B481-SD grown in media amended with 10 and 20 g L⁻¹ NaCl was observed (Figure 33). However, the transformant exhibited a 41% increase in growth compared to WT in media amended with 40 g L⁻¹ NaCl. Since B481-

SD was capable of growth in BG-11/HEPES medium at concentrations up to 40 g L⁻¹ NaCl, this concentration was selected for the further experiments.

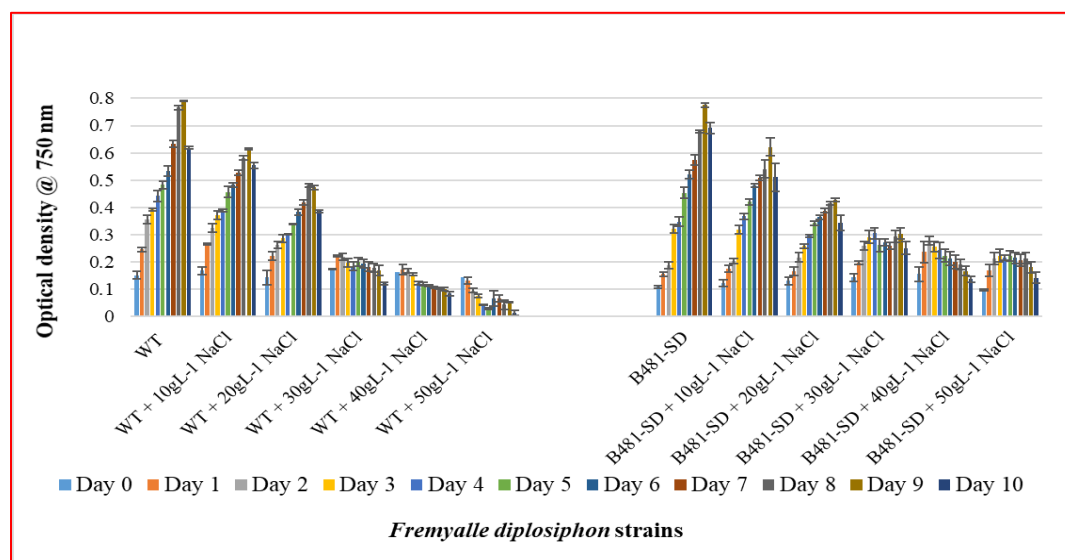


Figure 33 Effect of 0, 10, 20, 30, 40, and 50 g L⁻¹ sodium chloride (NaCl) on *Fremyella diplosiphon* wild type (B481-WT) and transformant (B481-SD) growth.

4.1.3.2 RT-qPCR analysis confirms overexpression of sterol desaturase gene in *F. diplosiphon* halotolerant transformant

RT-qPCR was performed to quantify transcript level of sterol desaturase gene in *F. diplosiphon* transformant grown in 40 g L⁻¹ NaCl. Our results revealed a 38-fold increase in halotolerant transformant transcript abundance relative to the WT (Figure 34). The *F. diplosiphon* halotolerant transformant strain was designated as B481-SDH. In a previous study, 1.7- and 8.5-fold increases in transcript level of fatty acid desaturase (delta 12) gene

were reported when *Chlorella vulgaris* strain NJ-7 was exposed to 3% and 6% NaCl concentrations (Lu et al., 2009).

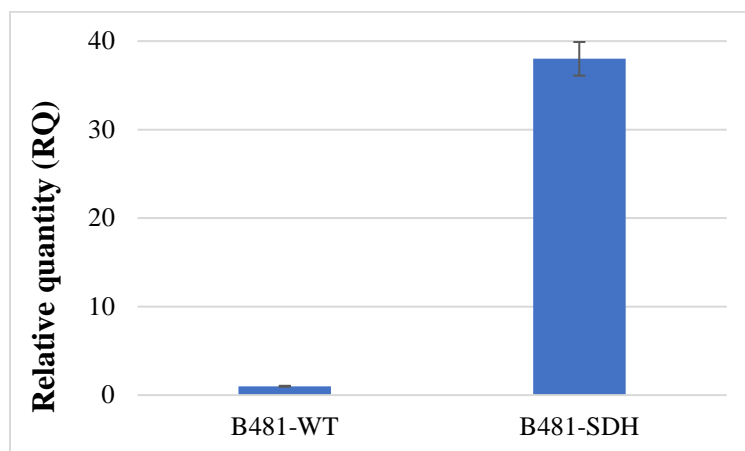


Figure 34 Relative quantification (RQ) of transcript level in *Fremyella diplosiphon* wild type (WT) and halotolerant transformant (B481-SDH) using reverse transcription-quantitative PCR.

4.1.3.3 Enhancement of total lipid content in halotolerant transformant strain

Results of gravimetric analysis revealed a significant increase ($P \leq 0.05$) in *F. diplosiphon* halotolerant transformant B481-SDH total lipid yield compared to the WT-B481 (Figure 35). In a recent study in our laboratory, no significant differences were observed in total lipid content of *F. diplosiphon* wild type (17.83%) and halotolerant strains, HSF33-1 (18.67%) and HSF33-2 (19.66%) indicating that overexpression of the *hlyB* and *mdh* halotolerance genes did not alter the lipid biosynthesis pathway (Tabatabai et al., 2018). However, results of our present study revealed a 28% increase in total lipid content of B481-SDH relative to WT indicating that salinity stress had a positive effect on

enhancing impact on *F. diplosiphon* B481-SDH total lipid yield. In another study, Bhakar et al., (2013) reported up to a 25.53% increase in total lipid content of the cyanobacterium species *Spirulina* when exposed to 5 g L⁻¹ NaCl.

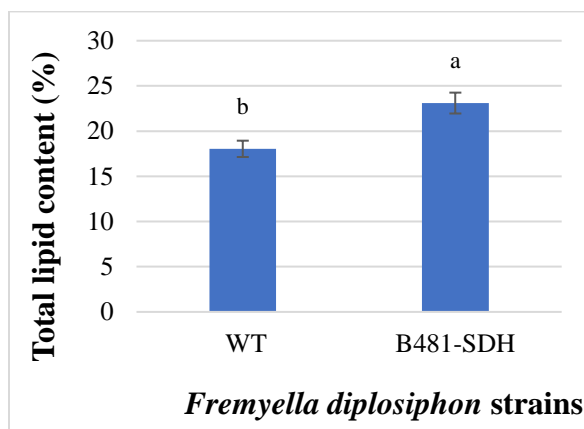


Figure 35 Comparison of total lipid content in wild type (WT) and halotolerant transformant (B481-SDH) *Fremyella diplosiphon*.

4.1.3.4 Comparison of fatty acid methyl ester profile in wild-type and halotolerant transformant via direct transesterification and GC-MS.

FAMES derived by transesterification of fatty acids were identified as primary molecules for biofuel. In this study, methyl palmitate (C16:0), the most abundant FAME, accounted for 85.67% and 84.58% of total FAMES produced from WT and B481-SDH total transesterified lipids respectively. In addition, total saturated FAMES produced from WT and B481-SDH total transesterified lipids accounted for 91.97% and 86.10% respectively (Table 6). We also identified other FAMES components such as methyl tetradecanoate (C14:1), methyl hexadecenoate (C16:1), methyl octadecanoate (C18:0), methyl octadecenoate (C18:1), and methyl octadecadienoate (C18:2) which accounted for 4.44%, 1.81%, 6.30%, 1.03% and 0.79% for WT and 4.03%, 1.9%, 1.51%, 3.9% and

4.08% for B481-SDH respectively (Table 7). In cyanobacteria, membrane integrity and function, which are determined by structure and fluidity, are affected by lipid composition as well as the degree of unsaturated FAMES (Zhang et al., 2005). Several studies have reported that salinity stress alters fatty acids composition, especially the unsaturated FAs (Olsson, 1995; Matos et al., 2002; Zhang et al., 2005).

Strain	FAME Type (%)		Ratio of FAME
	Saturated	Unsaturated	Saturated/Unsaturated
WT	91.97	8.02	11.46
B481-SDH	86.10	13.89	6.19

Table 6 Breakdown of saturated and unsaturated fatty acid methyl ester (FAME) proportions in *Fremyella diplosiphon* wild type (WT) and halotolerant transformant (B481-SDH).

	WT				B481-SDH			
	:0 ^b	:1	:2	SUM	:0	:1	:2	SUM
C14^a	-	4.4	-	4.4	-	4.03	-	4.03
C16	85.67	1.81	-	87.48	84.58	1.9	-	86.48
C18	6.30	1.03	0.79	8.12	1.51	3.9	4.08	9.49
SUM	91.97	7.24	0.79	100	86.09	9.83	4.08	100

^a Column represents length of the carbon chain.

^b Row represents degree of saturation (number of double bonds in chain).

Table 7 Quantitative composition of fatty acid methyl ester in *Fremyella diplosiphon* wild type (WT-B481) and halotolerant transformant (B481-SDH) transesterified lipids.

Significant increases ($P \leq 0.05$) in methyl octadecenoate (C18:1) and methyl octadecadienoate (C18:2) levels from B481-SDH transesterified lipids were also detected. These results suggest that salinity stress enhances desaturated FAMES, which are the key constituents in biofuel production. These results are in accordance with previous studies where a direct correlation between salinity stress and desaturated fatty acids was observed (Zhang et al., 2005; Bhakar et al., 2013). Overexpression of the fatty acid desaturase gene in tobacco cells (By-2) significantly increased desaturated FAs enhancing the tolerance of the organism to salinity stress. An increase in linolenic (C18:3) and linoleic acids (C18:2) in *Spirulina* exposed to 3 g L⁻¹ salt after 21 days of incubation was reported (Bhakar et al., 2013). These findings indicate that higher proportion of unsaturated FAs, particularly the C18 group, are enhanced in response to salinity stress in *F. diplosiphon*. Our results

exhibited no significant differences ($P>0.05$) in other desaturated FAMES components such as methyl tetradecanoate (C14:1) and methyl hexadecenoate (C16:1) in WT and B481-SDH (Figure 36-38). In addition, no significant difference ($P>0.05$) was observed in methyl palmitate (C16:0) between the B481-WT and halotolerant transformant (Figure 36 and 37). However, a significant decrease ($P\leq 0.05$) was observed in octadecanoic acid (C18:0) level in B481-SDH transesterified lipids compared to WT (Figure 36). In addition, 1.26 % and 76% decreases of methyl palmitate (C16:0) and methyl octadecanoate acid (C18:0) in the halotolerant transformant suggest that exposure to salinity stress resulted in decrease proportion of desaturated fatty acids due to alterations in cyanobacterial membrane lipid composition (Zhang et al., 2005; Bhakar et al., 2013).

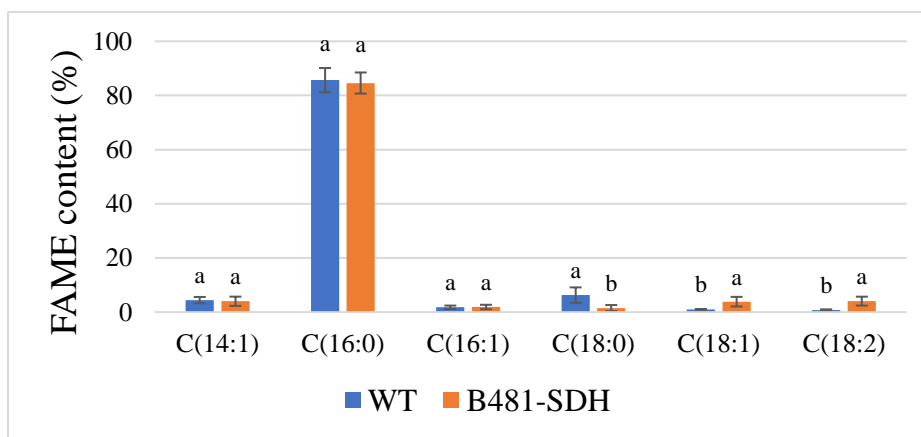


Figure 36 Comparison of fatty acid methyl ester (FAME) composition in *Fremyella diplosiphon* wild type (WT) and halotolerant transformant (B481-SDH) total lipids subjected to direct transesterification.

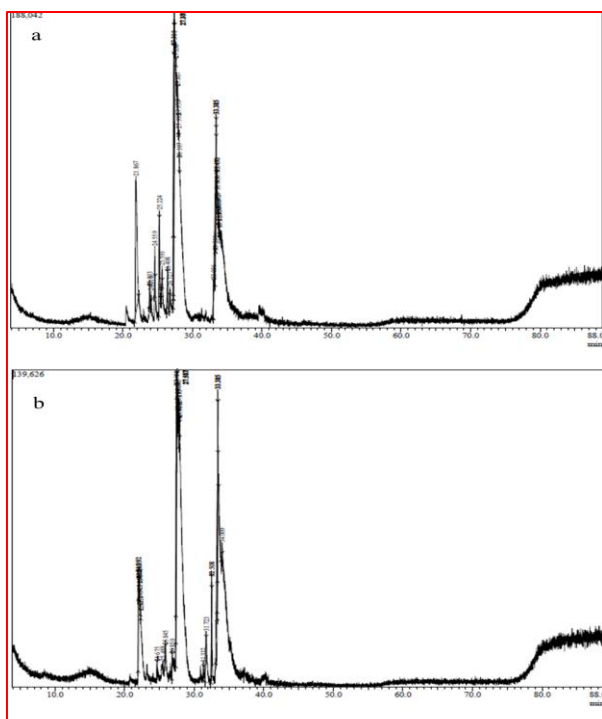


Figure 37 Representative one-dimensional gas chromatogram of *Fremyella diplosiphon* strains (a) wild type (WT-B481) and (b) halotolerant transformant B481-SDH total lipids subjected to direct transesterification.

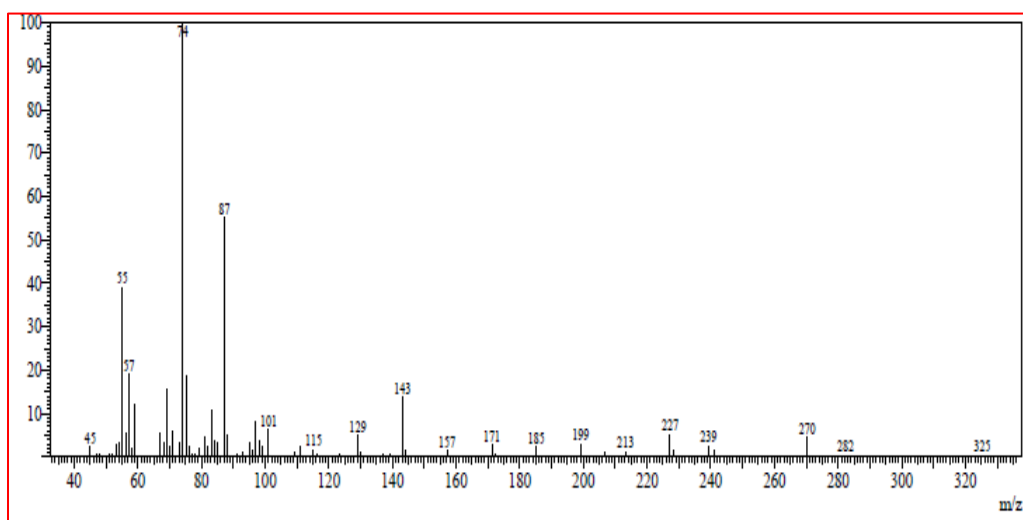


Figure 38 Representative mass spectra of methyl palmitate (C16:0) in *Fremyella diplosiphon* halotolerant transformant (B481-SDH) extracted total lipids when subjected to direct transesterification.

To evaluate the potential of the halotolerant strain as an ideal biofuel agent, different theoretical chemical and physical properties were identified. Calculation of these properties revealed a product with high cetane number (71.750 for WT and 69.695 for B481-SDH). Oxidative stabilities were determined to be 160.613 h for WT and 31.442 h for B481-SDH, which are higher than fuel standards (Masera and Hossain, 2017). In addition, we calculated values including density (0.827 g/cm^3 for WT and 0.832 g/cm^3 for B481-SDH), viscosity ($3.650 \text{ mm}^2/\text{s}$ for WT and $3.614 \text{ mm}^2/\text{s}$ for B481-SDH), and iodine ($4.074 \text{ g I}_2/100 \text{ g}$ for WT and $12.879 \text{ g I}_2/100 \text{ g}$ for B481-SDH) (Table 8 and Figure 39). These findings indicate that the characteristics of WT and B481-SDH-derived biofuel for cetane number are considerably higher than minimum acceptable fuel standards. In addition, other biofuel properties such as iodine value, density, and viscosity were detected to be higher than the acceptable range for both fuel standards. These findings indicate the ability of the halotolerant strain as a source for efficient biofuel production which can further reduce our dependence on petroleum-based fuels.

Biodiesel Properties	WT	B481-SDH
Saponification Value (mg KOH/g fat)	207.006	207.750
Iodine Value (g I ₂ /100 g)	4.074	12.789
Cetane number	71.750	69.695
Long Chain Saturated Factor	11.720	9.216
Cold Filter Plugging Point (°C)	20.345	12.477
Cloud Point (°C)	40.071	39.502
Pour Point (°C)	36.679	36.060
Allylic Position Equivalent	2.509	12.043
Bis-Allylic Position Equivalent	0.746	4.087
Oxidation Stability (h)	160.613	31.442
Higher Heating Value (mJ/kg)	37.495	37.643
Kinematic Viscosity (mm ² /s)	3.650	3.614
Density (g/cm ³)	0.827	0.832

Table 8 Theoretical biodiesel properties of *Fremyella diplosiphon* wild type (WT) and halotolerant transformant (B481-SDH) transesterified lipids.

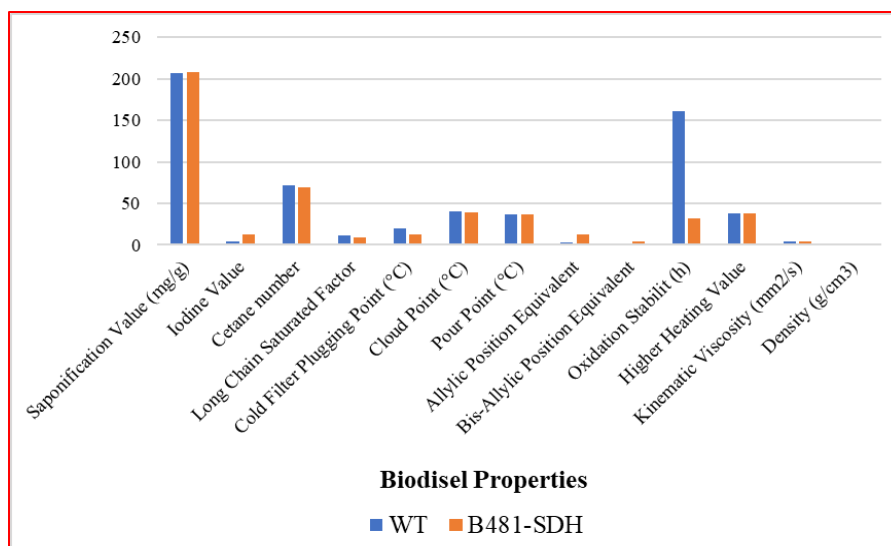


Figure 39 Theoretical biodiesel properties of *Fremyella diplosiphon* wild type (WT) and halotolerant transformant (B481-SDH) transesterified lipids.

4.1.3.5 Growth of the wild-type and halotolerant transformant strains in sea water

Halotolerance of the *F. diplosiphon* B481-SDH strain was tested by growing the strain in sea water at a salinity of 37.1 g L⁻¹ NaCl. The halotolerant transformant exhibited significantly higher ($P \leq 0.05$) growth compared to the wild type (Figure 40). The growth of WT gradually declined after day 6 while, the halotolerant transformant thrived and achieved peak growth on day 9 (Figure 40). The ability of the halotolerant strain to thrive in naturally available sea water makes this strain preferable for large-scale biofuel production. In a previous effort in our laboratory, significant increases were observed in growth of the halotolerant *hlyB*- and *mdh*-expressing transformants when grown in sea water salinity conditions.

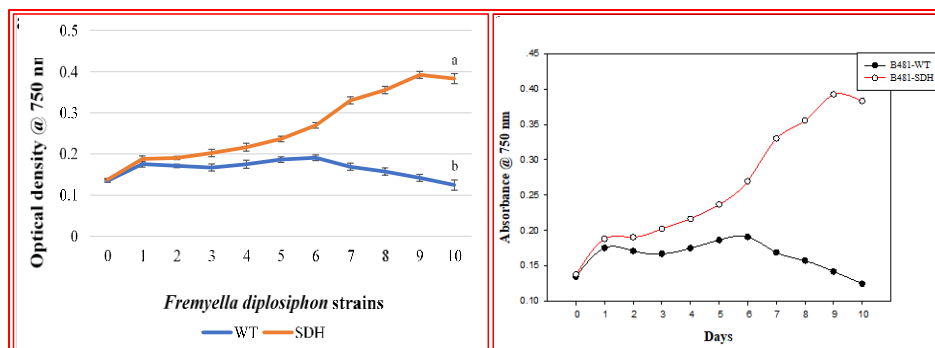


Figure 40 Growth of WT and halotolerant transformant (B481-SDH) strains in sea water containing 37.1 g L⁻¹ sodium chloride (NaCl).

4.1.3.6 Growth of the wild-type and halotolerant transformant strains in sea water and brackish water amended with BG11 media

The *F. diplosiphon* WT and halotolerant transformant (B481-SDH) strains were grown in sea water and brackish water containing 37.1 g L⁻¹ and 9 g L⁻¹ NaCl respectively. As a start-up for culture growth, brackish and sea-water were amended with 6% BG11 /HEPES media as described previously (Tabatabai et al., 2017-b). Results of the study revealed a significant increase ($P \leq 0.05$) in growth of B481-SDH compared to wild type in both marine (sea water) and brackish waters (Figure 41 and 42). In addition, *F. diplosiphon* WT and halotolerant transformant cultures grew for nine days. These findings suggest that sea/brackish waters contain nutrients required for cyanobacterial cultivation; however, addition of 6% BG11 media enhanced its growth. In a previous study, comparison of salinity tolerance of the cyanobacterial strains *Anabaena aphanizomenoides* and *Cylindrospermopsis* in the Baltic Sea revealed that *Anabaena* grew up to 15 g L⁻¹ NaCl, however, its growth was inhibited at 20 g L⁻¹ salinity (Moisander et al., 2002). The upper

limit for salinity tolerance of *Cylindrospermopsis* was 4 g L⁻¹ NaCl. In our study, overexpression of the sterol desaturase gene resulted in enhanced salinity tolerance in which B481-SD and B481-SDH were capable of growth in salinity levels of up to 40 g L⁻¹. This is an advantage since the strain can be cultivated in freely available brackish waters.

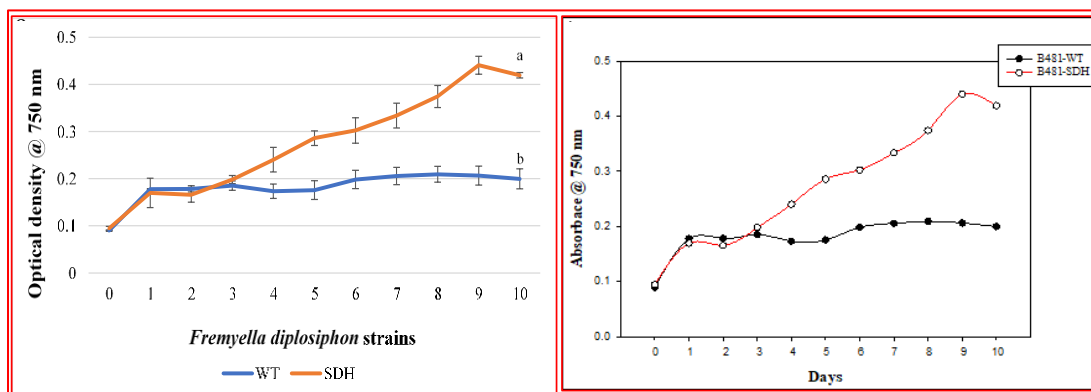


Figure 41 Growth of WT and halotolerant transformant (B481-SDH) in sea water which contained 37.1 g L⁻¹ sodium chloride (NaCl) amended with 6% BG11 /HEPES media.

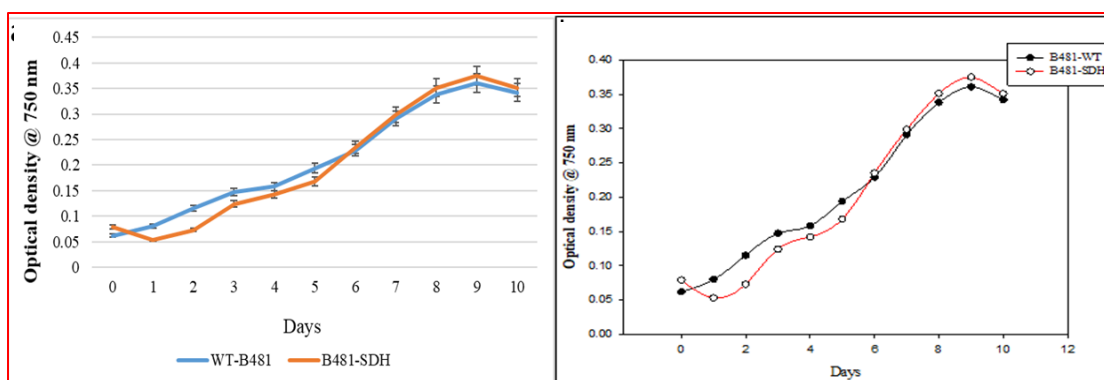


Figure 42 Growth of WT and halotolerant transformant (B481-SDH) in brackish water which contained 9 g L⁻¹ sodium chloride (NaCl) amended with 6% BG11 /HEPES media.

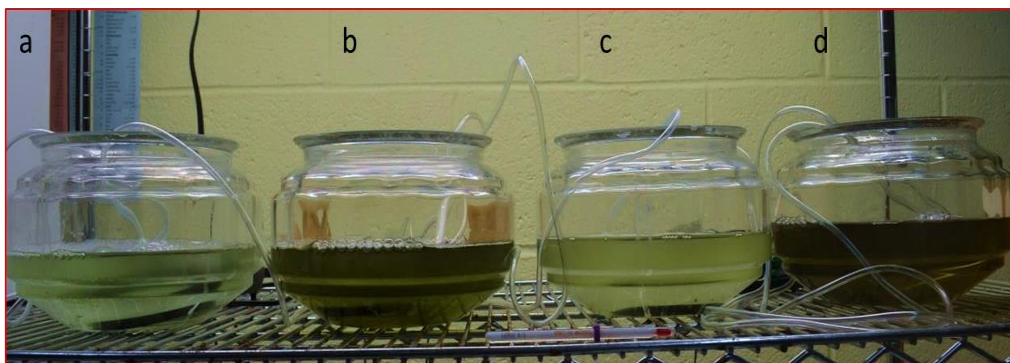


Figure 43 Representative growth of WT and halotolerant transformant (B481-SDH) strains in sea water (a, c respectively) and brackish water (b, d respectively) which contained 37.1 and 9 g L⁻¹ sodium chloride (NaCl) amended with 6% BG11 /HEPES media.

4.1.4 Proteomic comparison of *F. diplosiphon* B481-wild type, B481-SD, and B481-SDH

Protein is one of the major constituents involved in cyanobacterial photosystem I and II activities and encompasses a large fraction of their biomass (Pade and Hagemann, 2014). Comparison of total proteins using SDS-PAGE revealed a single band at the expected size of 48-49 kDa for B481-WT, B481-SD, and B481-SDH (Figure 44). These results indicate the expression of sterol desaturase protein in all *F. diplosiphon* strains. Our results are in accordance with a previous report, where an increase in protein expression level of *Synechocystis* exposed to long-term salt shock was observed (Fulda et al., 2006).

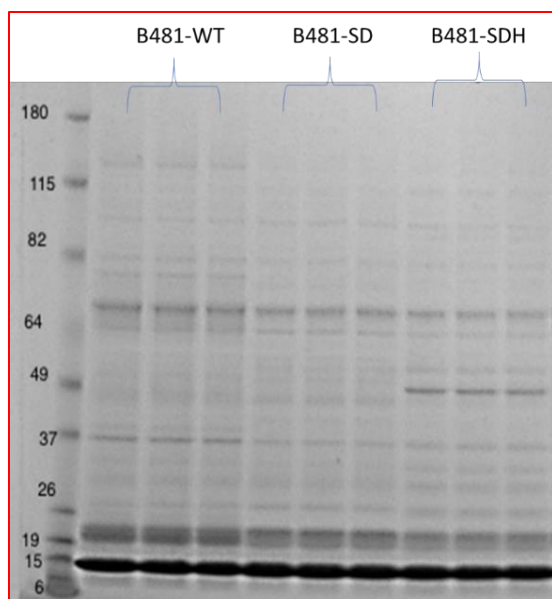


Figure 44 Protein expression in *Fremyella diplosiphon* wild type (B481-WT), transformant (B481-SD), and halotolerant transformant (B481-SDH).

Differential protein expression in the WT, B481-SD transformant, and B481-SDH halotolerant transformant strains revealed bands at the expected sizes on 1D-PAGE, which was further confirmed using 2D-PAGE (Figure 45). The sterol desaturase gene encodes 438 amino acids with a predicted theoretical isoelectric point (pI) of 7.15 and molecular weight (MW) of 48582.19 Da (ExPASy data base). Based on pI and MW, we identified four candidate spots representing sterol desaturase in the expected region. In addition, these spots were overexpressed in transformants SD and SDH when compared to WT-B481. These findings indicate that overexpression of the SD gene and exposure to salinity stress resulted in alteration of *F. diplosiphon*. In a recent study at our laboratory, Tabatabai et al., (2017-b) reported an up-regulation *F. diplosiphon* proteins in a heat mutant strain (Fd33) when exposed to 10 g L^{-1} NaCl. In another study, Singh et al., (2013) reported a transcript encoding protein similar to glycine-betaine transport system in *F. diplosiphon* exposed to 200 mM sodium chloride.

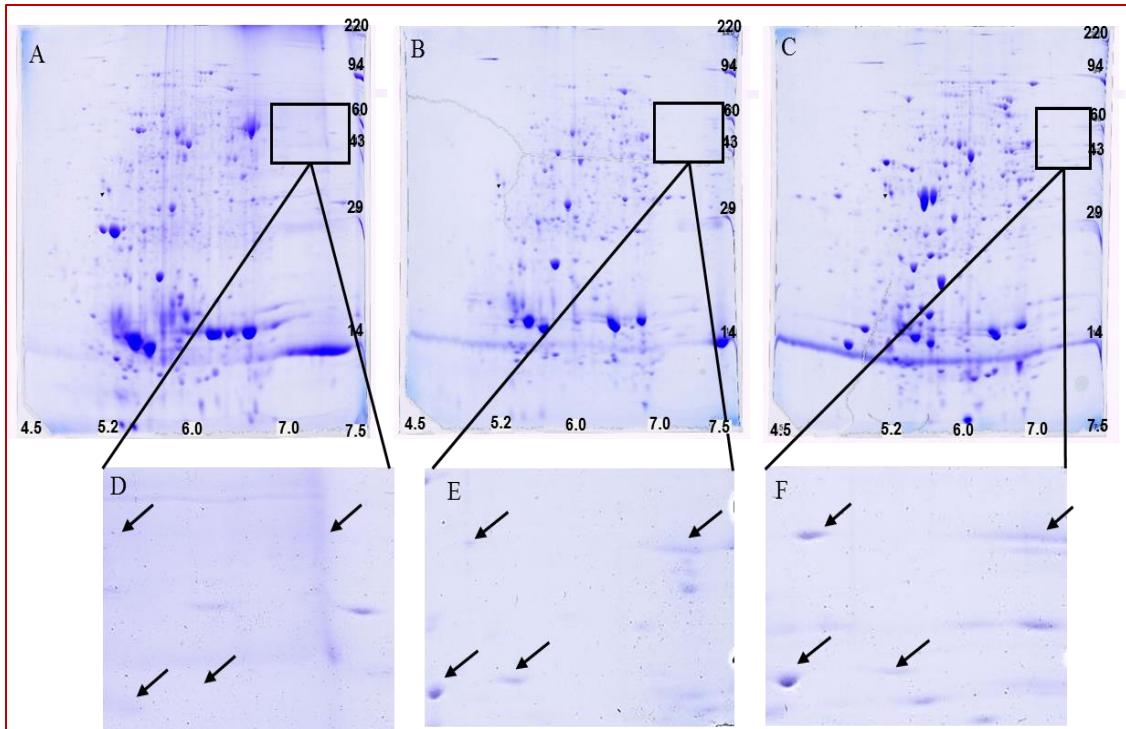


Figure 45 Two-dimensional polyacrylamide gel electrophoresis (2D-PAGE) of *Fremyella diplosiphon* wild type-B481 (A and D), B481-SD transformant (B and E), and halotolerant transformant (C and F).

4.2 ENHANCEMENT OF LIPIDS AND FATTY ACIDS IN *F. DIPLOSIPHON* USING IRON NANOPARTICLES

4.2.1 Impact of iron nanoparticles (Nanofer 25 and Nanofer 25s) on growth and photosynthetic efficacy of two *F. diplosiphon* strains (B481 and SF33)

4.2.1.1 Effect of iron nanoparticles concentrations ranging from 1.5-600 mg L⁻¹ on *F. diplosiphon* growth

Iron plays an important role as an essential trace element in cyanobacterial cell growth. Thus, nZVIs have been increasingly used to clean up polluted waters, soils and sediments (Padrova et al., 2015). Iron serves as a final acceptor in electron transfer chain and provides the electrons needed to convert NADP⁺ to NADPH which is the primary source of ROS. In another mechanism, H₂O₂ reacts with ferrous iron resulting in the generation of highly reactive hydroxyl radicals which add to the oxidative stress. In cyanobacteria, iron is mediated by ferric uptake regulator (Fur) transcriptional regulator which is the repressor for iron-transport proteins. Under optimal iron levels, Fur acts as a positive regulator of genes encoding iron storage proteins. This reaction which is a defense mechanism against ROS indicates that iron regulation could possibly induce oxidative stress in cyanobacteria (Latifi et al., 2009).

Since application of nZVIs in green technologies can have negative effects due to its toxicity related to ROS activity (Sevcu et al., 2011), determining optimal concentrations of nZVIs which are non-toxic to the *F. diplosiphon* growth was one of our major concerns. Our results revealed no significant increase ($P > 0.05$) in *F. diplosiphon* B481 and SF33 growth when exposed to 5-50 mg L⁻¹ Nanofer 25 and Nanofer 25s. No growth was observed

in *F. diplosiphon* B481 and SF33 exposed to Nanofer 25s ranging from 50-600 mg L⁻¹ and 200-600 mg L⁻¹ and Nanofer 25 ranging from 200-600 mg L⁻¹ and 50-600 mg L⁻¹ respectively. (Figure 46-49), indicating that high nanoparticle concentrations (50-600 mg L⁻¹) could result in cellular death (Figure 50). Since no significant increase in growth ($P>0.05$) was observed in *F. diplosiphon* B481 and SF33 exposed to 5 mg L⁻¹ nZVIs and higher, nZVI concentrations ranging from 0.05 to 3.2 mg L⁻¹ were used in further efforts.

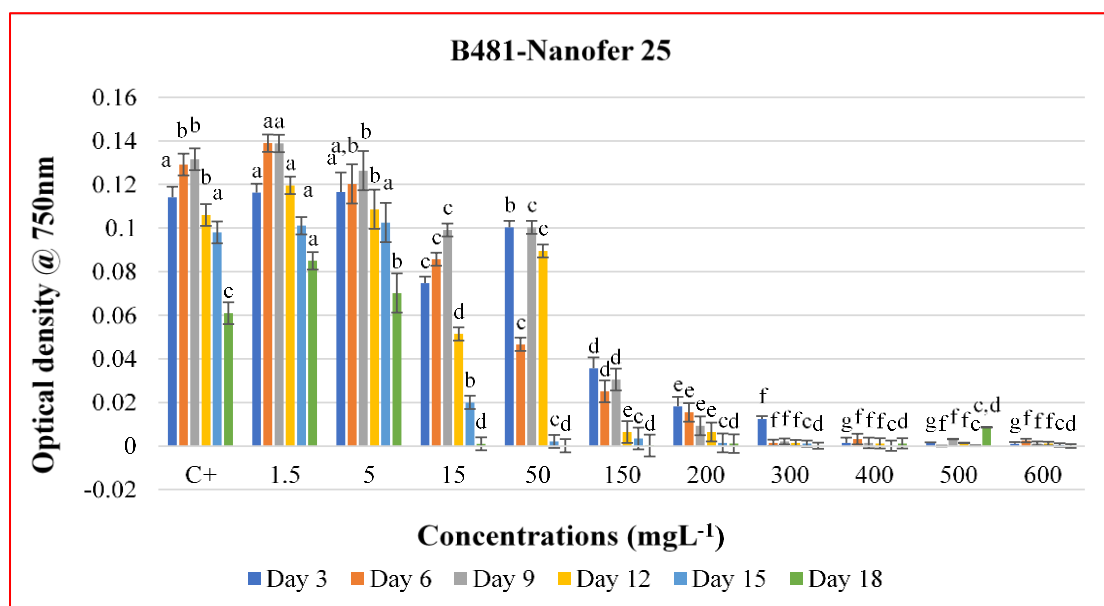


Figure 46 Growth of *Fremyella diplosiphon* B481 strain in BG11/HEPES medium with different concentrations of Nanofer 25 over a period 18 days.

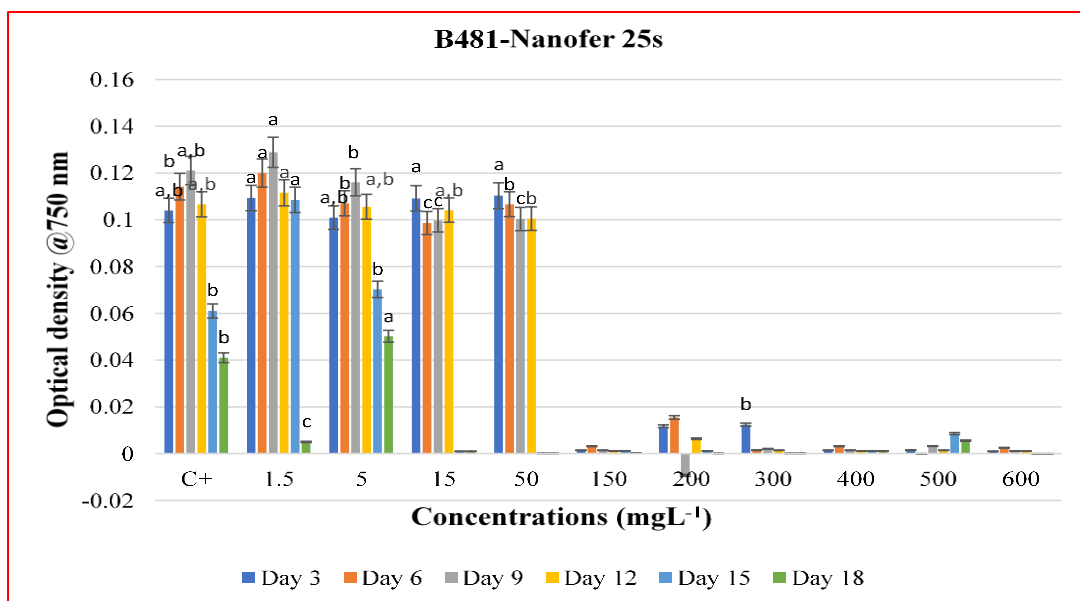


Figure 47 Growth of *Fremyella diplosiphon* B481 strain in BG11/HEPES medium with different concentrations of Nanofer 25s over a period 18 days.

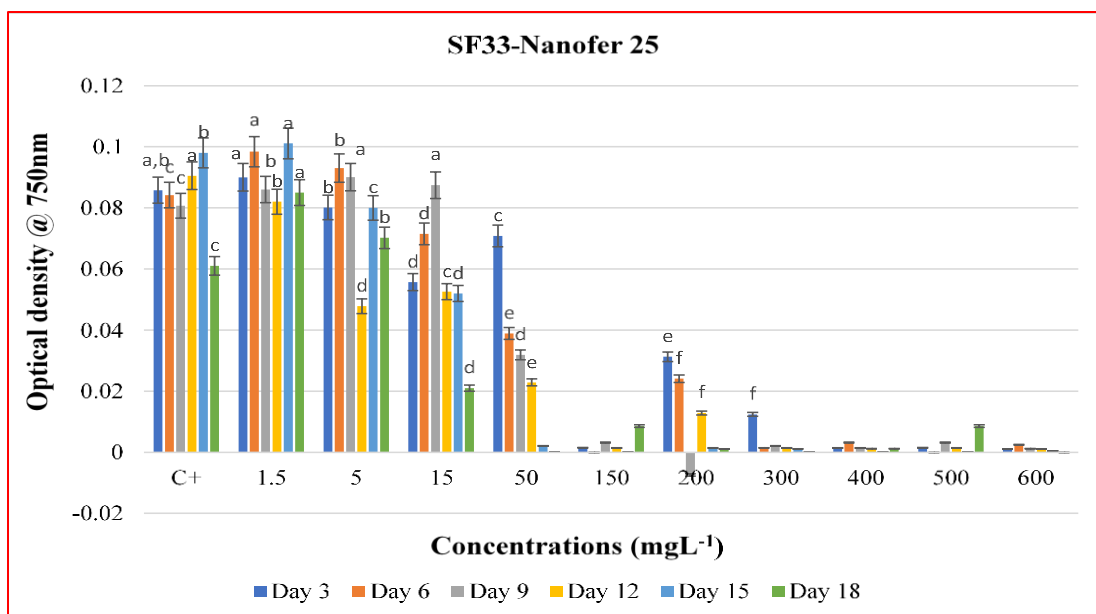


Figure 48 Growth of *Fremyella diplosiphon* SF33 strain in BG11/HEPES medium with different concentrations of Nanofer 25 over a period 18 days.

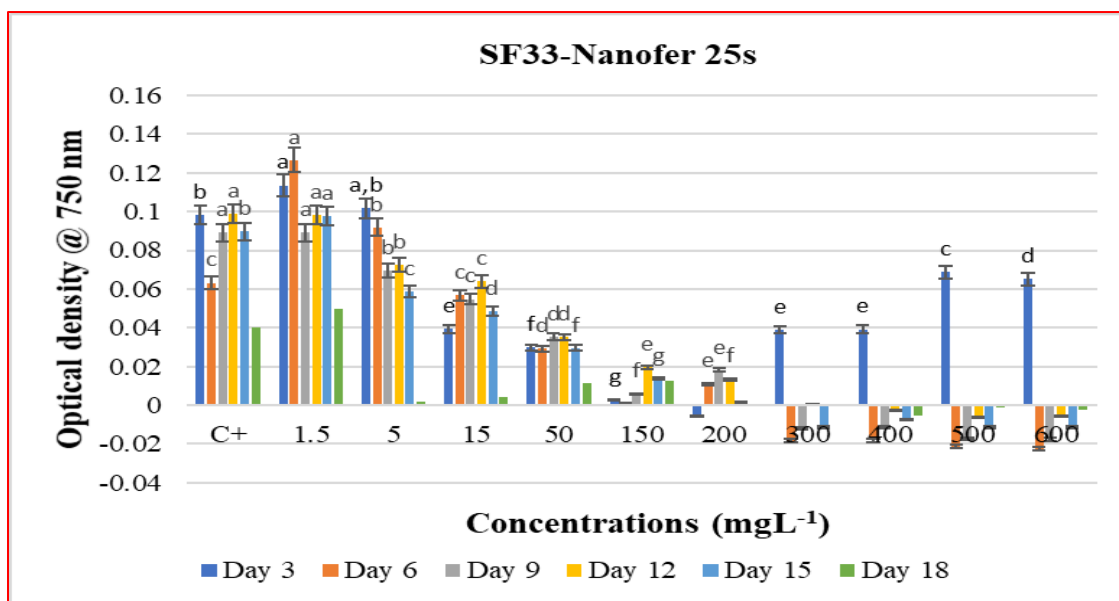


Figure 49 Growth of *Fremyella diplosiphon* SF33 strain in BG11/HEPES medium with different concentrations of Nanofer 25s over a period 18 days.



Figure 50 Representative of *F. diplosiphon* growth in BG11 media amended with different concentrations of nZVIs.

1) Control (60ml cells + 0.5mg Fe-EDTA as an iron source) 2) 60ml cell + 1.5 mg/l NP 3) 60ml cell + 5 mg/l NP 4) 60ml cell + 15 mg/l NP 5) 60ml cell + 50 mg/l NP 6) 60ml cell + 150 mg/l NP 7) 60ml cell + 200 mg/l NP 8) 60ml cell + 300 mg/l NP 9) 60ml cell + 400 mg/l NP 10) 60ml cell + 500 mg/l NP 11) 60ml cell + 600 mg/l NP

4.2.1.2 Effect of iron nanoparticles concentrations ranging from 0.05-3.2 mg L⁻¹ on *F. diplosiphon* growth

The impact of 0.05, 0.1, 0.2, 0.4, 0.8, 1.6, and 3.2 mg L⁻¹ Nanofer 25 and Nanofer 25s, on *F. diplosiphon* growth was investigated. Significant increases in growth of the *F. diplosiphon* SF33 (17.17%, 16.71%, 19.95%, and 13.52%.) and in the B481 strain (27.57%, 27.42%, 25.21% and 22.62%) was observed when they were exposed to Nanofer 25s concentrations ranging from 0.2 to 1.6 mg L⁻¹ at day 9 (growth peak). In addition, no significant differences ($P>0.05$) were observed in nano-treated cultures exposed to various concentrations of Nanofer 25 (Figures 51-55).

Depending on environmental conditions, the nZVI surface rapidly changes over time due to their reactive properties. The key advantage of using nZVIs is their protection from rapid oxidation in the air due to their specific core which contains zero-valent iron covered by a protective shell (Sevcu et al., 2011; Padrova et al., 2015), resulting in a strong oxidation reduction potential. Our results indicate that trace concentrations of nZVIs provide a suitable source of iron required for *F. diplosiphon* growth. The significant increase ($P\leq 0.05$) in growth of *F. diplosiphon* exposed to concentrations ranging from 0.2 to 1.6 mg L⁻¹ Nanofer 25s suggest improved adsorption of this nanoparticle to cyanobacterial outer cell membranes leading to enhanced membrane permeability. This resulted in more robust nZVI-*F. diplosiphon* interactions. Since Nanofer 25 is unmodified, no significant increase ($P>0.05$) in growth was observed, suggesting that this activity could have been lost when exposed to air. Similar results have been reported by Kirschling et al., (2010) where coated iron nanoparticles stimulated *Escherichia coli* growth in different

trichloroethylene contaminated sites. Since *F. diplosiphon* SF33 and B481 strains exposed to different concentrations of Nanofer 25s exhibited significant increases ($p \leq 0.05$) in growth, this nZVI type was chosen for use in further experiments.

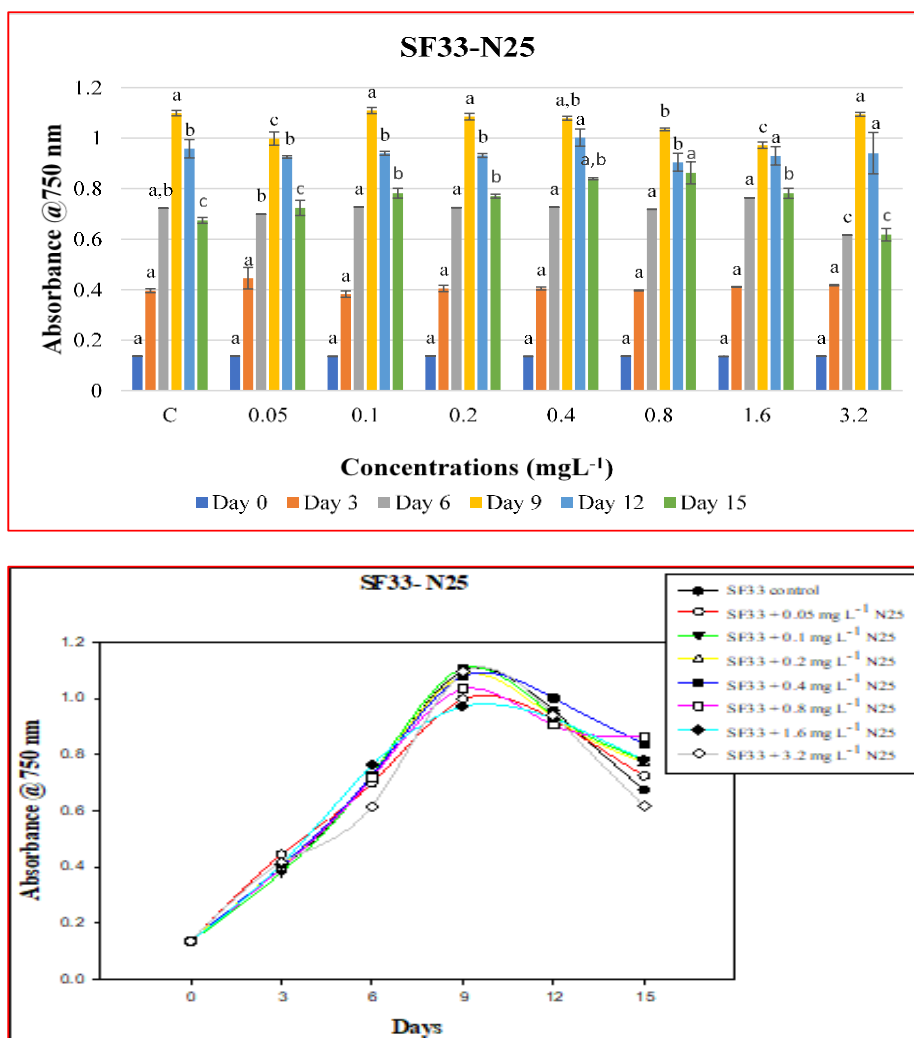


Figure 51 Growth of *Fremyella diplosiphon* SF33 strain in BG11/HEPES medium with different concentrations of Nanofer 25 over a period 15 days.

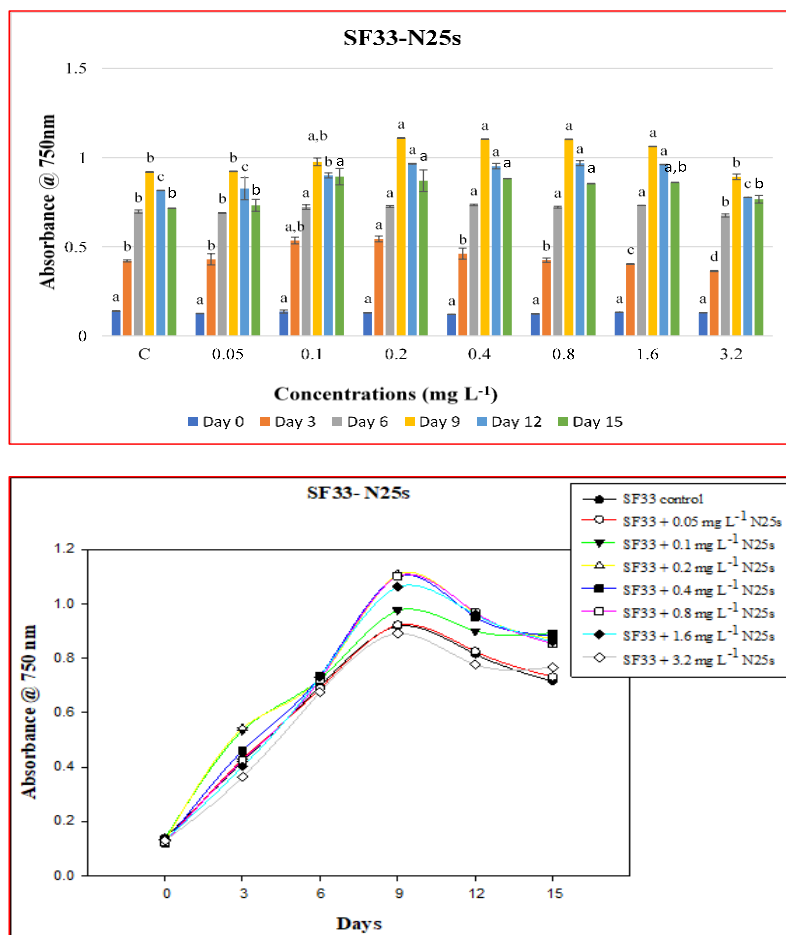


Figure 52 Growth of *Fremyella diplosiphon* SF33 strain in BG11/HEPES medium with different concentrations of Nanofer 25s over a period 15 days.

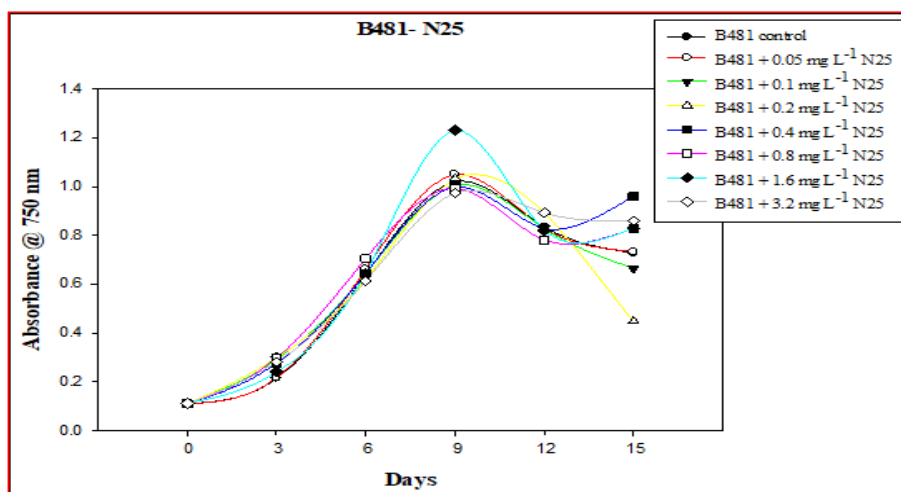
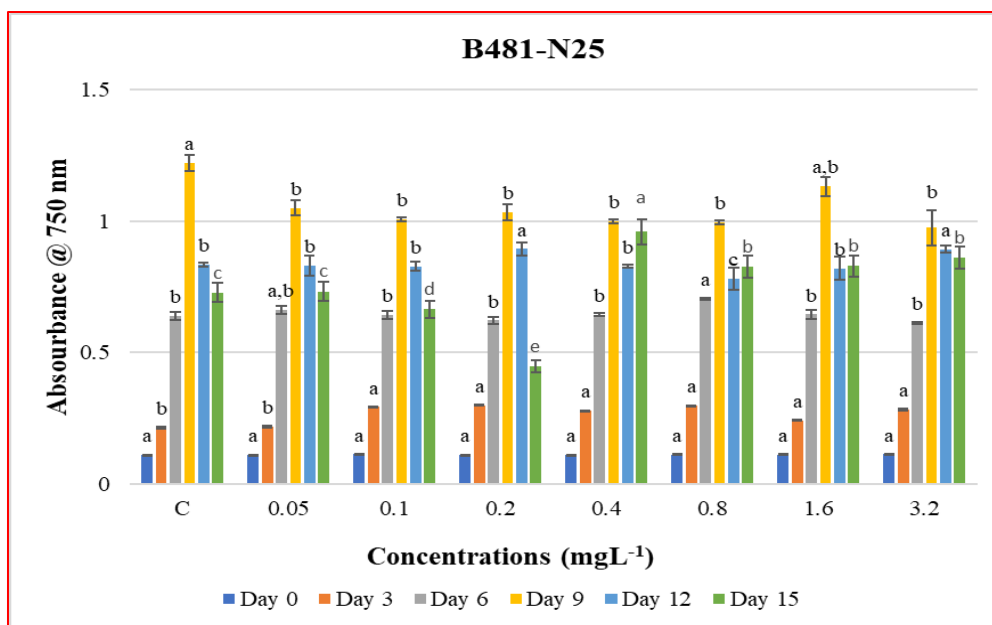


Figure 53 Growth of *Fremyella diplosiphon* B481 strain in BG11/HEPES medium with different concentrations of Nanofer 25 over a period 15 days.

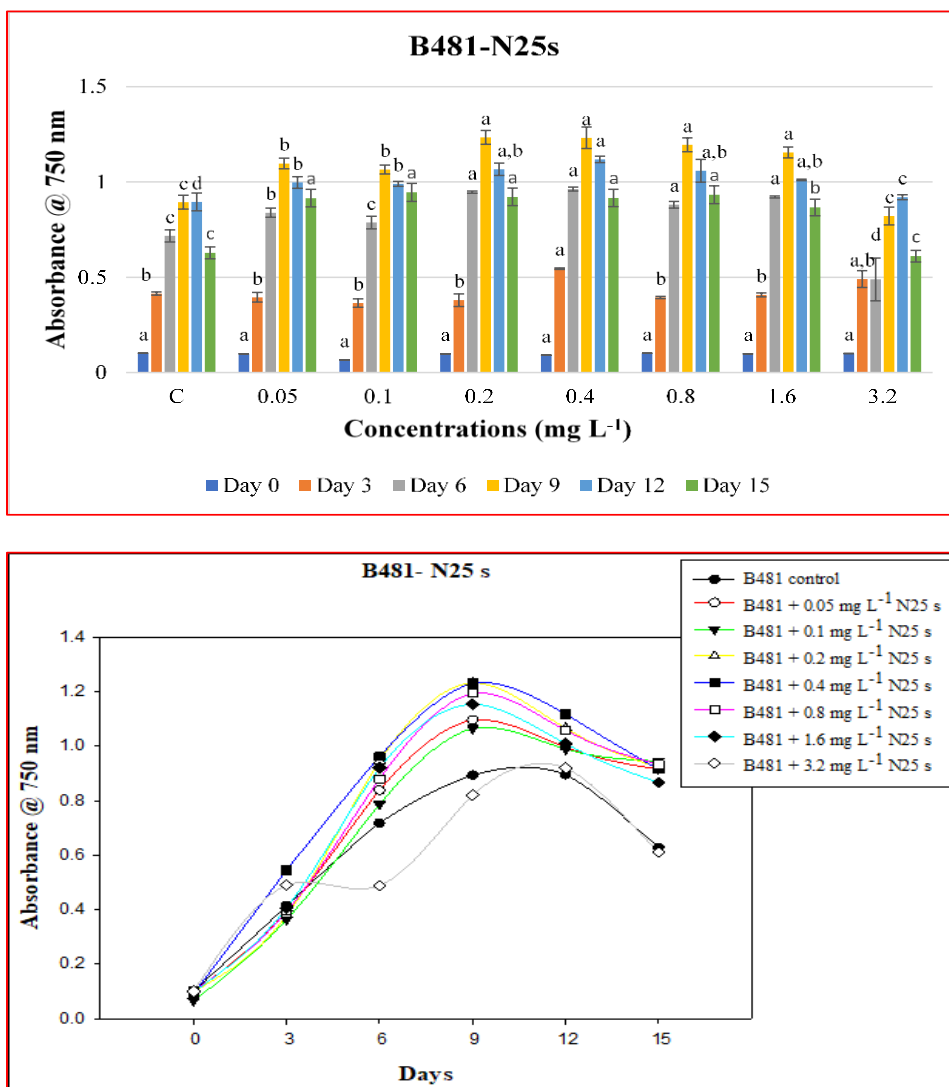
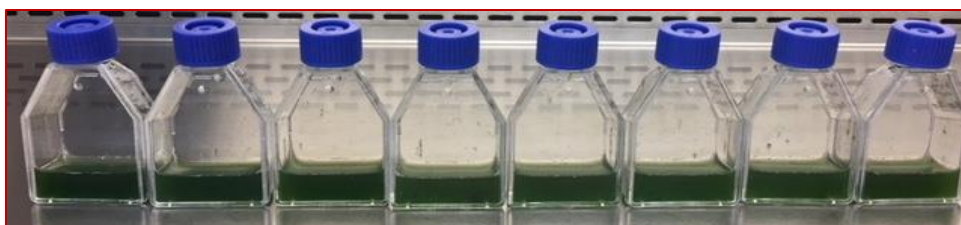


Figure 54 Growth of *Fremyella diplosiphon* B481 strain in BG11/HEPES medium with different concentrations of Nanofer 25s over a period 15 days.



Control 0.05mg/L 0.1mg/L 0.2mg/L 0.4mg/L 0.8mg/L 1.6mg/L 3.2mg/L

Figure 55 Representative samples of *F. diplosiphon* growth in BG11 media amended with different concentrations of nZVIs.

4.2.2 Effect of Nanofer 25s on *F. diplosiphon* photosynthetic efficacy

Since high concentrations of nanoparticles could be detrimental to cyanobacterial photosynthetic capacity (Ko et al., 2018), pigment accumulation in nano-treated cells was investigated. A 2.35%, 9.92%, and 6.69% increase in SF33 and a 5.58%, 12.30%, and 11.73% in B481 *chl a* levels, respectively, was observed when exposed to 0.4, 0.8, and 1.6 mg L⁻¹ Nanofer 25s (Figure 56). In addition, a 6.59%, 10.40%, and 14.09% increase in carotenoid levels in SF33, and 3.5%, 10.20%, and 7.50% increase in B481, respectively, when exposed to 0.4, 0.8, and 1.6 mg L⁻¹ Nanofer 25s was observed. However, increase in *chl a* and carotenoid levels of nano-treated cultures were not significant (Figure 57). These findings suggest that trace concentrations of iron nanoparticles can enhance photosynthetic activity. Our results are in accordance with Ko et al., (2018) who identified 38% and 30% increase in *chl a* content of *Chlorella vulgaris* when exposed to 5 mg L⁻¹ ZnO and 100 mg L⁻¹ Fe₂O₃ nanoparticles respectively. However, Vadivel et al., (2012) reported a slight decrease in *chl a* content of *Anabaena sp.* when exposed to 25% iron nanoparticles.

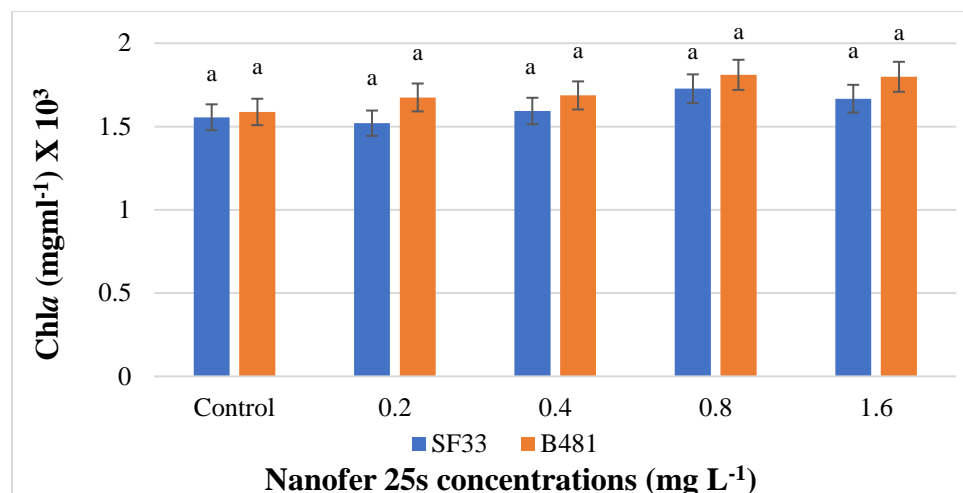


Figure 56 Impact of different concentrations of Nanofer 25s on chlorophyll *a* (chl_a) accumulation in *Fremyella diplosiphon* strains (SF33 and B481).

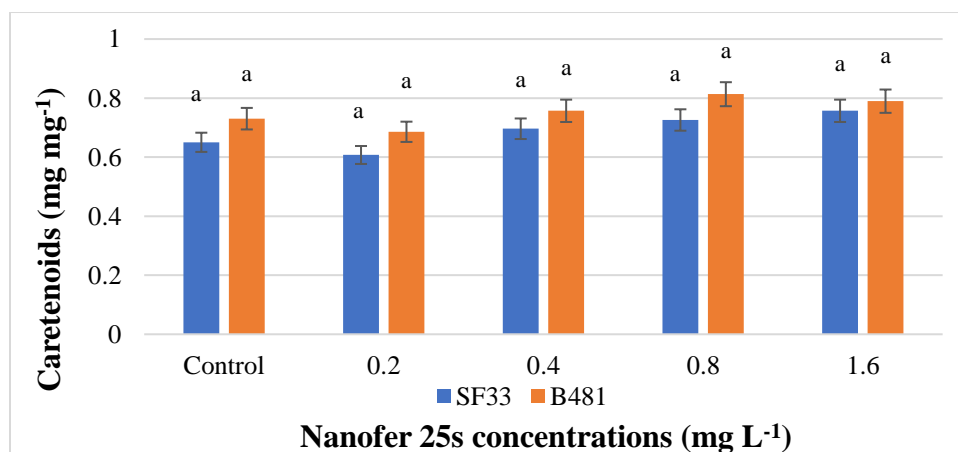


Figure 57 Impact of different concentrations of Nanofer 25s on carotenoid accumulation in *Fremyella diplosiphon* strains (SF33 and B481).

We identified 6.88%, 4.95%, and 10.45% increases in phycocyanin (PC) levels in SF33, and 18.32%, 18.61%, and 14.36% in B481 when exposed to 0.4, 0.8, and 1.6 mg L⁻¹ Nanofer 25s, respectively, relative to their control (Figure 58). Our results also revealed, 0.78%, 11.87%, and 13.90% increases in allophycocyanin (AP) levels in SF33 and 7.73%, 4.54%, and 10.04% in B481 when exposed to 0.4, 0.8, and 1.6 mg L⁻¹ Nanofer 25s respectively (Figure 59). In addition, we observed 2.39%, 14.97%, and 9.04% increases in phycoerythrin (PE) levels in SF33 and 6.81%, 7.99%, and 0.44% increases in B481 when exposed to 0.4, 0.8, and 1.6 mg L⁻¹ Nanofer 25s (Figure 60). Increase in phycobiliprotein (PC, AP, and PE) levels suggest that pigment accumulation is directly affected by iron stress since they are quantified as a function of *chl a*. These findings indicate that Nanofer 25s enhances photosynthetic efficacy in *F. diplosiphon*. In a previous study, no significant differences ($P>0.05$) in carotenoid content of the microalgae *Arthrospira platensis* was observed when exposed to 10 mg L⁻¹ Fe⁺² (Akbarnezhad et al., 2016). However, an increase in Fe⁺² concentration (up to 10 mg L⁻¹) resulted in reduced phycobiliprotein levels. Similar studies were reported by Tabatabai et al., (2019) where no significant differences were observed in *F. diplosiphon* phycobiloprotein accumulation when exposed to 20, 100, and 200 nm gold nanoparticles.

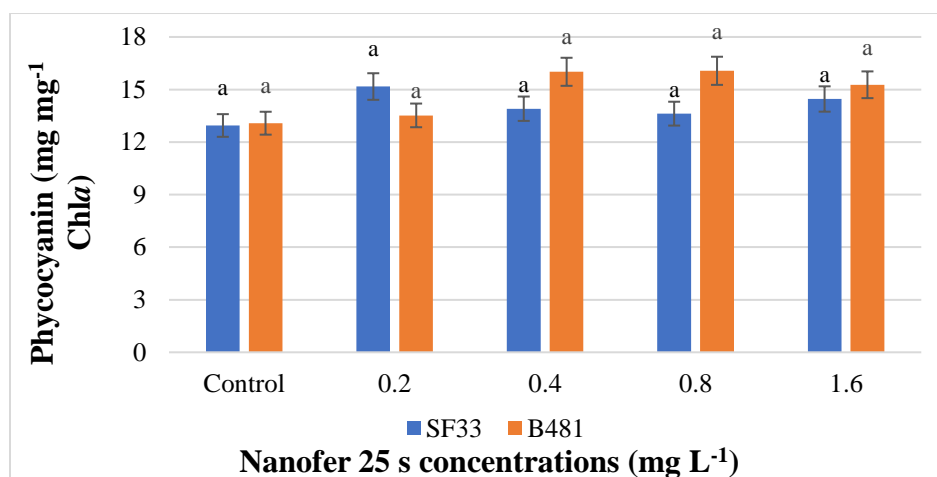


Figure 58 Impact of different concentrations of Nanofer 25s on phycocyanin (PC) accumulation in *Fremyella diplosiphon* strains (SF33 and B481). means ($P \geq 0.05$).

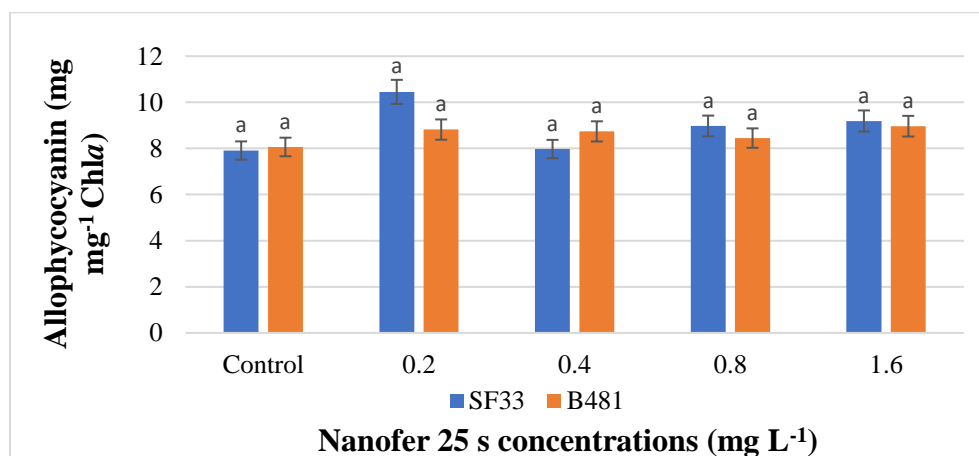


Figure 59 Impact of different concentrations of Nanofer 25s on allophycocyanin (AP) accumulation in *Fremyella diplosiphon* strains (SF33 and B481).

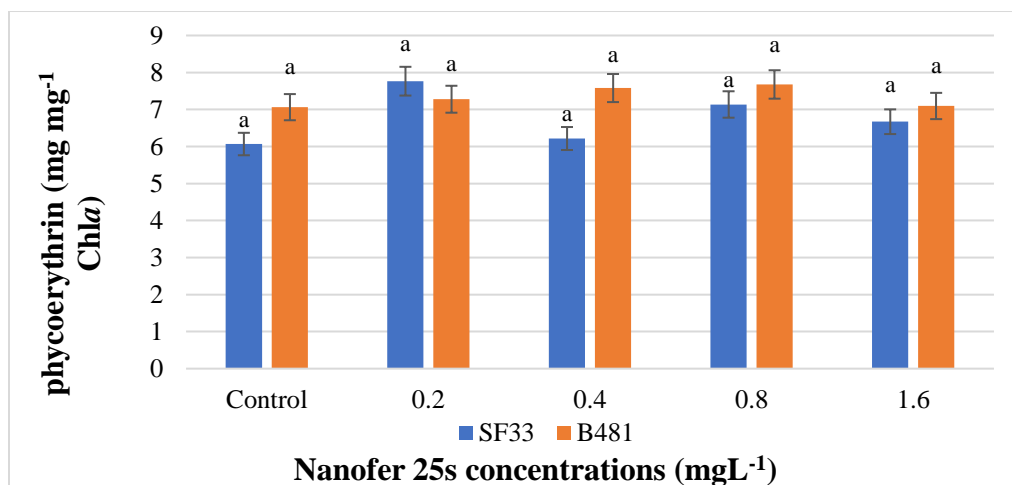


Figure 60 Impact of different concentrations of Nanofer 25s on phycoerythrin (PE) accumulation in *Fremyella diplosiphon* strains (SF33 and B481).

4.2.3 Enhancement of total lipid content in *F. diplosiphon* Nanofer 25s-treated cells

Iron is one of the major elements for cyanobacterial growth, which influences essential processes such as photosynthesis and respiration (Nozzi et al., 2013; Padrova et al., 2015). Iron stress leads in an elevated ROS level, followed by increasing oxidative stress in cyanobacterial cells resulting in lipid production. Our results revealed significant increases ($P \leq 0.05$) in total lipid yield of *F. diplosiphon* B481 (19.02%, 29.29%, and 44.51%) when exposed to 0.4, 0.8, and 1.6 mg L⁻¹ Nanofer 25s compared to the control. In addition, significant increases ($P \leq 0.05$) were observed in SF33 total lipid content (28.13%, 48.2%, 58.45%, and 49.75%) when exposed to Nanofer 25s ranging from 0.2 to 1.6 mg L⁻¹. However, no significant increases in total lipid content of *F. diplosiphon* B481 strain was observed when exposed to 0.2 mg L⁻¹ Nanofer 25s (Figure 61). In addition, we detected

22.57%, 7.04%, 0.02%, and 18.29% higher lipid content in *F. diplosiphon* B481 cultivated with 0, 0.2, 0.8, and 1.6 mg L⁻¹ Nanofer 25s respectively compared to SF33 in similar concentrations. Significant increases in total lipid content of *F. diplosiphon* SF33 cultivated in 0.2, 0.4, 0.8, and 1.6 mg L⁻¹, and B481 in 0.4, 0.8, and 1.6 mg L⁻¹ Nanofer 25s, respectively, suggest that Nanofer 25s-catalyzed NADP (H)-dependent reactions which are primary source of ROS, could have resulted in lipid augmentation. In a previous study, an increase in total lipid content of 26.2-35% was reported when *Trachydiscus minutus* was exposed to 5.1 mg L⁻¹ nZVIs (Padrova et al., 2015). In addition, maximal lipid content was reported in *Chlorella vulgaris* exposed to 0.1 g L⁻¹ of TiO₂ nanoparticles due to increased reactive oxidative stress (Kang et al., 2014). These findings suggest that enhanced lipid accumulation in cyanobacteria/microalgae cultivated with iron or titanium could be related to oxidative stress induced by exposure to nanoparticles.

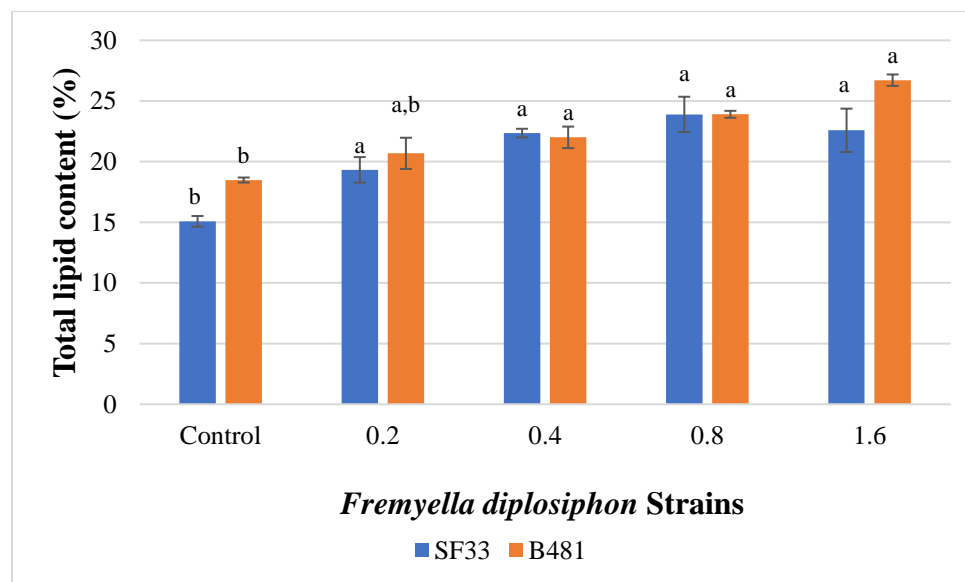


Figure 61 Comparison of total lipid content in *Fremyella diplosiphon* SF33 and B481 strains (control) and cultures amended with different concentrations of Nanofer 25s.

4.2.4 Comparison of fatty acid methyl ester profile in *F. diplosiphon* wild-type and Nanofer 25s-treated cells via direct transesterification and GC-MS

Quantification of total lipid content provides important information on the capability of the organism for their production; however, it is not determinative for biodiesel potential since this includes all cellular lipids. Thus, it is critical to evaluate FAME composition of *F. diplosiphon* transesterified lipids as well as calculate their corresponding physical and chemical properties to gain more comprehensive understanding of its capacity as a biofuel agent.

We identified both saturated and unsaturated FAMES from SF33 and B481 transesterified lipids (Figure 62 and 63; Table 9 and 10). Our results revealed that methyl palmitate was the dominant FAME in *F. diplosiphon* B481 and SF33 controls and nano-

treated cultures (Figure 64). In *F. diplosiphon* SF33, methyl palmitate accounted for 82.55%, 59.67%, 56.64%, 69.69%, and 49.05% of total FAMES produced from overall lipid content of strain treated with 0, 0.2, 0.4, 0.8, and 1.6 mg L⁻¹ Nanofer 25s respectively. This component accounted for 66.00%, 61.43%, 57.87%, 55.42%, and 60.95% of total FAME in B481 treated with similar nZVI concentrations (Figure 62-64). In a previous study, a 57% increase in *Scenedesmus obliquus* saturated FAs was identified when exposed to 20 mg L⁻¹ iron (El Baky et al., 2012).

In addition, we have detected other FAME components such as methyl tetradecanoate (C14:1), methyl hexadecenoate (C16:1), methyl octadecanoate (C18:0), methyl octadecenoate (C18:1), and methyl octadecadienoate (C18:2) in all *F. diplosiphon* cultures (Table 11 and 12). We observed significant increases ($P \leq 0.05$) in methyl octadecenoate (C18:1), and methyl octadecadienoate (C18:2) levels from SF33 treated with 0.4, 0.8, and 1.6 mg L⁻¹ Nanofer 25s transesterified lipids compared with control, while no significant differences ($P > 0.05$) were exhibited in cultures treated with 0.2 mg L⁻¹ transesterified lipids relative to the control (Figure 62 and 63). These findings suggest that Nanofer 25s enhanced unsaturated FAMES which are primary components in biofuel.

Under oxidative stress, free radicals affect cyanobacterial cellular and physiological functions resulting in cell damage. Unsaturated FAs have a radical scavenging potential that contributes to cell protection against augmented ROS concentration (Adarme-Vega et al., 2014). This leads to increased unsaturated FAs in *F. diplosiphon* cells, which could be a cellular response to oxidative stress induced by ROS and may play a critical role in protection mechanism. Our study is the first to report the use of iron nanoparticles to

enhance total lipid content and essential FAs in *F. diplosiphon*. These results suggest that Nanofer 25s could be an ideal nZVI to enhance biodiesel production capacity of *F. diplosiphon*. A Provisional Patent Application (No. 62778617) describing application of iron nanoparticles to enhance total lipid content and essential unsaturated FAs has been filed (Sittler and Gharaie Fathabad, 2018).

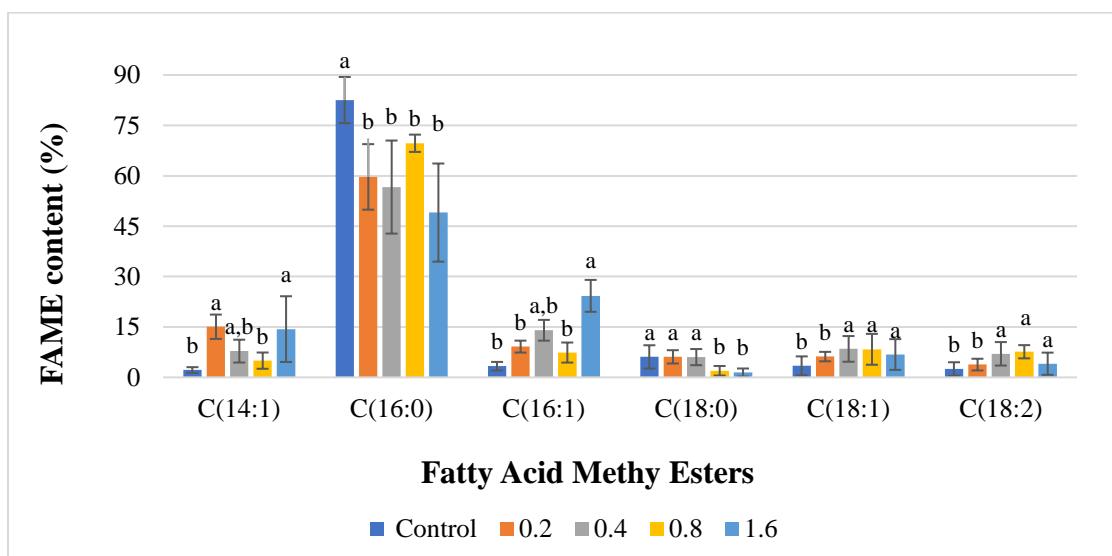


Figure 62 Comparison of fatty acid methyl ester (FAME) composition of *Fremyella diplosiphon* SF33 strain total lipids subjected to direct transesterification.

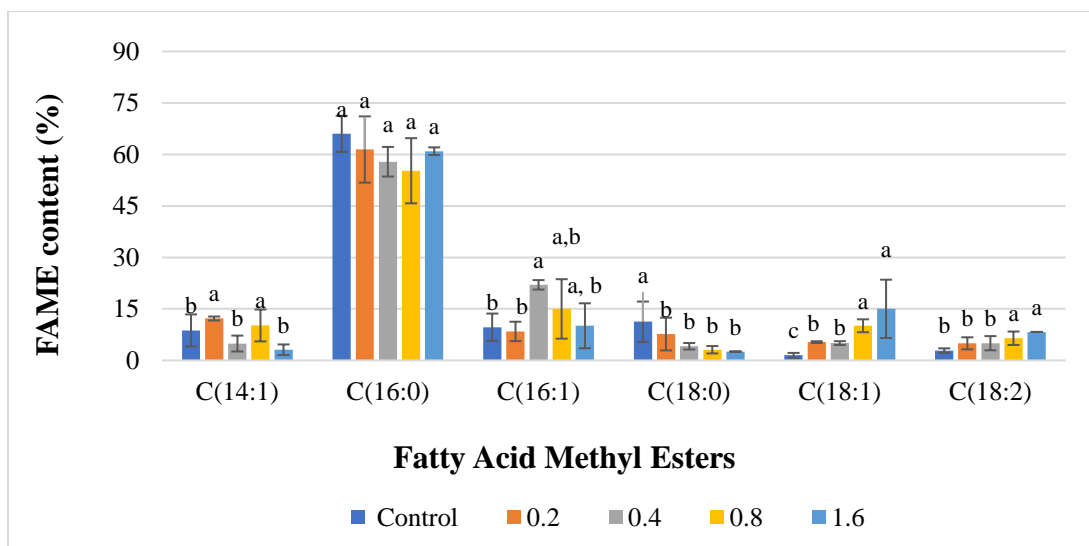


Figure 63 Comparison of fatty acid methyl ester (FAME) composition of *Fremyella diplosiphon* B481 strain total lipids subjected to direct transesterification.

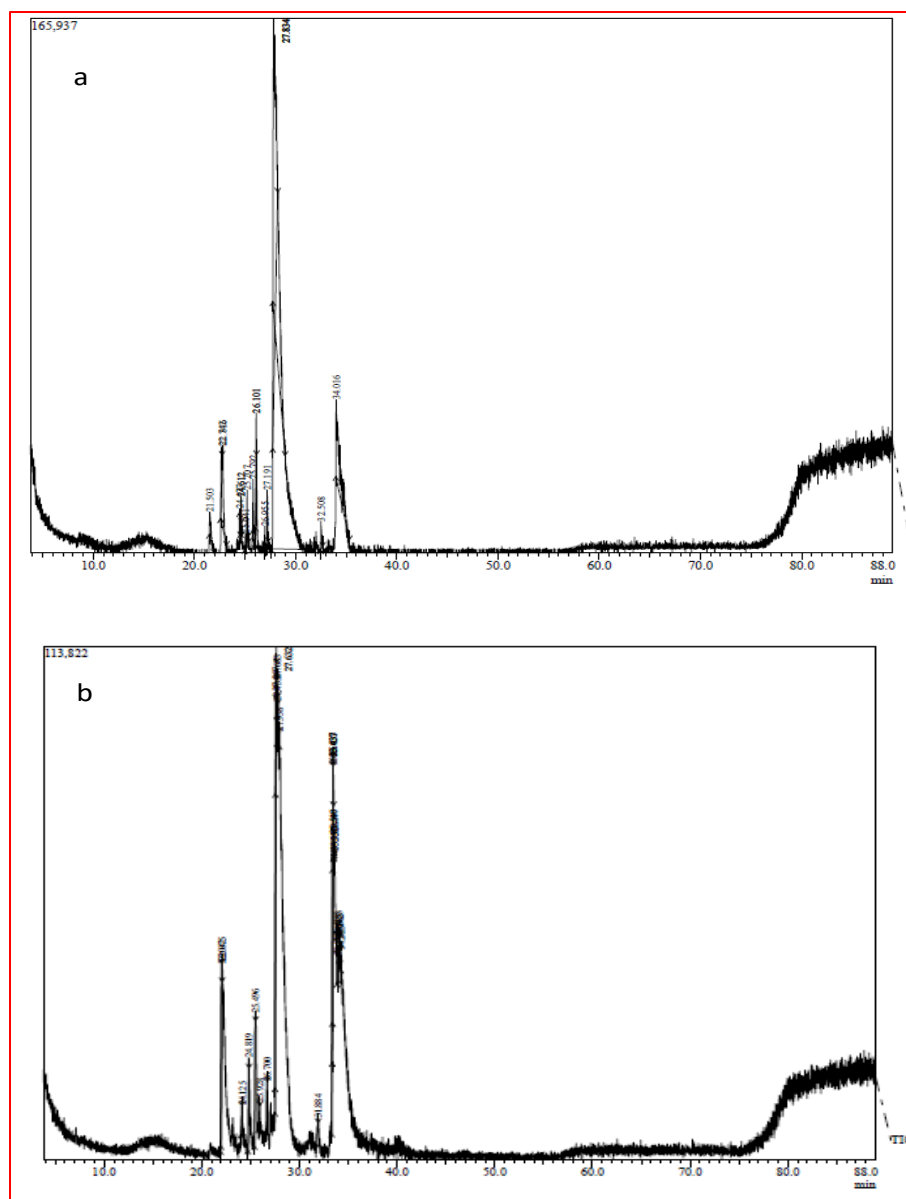


Figure 64 Representative one dimensional gas chromatogram of *Fremyella diplosiphon* strains SF33 (a) control, (b) nanotreated cells (1.6 mg L^{-1} Nanofer 25s) total lipid subjected to direct transesterification.

Strains	FAME Type (%)		Ratio of FAME
	Saturated	Unsaturated	Saturated/ Unsaturated
SF33 control	88.64	11.44	7.75
SF33 + 0.2 mg L ⁻¹ N25s	65.78	34.22	1.92
SF33 + 0.4 mg L ⁻¹ N25s	62.67	37.33	1.68
SF33 + 0.8 mg L ⁻¹ N25s	71.66	28.34	2.53
SF33 + 1.6 mg L ⁻¹ N25s	50.50	49.50	1.02

Table 9 Breakdown of saturated and unsaturated fatty acid methyl ester (FAME) proportions in *Fremyella diplosiphon* SF33.

Strains	FAME Type (%)		Ratio of FAME
	Saturated	Unsaturated	Saturated/ Unsaturated
B481 control	77.27	22.74	3.40
B481 + 0.2 mg L ⁻¹ N25s	69.11	30.95	2.23
B481 + 0.4 mg L ⁻¹ N25s	62.00	36.97	1.68
B481 + 0.8 mg L ⁻¹ N25s	58.35	41.72	1.40
B481 + 1.6 mg L ⁻¹ N25s	63.51	36.50	1.74

Table 10 Breakdown of saturated and unsaturated fatty acid methyl ester (FAME) proportions in *Fremyella diplosiphon* B481.

FAME	C-SF33	0.2 mg L ⁻¹	0.4 mg L ⁻¹	0.8 mg L ⁻¹	1.6 mg L ⁻¹
Methyl myristate (C14:1)	2.19	15.07	7.82	4.98	14.36
Methyl palmitate (C16:0)	82.55	59.67	56.64	69.69	49.05
Methyl hexadecanoate (C16:1)	3.33	9.16	14.02	7.39	24.27
Methyl octadecanoate (C18:0)	6.09	6.11	6.03	1.97	1.45
Methyl octadecenoate (C18:1)	3.44	6.19	8.48	8.35	6.81
Methyl octadecadienoate (C18:2)	2.49	3.80	7.01	7.63	4.06

Table 11 Fatty acid methyl ester (FAME) composition in *Fremyella diplosiphon* SF33.

FAME	C-B481	0.2 mg L ⁻¹	0.4 mg L ⁻¹	0.8 mg L ⁻¹	1.6 mg L ⁻¹
Methyl myristate (C14:1)	8.73	12.20	4.92	10.17	3.10
Methyl palmitate (C16:0)	66.00	61.43	57.87	55.24	60.95
Methyl hexadecanoate (C16:1)	9.66	8.45	22.01	15.00	10.09
Methyl octadecanoate (C18:0)	11.27	7.68	4.13	3.10	2.56
Methyl octadecenoate (C18:1)	1.49	5.32	5.04	10.09	15.02
Methyl octadecadienoate (C18:2)	2.86	4.98	5.01	6.46	8.29

Table 12 Fatty acid methyl ester (FAME) composition in *Fremyella diplosiphon* B481.

Calculation of theoretical chemical and physical biodiesel properties revealed a product with elevated cetane number (62.6–68.81 for SF33 and 63.09-67.74 for B481) and oxidative stability (49.39–18.05 h for SF33 and 43.83-16.82 h for B481). We detected values including density (0.868–0.870 g/cm³ for SF33 and 0.861-0.870 g/cm³ for B481), viscosity (3.508–3.808 mm²/s for SF33 and 3.588-3.759 mm²/s for B481), and iodine (11.56–37.71 g I₂/100 g for SF33 and 16.17-38.60 g I₂/100 g for B481) (Table 13 and 14). These findings indicate that the properties of *F. diplosiphon* control and nano-treated-derived biofuel for cetane number are significantly higher than conventional fuels. In addition, in both controls (SF33 and B481) and nano-treated cells iodine value, density, and viscosity were comparable to the fuels currently in the market, suggesting the ability of the *F. diplosiphon* control and nano-treated strains as a potential source for efficient biofuel production.

Biodiesel Properties	SF33	0.2 mgL⁻¹	0.4 mgL⁻¹	0.8 mgL⁻¹	1.6 mgL⁻¹
Saponification Value	217.314	219.319	216.413	216.344	220.219
Iodine Value (g I ₂ /100 g)	11.564	21.595	34.321	28.708	37.709
Cetane number	68.814	66.327	63.798	65.069	62.6
Long Chain Saturated Factor	10.181	9.022	8.679	7.954	5.63
Cold Filter Plugging Point (°C)	15.509	11.867	10.79	8.512	1.211
Cloud Point (°C)	39.434	26.394	24.801	31.665	20.808
Pour Point (°C)	35.987	21.832	20.101	27.553	15.768
Allylic Position Equivalent	8.66	13.79	22.5	23.61	14.93
Bis-Allylic Position Equivalent	2.52	3.8	7.01	7.63	4.06
Oxidation Stability (h)	49.388	33.625	19.414	18.047	31.637
Higher Heating Value (MJ/kg)	39.244	39.116	39.18	39.199	39.053
Kinematic Viscosity (mm ² /s)	3.808	3.651	3.681	3.718	3.508
Density (g/cm ³)	0.868	0.868	0.87	0.869	0.87

Table 13 Theoretical biodiesel properties of *Fremyella diplosiphon* SF33.

Biodiesel Properties	Control	0.2	0.4	0.8	1.6
Saponification Value	217.659	218.284	215.022	217.60	214.292
Iodine Value	16.165	22.241	35.582	35.751	38.597
Cetane number	67.739	66.3	63.678	63.339	63.086
Long Chain Saturated Factor	12.235	9.983	7.852	7.074	7.375
Cold Filter Plugging Point (°C)	21.962	14.887	8.192	5.747	6.693
Cloud Point (°C)	29.724	27.32	25.448	24.064	27.068
Pour Point (°C)	25.446	22.837	20.804	19.302	22.562
Allylic Position Equivalent	7.21	15.28	15.06	23.01	31.6
Bis-Allylic Position Equivalent	2.86	4.98	5.01	6.46	8.29
Oxidation Stability (h)	43.825	26.271	26.129	20.846	16.816
Higher Heating Value (mJ/kg)	39.186	39.175	38.753	39.167	39.242
Kinematic Viscosity (mm ² /s)	3.759	3.696	3.588	3.631	3.737
Density (g/cm ³)	0.867	0.869	0.861	0.87	0.87

Table 14 Theoretical biodiesel properties of *Fremyella diplosiphon* B481.

To further separate polar and aromatic compounds, samples were subjected to high-resolution GC × GC-TOFMS was performed. Our results revealed that FAME abundance was significantly higher ($P \leq 0.05$) in *F. diplosiphon* SF33 and B481 exposed to 0.8 and 1.6 mg L⁻¹ Nanofer 25s (Figure 65 and 66). A significant increase (16% and 13.41%) in octadecatrienoic acid (C18:3) in SF33 transesterified lipids was observed when supplemented with 0.8 and 1.6 mg L⁻¹ Nanofer 25s compared to the control. In addition, we detected a significant increase (49.13% and 14.67%) in octadecatrienoic acid (C18:3) in B481 transesterified lipids when treated with 0.8 and 1.6 mg L⁻¹ Nanofer 25s compared to the control. We identified FAME components such as C18:3 and C18:4 by GC×GC-TOFMS which were not detected in 1D GC-MS suggesting additional benefits of *F. diplosiphon*-derived biofuel. These findings indicate that *F. diplosiphon* nano-treated cultures could have higher biofuel capacity due to their higher FAME abundance.

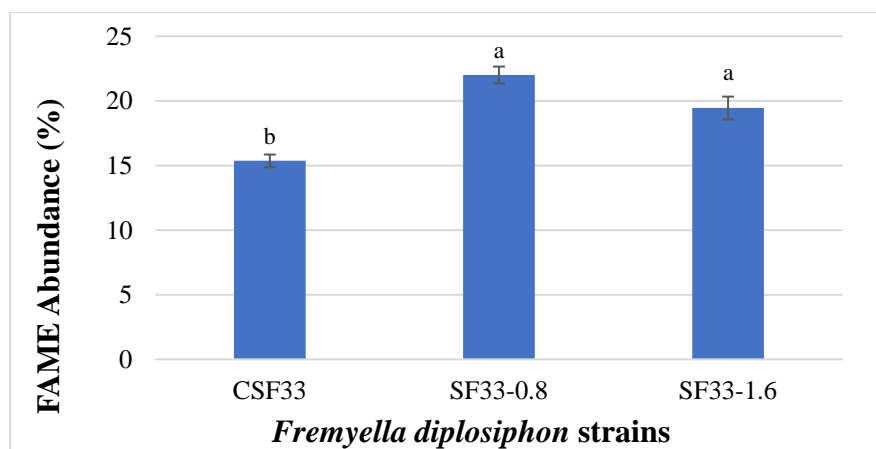


Figure 65 Fatty acid methyl ester (FAME) abundance in transesterified extractable lipids of *Fremyella diplosiphon* SF33.

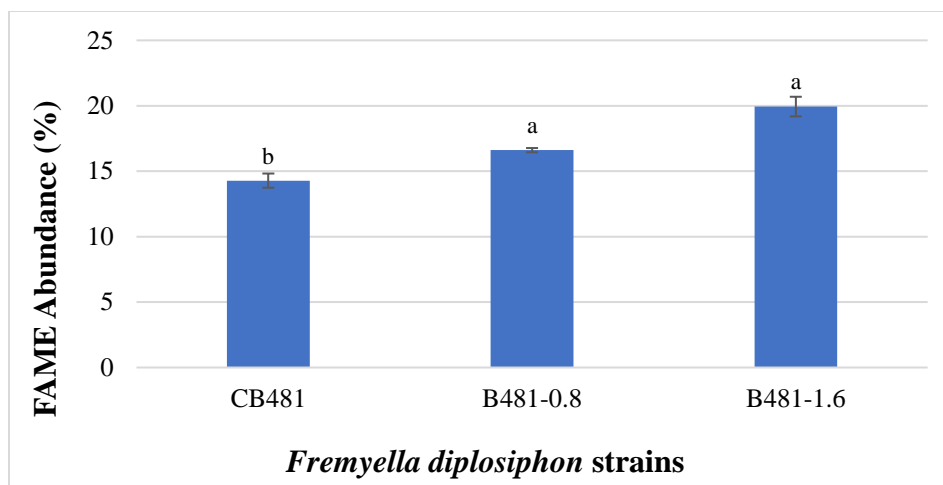


Figure 66 Fatty acid methyl ester (FAME) abundance in transesterified extractable lipids of *Fremyella diplosiphon* B481.

4.2.5 Microscopy studies to visualize the presence of iron nanoparticle in *F. diplosiphon* cell

Microscopy techniques including optical and transmission electron microscopy (TEM) are frequently used to identify the cyanobacterial morphology, ecology and physiological adaptations (Marine et al., 2004). In this study, *F. diplosiphon* B481 supplemented with 1.6 mg L⁻¹ Nanofer 25s labeled with Prussian blue was visualized under the optical microscopy to identify the effect of nZVI on filaments growth and morphological changes. Results of optical microscopy revealed that Nanofer 25s has no negative effect impact on *F. diplosiphon* growth and morphology (Figure 67).

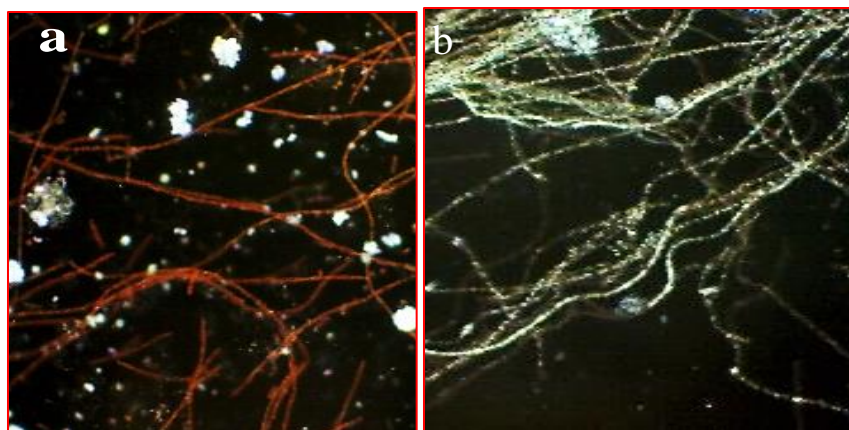


Figure 67 Dark field of optical microscopy of *Fremyella diplosiphon* B481 exposed to Nanofer 25s stained with Prussian blue at (a) day 0 and (b) day 3.

TEM offers morphological evidence about the size and shape of organelles as well as the presence of nanomaterial inside the cells (Marine et al., 2004). We visualized the presence of iron nanoparticles (Nanofer 25s) in *F. diplosiphon* cells using TEM (Figure 68). In a previous study, the ability of selected cyanobacteria species *Anabaena* sp., *Aphanizomenon* sp., and *Cylindrospermopsis* sp. to biosynthesize silver nanoparticles was identified using TEM (Patel et al., 2015). They reported the presence of nanoparticles inside the cyanobacterial cells in various shapes and sizes that ranged between 13 and 31 nm based on the host species.

Nanoparticles are composed of a wide array of materials and vary in size from 20 to 100 nm with a surface area of 25–30 m²g⁻¹ (Eglal and Ramamurthy, 2014). Since iron colloids tend to aggregate easily, variously sized nanoparticles have been investigated. It is also known that zero valent iron nanoparticles larger than 80 nm are toxic for bacteria such as *Escherichia coli* strain 8739 (Keller et al., 2012). Our findings indicate that iron

nanoparticles penetrate into *F. diplosiphon* cells due to their small size (50 nm) and act as a stress inducer, thus resulting in enhanced lipid production.

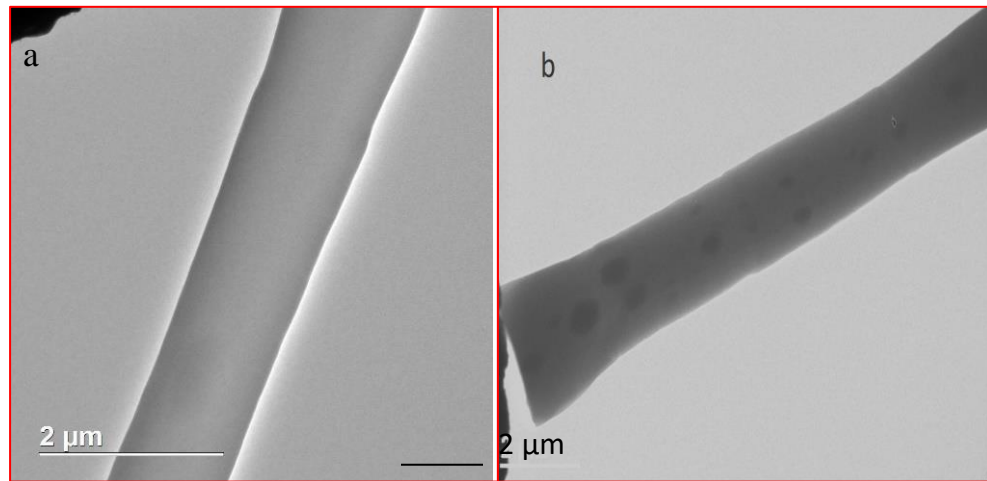


Figure 68 Transmission electron microscopy (TEM) micrographs (a) *Fremyella diplosiphon* B481 strain and (b) *F. diplosiphon* treated with 1.6 mg L⁻¹ Nanofer 25s.

CHAPTER V

CONCLUSIONS

5.1 ENHANCEMENT OF LIPID IN *F. DIPLOSIPHON* USING GENETIC TRANSFORMATION VIA. ELECTROPORATION

5.1.1 Overexpression of sterol desaturase and acyl-lipid desaturase genes in *F. diplosiphon* via electroporation-mediated genetic transformation.

Large-scale biofuel production from microalgae/cyanobacteria is greatly hindered by low lipid productivity during cultivation. Thus, enhancing total lipid content and fatty acid abundance are indispensable to reduce the cost of biofuel production. In this study, we constructed, cloned, and overexpressed plasmids containing the acyl-lipid desaturase and sterol desaturase genes in *F. diplosiphon* B481 strain. Isolated sequences were confirmed to encode these genes using primer-specific amplification and BLAST analysis. Real-time PCR identified a transformant exhibiting a 64-fold increase in SD transcript abundance. This transformed strain, B481-SD, thrived in liquid BG-11/HEPES medium containing 80 mg L⁻¹ ampicillin for 28 generations with no loss in photosynthetic pigment accumulation indicating the success of SD overexpression. With increasing demand for alternative energy sources, the development of transformant strains using genetic engineering approach, has paved the way for enhanced lipid productivity making it a promising commercial-scale biofuel agent.

5.1.2 Comparison of total lipid content and fatty acid compositions in the WT and transformant by gravimetric analysis, GC-MS and GC-TOFMS.

Gravimetric analysis of *F. diplosiphon* revealed a significant increase (27%) in total lipid content of B481-SD relative to the B481-WT, indicating that the SD-overexpressing strain is preferable for large-scale biofuel production. The presence of FAMES in *F. diplosiphon* B481-WT and B481-SD transesterified lipids demonstrates the potential of this species as a viable biofuel source due to its amenable fatty acid profile. In addition, increase in unsaturated FAME proportion was observed, which we hypothesize is most likely due to overexpression in the SD transformant. Theoretical biofuel properties were calculated and confirmed that *F. diplosiphon*-derived FAMES have a strong potential for high quality biofuel production. Comprehensive GC x GC-TOFMS revealed significantly higher FAME abundance (80.92% TL) in the transformant relative to the WT (77.92% TL) indicating that B481-SD has a higher biofuel capacity than B481-WT. Results demonstrated in this study offer a novel pathway for a highly efficient and cost-effective production system for renewable fuel and chemical feedstock.

5.1.3 Enhancement of total lipid content and essential fatty acid methyl esters by exposure to salinity stress.

Growth of the *F. diplosiphon* B481-SD strain in elevated salinity conditions (0 to 50 g L⁻¹ NaCl) indicate the impact of SD overexpression on halotolerance of the strain. While all strains exhibited declining growth in media amended with NaCl, B481-SD demonstrated sustained growth compare to B481-WT when exposed to 40 g L⁻¹ NaCl.

RT-qPCR of the halotolerant strain, B481-SDH, detected a 38-fold increase in SD expression confirming that this gene was still capable of overexpression in the presence of elevated salinity. Gravimetric analysis revealed a significantly higher total lipid content in B481-SDH relative to the B481-WT indicating that salinity stress induces additional lipid production. Additionally, FAME analysis detected significant increases in methyl octadecenoate (C18:1) and methyl octadecadienoate (C18:2) levels abundance from B481-SDH transesterified lipids when compared to the WT suggesting that salinity stress augments desaturated FAME yields. Further studies have confirmed that FAME profile of B481-SDH is ideal for biofuel production, and that this strain is capable of growth in sea water and brackish water. These findings demonstrate that cultivation of *F. diplosiphon* B481-SD in NaCl concentrations up to 40 g L⁻¹ has great potential as a source of clean and renewable biofuel.

5.1.4 Proteomic comparison of *F. diplosiphon* B481-wild type, B481-SD, and B481-SDH

Understanding the effect of SD overexpression and exposure to elevated salinity on *F. diplosiphon* proteome analysis is important to confirm whether overexpression is correlated with translation of the SD protein. SDS-PAGE revealed the presence of a band near the expected size of sterol desaturase in all strains, confirming expression of this protein in *F. diplosiphon*. Further studies using 2D-PAGE to determine differential protein expression revealed four spots that potentially represent sterol desaturase up-regulated in B481-SD and B481-SDH.

5.2 ENHANCEMENT OF LIPIDS AND FATTY ACIDS IN *F. DIPLOSIPHON* USING IRON NANOPARTICLES

5.2.1 Impact of iron nanoparticles (Nanofer 25 and Nanofer 25s) on growth and photosynthetic efficacy of two *F. diplosiphon* strains (B481 and SF33)

Growth of *F. diplosiphon*, B481 and SF33, in solution with nZVIs ranging from 0.05-3.2 mg L⁻¹ revealed that slight concentrations of iron nanoparticles are non-toxic to survival of the organism. Additionally, cultures supplemented with Nanofer 25s ranging from 0.2-1.6 mg L⁻¹ exhibited a significant increase in growth compared to the control indicating that trace concentrations of this nZVI provides a suitable source of iron required for *F. diplosiphon* growth. In addition, no significant increase in growth of cultures exposed to Nanofer 25 suggests that this nanoparticle could have lost its activity when exposed to air due to its lack of modification by organic/inorganic chemicals. Photosynthetic pigment quantification detected increase in *chl a* and carotenoid accumulations in B481 and SF33 exposed to Nanofer 25s ranging from 0.4-1.6 mg L⁻¹ relative to the control indicating higher photosynthetic activity. In addition, increase in phycocyanin, allophycocyanin, and phycobiliprotein levels indicates that pigment accumulation is directly affected by iron stress. These results confirm that adsorption of Nanofer 25s to cyanobacterial outer cell membranes could have resulted in enhanced membrane permeability and increased lipid production, with no lossess in pigmentation.

5.2.2 Comparison of total lipid content, fatty acid methyl ester profile in *F. diplosiphon* wild-type and Nanofer 25s-treated cells using gravimetric analysis, direct transesterification and GC-MS

Gravimetric analysis in *F. diplosiphon* revealed significant increases in total lipid yield of B481 when exposed to 0.4, 0.8 and 1.6 mg L⁻¹ Nanofer 25s and SF33 when exposed to 0.2 to 1.6 mg L⁻¹ of this nZVI which indicates iron stress leads in an elevated ROS level followed by increasing oxidative stress in cyanobacterial cells resulting in lipid production.

The presence of FAMES in B481 and SF33 nano-treated cells was confirmed by CG/MS and GC-TOF/MS. Significant increases in methyl octadecenoate (C18:1), and methyl octadecadienoate (C18:2) levels from SF33 and B481 transesterified lipids confirm that Nanofer 25s enhances unsaturated FAMES which are primary constituents in biofuel. *F. diplosiphon* transesterified lipids prove the potential of nano-treated strains as a practicable biofuel source due to its acquiescent fatty acid profile. In addition, higher FAME abundance in the nano-treated cultures compare to the WT was observed using GC x GC-TOFMS that indicate *F. diplosiphon* nano-treated cultures have a higher biofuel capacity than control. Theoretical biofuel properties of *F. diplosiphon* nano-treated cells confirmed a strong potential of the organism for efficient biofuel production. The presence of Nanofer 25s inside the *F. diplosiphon* filaments was visualized using TEM. In addition, visualization of *F. diplosiphon* nano-treated cells using optical microscopy confirmed that trace concentration of nZVI has no negative impact on filaments growth and morphology.

5.3 PERSPECTIVES AND APPLICATIONS

The fuel industry is considerably affected by government initiatives which play an important role in influencing capital interest. My dissertation research addresses two significant barriers to viability of cyanobacteria-based biofuels: enhanced total lipid content and essential fatty acid composition of the organism using genetic engineering and nanotechnological approaches to minimize freshwater input and artificial light supply respectively. These novel approaches were aimed towards overcoming other obstacles associated with cultivation, harvesting, and bioproductivity which would maximize its commercial potential.

This innovative approach to produce biofuel using brackish water and seawater by the overexpression of genes encoding lipid production in *F. diplosiphon* has great potential for commercialization. A non provisional patent application (No. 16/123,484) describing the process of genetic engineering to enhance total lipid content and fatty acid composition has been filed (Sitther and Gharaie Fathabad, 2018). In addition, Nanofer 25s-enhanced total lipid content and essential fatty acids have the prospective to reduce costs associated with large scale production. A provisional patent application (No. 62778617) explaining this process has also been filed (Sitther and Gharaie Fathabad, 2018). Achievement of the research objectives stated in this dissertation can be applied towards large-scale cultivation to produce high quantities of lipid for effective biofuel production. Scale-up studies to determine the feasibility of the strains will advance the biofuel market to the next higher level.

5.4 FUTURE WORK

In this study, total lipid content and essential unsaturated fatty acids in *F. diplosiphon* was enhanced by genetic engineering and nanotechnological approaches. Future studies will be aimed towards optimizing large-scale cultivation, harvest, and lipid extraction/conversion to determine the viability of *F. diplosiphon* B481-SD, B481-SDH and nano-treated cells for efficient biofuel production. In addition, we will measure ROS levels in the thylakoid membranes of *F. diplosiphon* nano-treated cells, and also malondialdehyde levels, which is one of the major indicators determining oxidative stress. In addition to biofuel and bioenergy, we will identify other potential commercial biotechnological applications of *F. diplosiphon*. This will include evaluating raw biomass for application as food and nutritional supplements, and high value purified products such as pigments and proteins for cosmetics and medicinal uses.

REFERENCES

- Adarme-Vega, T. C., Thomas-Hall, S. R., & Schenk, P. M. (2014). Towards sustainable sources for omega-3 fatty acids production. *Current Opinion in Biotechnology*, 26, 14-18.
- Afify, A. E. M. M., Shalaby, E. A., & Shanab, S. M. (2010). Enhancement of biodiesel production from different species of algae. *Grasasy Aceites*, 61(4), 416-422.
- Aguilar, P. S., & De Mendoza, D. (2006). Control of fatty acid desaturation: a mechanism conserved from bacteria to humans. *Molecular Microbiology*, 62(6), 1507-1514.
- Akbarnezhad, M., Mehrgan, M. S., Kamali, A., & Baboli, M. J. (2016). Bioaccumulation of Fe²⁺ and its effects on growth and pigment content of *spirulina* (*Arthrospira platensis*). *Aquaculture, Aquarium, Conservation & Legislation-International Journal of the Bioflux Society (AAFL Bioflux)*, 9(2).
- Allakhverdiev, S. I., Sakamoto, A., Nishiyama, Y., Inaba, M., & Murata, N. (2000). Ionic and osmotic effects of NaCl-induced inactivation of photosystems I and II in *Synechococcus* sp. *Plant physiology*, 123(3), 1047-1056.
- Apte, S. K., & Bhagwat, A. A. (1989). Salinity-stress-induced proteins in two nitrogen-fixing *Anabaena* strains differentially tolerant to salt. *Journal of Bacteriology*, 171(2), 909-915
- Bhagwat, A. A., & Apte, S. K. (1989). Comparative analysis of proteins induced by heat shock, salinity, and osmotic stress in the nitrogen-fixing cyanobacterium *Anabaena* sp. strain L-31. *Journal of Bacteriology*, 171(9), 5187-5189.

- Bhakar, R. N., Kumar, R., & Pabbi, S. (2013). Total lipids and fatty acid profile of different *Spirulina* strains as affected by salinity and incubation time. *Vegetos*, 26(2s), 148-54.
- Bhattarai, K., Stalick, W. M., Mckay, S., Geme, G., & Bhattarai, N. (2011). Biofuel: an alternative to fossil fuel for alleviating world energy and economic crises. *Journal of Environmental Science and Health, Part A*, 46(12), 1424-1442.
- Biswas, B., Scott, P. T., & Gresshoff, P. M. (2011). Tree legumes as feedstock for sustainable biofuel production: Opportunities and challenges. *Journal of Plant Physiology*, 168(16), 1877-1884.
- Blank, C. E., & Sanchez-Baracaldo, P. (2010). Timing of morphological and ecological innovations in the cyanobacteria—a key to understanding the rise in atmospheric oxygen. *Geobiology*, 8(1), 1-23.
- Blankenship, R. E. (2008). Photosynthetic pigments: Structure and spectroscopy. *Molecular Mechanisms of Photosynthesis*, 2, 41-58.
- Blumwald, E., Wolosin, J. M., & Packer, L. (1984). Na⁺ H⁺ exchange in the cyanobacterium *Synechococcus 6311*. *Biochemical and Biophysical Research Communications*, 122(1), 452-459.
- Bohin, A., Bouchart, F., Richet, C., Kol, O., Leroy, Y., Timmerman, P., & Zanetta, J. P. (2005). GC/MS identification and quantification of constituents of bacterial lipids and glycoconjugates obtained after methanolysis as heptafluorobutyrate derivatives. *Analytical Biochemistry*, 340(2), 231-244.

- Bolhassani, A., Khavari, A., & Orafa, Z. (2014). Electroporation—Advantages and drawbacks for delivery of drug, gene and vaccine. In *Application of Nanotechnology in Drug Delivery*. IntechOpen.
- Boudière, L., Michaud, M., Petroutsos, D., Rébeillé, F., Falconet, D., Bastien, O., Roy, S., Finazzi, G., Rolland, N., Jouhet, J. & Block, M. A. (2014). Glycerolipids in photosynthesis: composition, synthesis and trafficking. *Biochimica et Biophysica Acta (BBA)-Bioenergetics*, 1837(4), 470-480.
- Burgess-Cassler, A., Johansen, J. J., Santek, D. A., Ide, J. R., & Kendrick, N. C. (1989). Computerized quantitative analysis of coomassie-blue-stained serum proteins separated by two-dimensional electrophoresis. *Clinical Chemistry*, 35(12), 2297-2304.
- Cai, P. L., He, X. P., Liu, N., & Zhang, B. R. (2007). Effect of over-expression of sterol C-22 desaturase on ergosterol production in yeast strains. *Wei Sheng Wu Xue Bao = Acta Microbiologica Sinica*, 47(2), 274-279.
- Castielli, O., De la Cerda, B., Navarro, J. A., Hervás, M., & Miguel, A. (2009). Proteomic analyses of the response of cyanobacteria to different stress conditions. *FEBS Letters*, 583(11), 1753-1758.
- Chen, G., Qu, S., Wang, Q., Bian, F., Peng, Z., Zhang, Y., ... & He, Q. (2014). Transgenic expression of delta-6 and delta-15 fatty acid desaturases enhances omega-3 polyunsaturated fatty acid accumulation in *Synechocystis sp.* PCC6803. *Biotechnology for Biofuels*, 7(1), 32.

- Chen, Y., Deng, W., Wu, J., Qian, J., Chu, J., Zhuang, Y., & Liu, W. (2008). Genetic modulation of the overexpression of tailoring genes *eryK* and *eryG* leading to the improvement of erythromycin A purity and production in *Saccharopolyspora erythraea* fermentation. *Appl. Environ. Microbiol.*, *74*(6), 1820-1828.
- Chi, X., Yang, Q., Zhao, F., Qin, S., Yang, Y., Shen, J., & Lin, H. (2008). Comparative analysis of fatty acid desaturases in cyanobacterial genomes. *Comparative and Functional Genomics*, 2008.
- Chisti, Y. (2007). Biodiesel from microalgae. *Biotechnology advances*, *25*(3), 294-306.
- Crowe, J. H., Carpenter, J. F., & Crowe, L. M. (1998). The role of vitrification in anhydrobiosis. *Annual Review of Physiology*, *60*(1), 73-103.
- De Marsac, N. T., & Houmard, J. (1988). Complementary chromatic adaptation: physiological conditions and action spectra. In *Methods in Enzymology* (Vol. 167, pp. 318-328). Academic Press.
- Deng, M. D., & Coleman, J. R. (1999). Ethanol synthesis by genetic engineering in cyanobacteria. *Appl. Environ. Microbiol.*, *65*(2), 523-528.
- Eglal, M. M., & Ramamurthy, A. S. (2014). Nanofer ZVI: morphology, particle characteristics, kinetics, and applications. *Journal of Nanomaterials*, 2014, 29.
- El Baky, H. H. A., El-Baroty, G. S., Bouaid, A., Martinez, M., & Aracil, J. (2012). Enhancement of lipid accumulation in *Scenedesmus obliquus* by optimizing CO₂ and Fe³⁺ levels for biodiesel production. *Bioresource Technology*, *119*, 429-432.
- Favretto, L. (2004). Basic Guidelines for Microwave Organic Chemistry Applications. *Milestone, Bergamo*.

- Federspiel, N. A., & Grossman, A. R. (1990). Characterization of the light-regulated operon encoding the phycoerythrin-associated linker proteins from the cyanobacterium *Fremyella diplosiphon*. *Journal of Bacteriology*, 172(7), 4072-4081.
- Ferreira, F., & Straus, N. A. (1994). Iron deprivation in cyanobacteria. *Journal of Applied Phycology*, 6(2), 199-210.
- Floch, J. (1957). A simple method for the isolation and purification of total lipids from animal tissues. *Journal of Biol. Chem.*, 226, 497-509.
- Fourie, R., Kuloyo, O. O., Mochochoko, B. M., Albertyn, J., & Pohl, C. H. (2018). Iron at the Centre of *Candida albicans* Interactions. *Frontiers in Cellular and Infection Microbiology*, 8.
- Froehlich, J.E., Poorman, R., Reardon, E., Barnum, S.R. & Jaworski, J.G. (1990). Purification and characterization of acyl carrier protein from two cyanobacteria species. *European Journal of Biochemistry*, 193(3), 817-825.
- Frysinger, G. S., Gaines, R. B., Xu, L., & Reddy, C. M. (2003). Resolving the unresolved complex mixture in petroleum-contaminated sediments. *Environmental Science & Technology*, 37(8), 1653-1662.
- Fu, P. (2009). Genome-scale modeling of *Synechocystis* sp. PCC 6803 and prediction of pathway insertion. *Journal of Chemical Technology & Biotechnology: International Research in Process, Environmental & Clean Technology*, 84(4), 473-483.

- Fulda, S., Huang, F., Nilsson, F., Hagemann, M., & Norling, B. (2000). Proteomics of *Synechocystis* sp. strain PCC 6803: Identification of periplasmic proteins in cells grown at low and high salt concentrations. *European Journal of Biochemistry*, 267(19), 5900-5907.
- Fulda, S., Mikkat, S., Huang, F., Huckauf, J., Marin, K., Norling, B., & Hagemann, M. (2006). Proteome analysis of salt stress response in the cyanobacterium *Synechocystis* sp. strain PCC 6803. *Proteomics*, 6(9), 2733-2745.
- Gabrielle, B. (2008). Significance and limitations of first generation biofuels. *Journal de la Société de Biologie*, 202(3), 161-165.
- Gelvin, S. B. (2003). Agrobacterium-mediated plant transformation: the biology behind the “gene-jockeying” tool. *Microbiol. Mol. Biol. Rev.*, 67(1), 16-37.
- Goda, N., Tenno, T., Takasu, H., Hiroaki, H., & Shirakawa, M. (2004). The PRESAT-vector: Asymmetric T-vector for high-throughput screening of soluble protein domains for structural proteomics. *Protein Science*, 13(3), 652-658.
- Griffiths, M. J., & Harrison, S. T. (2009). Lipid productivity as a key characteristic for choosing algal species for biodiesel production. *Journal of Applied Phycology*, 21(5), 493-507.
- Grossman, A. R., Bhaya, D., & He, Q. (2001). Tracking the light environment by cyanobacteria and the dynamic nature of light harvesting. *Journal of Biological Chemistry*, 276(15), 11449-11452.

- Gude, V. G., Patil, P., Martinez-Guerra, E., Deng, S., & Nirmalakhandan, N. (2013). Microwave energy potential for biodiesel production. *Sustainable Chemical Processes*, 1(1), 5.
- Guha, T., Ravikumar, K. V. G., Mukherjee, A., Mukherjee, A., & Kundu, R. (2018). Nanopriming with zero valent iron (nZVI) enhances germination and growth in aromatic rice cultivar (*Oryza sativa* cv. Gobindabhog L.). *Plant Physiology and Biochemistry*, 127, 403-413.
- Heaton, E. A., Dohleman, F. G., & Long, S. P. (2008). Meeting US biofuel goals with less land: the potential of *Miscanthus*. *Global Change Biology*, 14(9), 2000-2014.
- Hu, J., Jin, L., Wang, X., Cai, W., Liu, Y., & Wang, G. (2014). Response of photosynthetic systems to salinity stress in the desert cyanobacterium *Scytonema javanicum*. *Advances in Space Research*, 53(1), 30-36.
- Huang, F., Fulda, S., Hagemann, M. and Norling, B., 2006. Proteomic screening of salt-stress-induced changes in plasma membranes of *Synechocystis* sp. strain PCC 6803. *Proteomics*, 6(3), pp.910-920.
- Huang, X., Wei, L., Huang, Z., & Yan, J. (2014). Effect of high ferric ion concentrations on total lipids and lipid characteristics of *Tetraselmis subcordiformis*, *Nannochloropsis oculata* and *Pavlova viridis*. *Journal of Applied Phycology*, 26(1), 105-114.
- Kaczmarzyk, D., & Fulda, M. (2010). Fatty acid activation in cyanobacteria mediated by acyl-acyl carrier protein synthetase enables fatty acid recycling. *Plant Physiology*, 152(3), 1598-1610.

- Kahn, J. H., & Gelso, C. J. (1997). Factor structure of the Research Training Environment Scale-Revised: Implications for research training in applied psychology. *The Counseling Psychologist, 25*(1), 22-37.
- Kamthan, A., Kamthan, M., & Datta, A. (2017). Expression of C-5 sterol desaturase from an edible mushroom in *fiisson* yeast enhances its ethanol and thermotolerance. *PloS One, 12*(3), e0173381.
- Kaneko, T., Sato, S., Kotani, H., Tanaka, A., Asamizu, E., Nakamura, Y., & Kimura, T. (1996). Sequence analysis of the genome of the unicellular cyanobacterium *Synechocystis* sp. strain PCC6803. II. Sequence determination of the entire genome and assignment of potential protein-coding regions. *DNA Research, 3*(3), 109-136.
- Kanesaki, Y., Suzuki, I., Allakhverdiev, S. I., Mikami, K., & Murata, N. (2002). Salt stress and hyperosmotic stress regulate the expression of different sets of genes in *Synechocystis* sp. PCC 6803. *Biochemical and Biophysical Research Communications, 290*(1), 339-348.
- Kang, N. K., Lee, B., Choi, G. G., Moon, M., Park, M. S., Lim, J., & Yang, J. W. (2014). Enhancing lipid productivity of *Chlorella vulgaris* using oxidative stress by TiO₂ nanoparticles. *Korean Journal of Chemical Engineering, 31*(5), 861-867.
- Kehoe, D. M., & Grossman, A. R. (1998). Use of molecular genetics to investigate complementary chromatic adaptation: Advances in transformation and complementation. In *Methods in Enzymology* (Vol. 297, pp. 279-290). Academic Press.

- Keller, A. A., Garner, K., Miller, R. J., & Lenihan, H. S. (2012). Toxicity of nano-zero valent iron to freshwater and marine organisms. *PloS One*, 7(8), e43983.
- Kenyon, C. N. (1972). Fatty acid composition of unicellular strains of blue-green algae. *Journal of Bacteriology*, 109(2), 827-834.
- Kern, J., Zouni, A., Guskov, A., & Krauß, N. (2009). Lipids in the Structure of Photosystem I, Photosystem II and the Cytochrome b 6 f Complex. In *Lipids in Photosynthesis* (pp. 203-242). Springer, Dordrecht.
- Khatoon, T., Hussain, K., Majeed, A., Nawaz, K., & Nisar, M. F. (2010). Morphological variations in maize (*Zea mays* L.) under different levels of NaCl at germinating stage. *World Appl. Sci. J*, 8(10), 1294-1297.
- Kirschling, T. L., Gregory, K. B., Minkley, Jr, E. G., Lowry, G. V., & Tilton, R. D. (2010). Impact of nanoscale zero valent iron on geochemistry and microbial populations in trichloroethylene contaminated aquifer materials. *Environmental Science & Technology*, 44(9), 3474-3480.
- Ko, K. S., Koh, D. C., & Kong, I. (2018). Toxicity evaluation of individual and mixtures of nanoparticles based on algal chlorophyll content and cell count. *Materials*, 11(1), 121.
- Kramm, A., Kisiela, M., Schulz, R., & Maser, E. (2012). Short-chain dehydrogenases/reductases in cyanobacteria. *The FEBS Journal*, 279(6), 1030-1043.

- Lang, I., Hodac, L., Friedl, T., & Feussner, I. (2011). Fatty acid profiles and their distribution patterns in microalgae: a comprehensive analysis of more than 2000 strains from the SAG culture collection. *BMC Plant Biology*, *11*(1), 124.
- Latifi, A., Ruiz, M., & Zhang, C. C. (2009). Oxidative stress in cyanobacteria. *FEMS Microbiology Reviews*, *33*(2), 258-278.
- Lea-Smith, D.J., Biller, S.J., Davey, M.P., Cotton, C.A., Sepulveda, B.M.P., Turchyn, A.V., Scanlan, D.J., Smith, A.G., Chisholm, S.W. & Howe, C.J. (2015). Contribution of cyanobacterial alkane production to the ocean hydrocarbon cycle. *Proceedings of the National Academy of Sciences*, *112*(44), 13591-13596.
- Lepage, G., & Roy, C. C. (1984). Improved recovery of fatty acid through direct transesterification without prior extraction or purification. *Journal of Lipid Research*, *25*(12), 1391-1396.
- Lepage, G., & Roy, C. C. (1986). Direct transesterification of all classes of lipids in a one-step reaction. *Journal of Lipid Research*, *27*(1), 114-120.
- Lewis, T., Nichols, P. D., & McMeekin, T. A. (2000). Evaluation of extraction methods for recovery of fatty acids from lipid-producing microheterotrophs. *Journal of Microbiological Methods*, *43*(2), 107-116.
- Li-Beisson, Y., Shorrosh, B., Beisson, F., Andersson, M. X., Arondel, V., Bates, P. D., ... & Franke, R. B. (2013). Acyl-lipid metabolism. *The Arabidopsis book/American Society of Plant Biologists*, *11*.

- Lindberg, P., Park, S., & Melis, A. (2010). Engineering a platform for photosynthetic isoprene production in cyanobacteria, using *Synechocystis* as the model organism. *Metabolic Engineering*, *12*(1), 70-79.
- Liu, X., Sheng, J., & Curtiss III, R. (2011). Fatty acid production in genetically modified cyanobacteria. *Proceedings of the National Academy of Sciences*, *108*(17), 6899-6904.
- Los, D., & Mironov, K. (2015). Modes of fatty acid desaturation in cyanobacteria: an update. *Life*, *5*(1), 554-567.
- Los, D. A., Mironov, K. S., & Allakhverdiev, S. I. (2013). Regulatory role of membrane fluidity in gene expression and physiological functions. *Photosynthesis Research*, *116*(2-3), 489-509.
- Loto, I., Gutiérrez, M.S., Barahona, S., Sepúlveda, D., Martínez-Moya, P., Baeza, M., Cifuentes, V. & Alcaíno, J. (2012). Enhancement of carotenoid production by disrupting the C22-sterol desaturase gene (CYP61) in *Xanthophyllomyces dendrorhous*. *BMC Microbiology*, *12*(1), 235.
- Lu, Y., Chi, X., Yang, Q., Li, Z., Liu, S., Gan, Q., & Qin, S. (2009). Molecular cloning and stress-dependent expression of a gene encoding Δ 12-fatty acid desaturase in the Antarctic microalga *Chlorella vulgaris* NJ-7. *Extremophiles*, *13*(6), 875.
- Lunde, C., Jensen, P. E., Rosgaard, L., Haldrup, A., Gilpin, M. J., & Scheller, H. V. (2003). Plants impaired in state transitions can to a large degree compensate for their defect. *Plant and Cell Physiology*, *44*(1), 44-54.

- Machado, I. M., & Atsumi, S. (2012). Cyanobacterial biofuel production. *Journal of Biotechnology*, *162*(1), 50-56.
- Mansilla, M. C., Banchio, C. E., & de Mendoza, D. (2008). Signalling pathways controlling fatty acid desaturation. In *Lipids in Health and Disease* (pp. 71-99). Springer, Dordrecht.
- Marin, K., Kanesaki, Y., Los, D. A., Murata, N., Suzuki, I., & Hagemann, M. (2004). Gene expression profiling reflects physiological processes in salt acclimation of *Synechocystis* sp. strain PCC 6803. *Plant Physiology*, *136*(2), 3290-3300.
- Mariné, M. H., Clavero, E., & Roldán, M. (2004). Microscopy methods applied to research on cyanobacteria. *Limnetica*, *23*(1-2), 179-186.
- Masera, K., & Hossain, A. K. (2017). Production, characterisation and assessment of biomixture fuels for compression ignition engine application. *World Acad Sci Engn Technol Internat J Mech Aero Indust Mecha Manufact Engn*, *11*, 1852-1858.
- Matos, M.C., Campos, P.S., Ramalho, J.C., Medeira, M.C., Maia, M.I., Semedo, J.M., Marques, N.M. & Matos, A. (2002). Photosynthetic activity and cellular integrity of the Andean legume *Pachyrhizus ahipa* (Wedd.) Parodi under heat and water stress. *Photosynthetica*, *40*(4), 493-501.
- Meher, L. C., Sagar, D. V., & Naik, S. N. (2006). Technical aspects of biodiesel production by transesterification—a review. *Renewable and Sustainable Energy Reviews*, *10*(3), 248-268.

- Michel, K. P., & Pistorius, E. K. (2004). Adaptation of the photosynthetic electron transport chain in cyanobacteria to iron deficiency: the function of *IdiA* and *IsiA*. *Physiologia Plantarum*, *120*(1), 36-50.
- Minhas, A. K., Hodgson, P., Barrow, C. J., & Adholeya, A. (2016). A review on the assessment of stress conditions for simultaneous production of microalgal lipids and carotenoids. *Frontiers in Microbiology*, *7*, 546.
- Modiri, S., Sharafi, H., Alidoust, L., Hajfarajollah, H., Haghghi, O., Azarivand, A., Zamanzadeh, Z., Zahiri, H.S., Vali, H. & Noghabi, K.A. (2015). Lipid production and mixotrophic growth features of cyanobacterial strains isolated from various aquatic sites. *Microbiology*, *161*(3), 662-673.
- Molitor, V., Erber, W., & Peschek, G. A. (1986). Increased levels of cytochrome oxidase and sodium-proton antiporter in the plasma membrane of *Anacystis nidulans* after growth in sodium-enriched media. *FEBS Letters*, *204*(2), 251-256.
- Montgomery, B. L. (2016). Mechanisms and fitness implications of photomorphogenesis during chromatic acclimation in cyanobacteria. *Journal of Experimental Botany*, *67*(14), 4079-4090.
- Müller, V., & Oren, A. (2003). Metabolism of chloride in halophilic prokaryotes. *Extremophiles*, *7*(4), 261-266.
- Murata, N., & Wada, H. (1995). Acyl-lipid desaturases and their importance in the tolerance and acclimatization to cold of cyanobacteria. *Biochemical Journal*, *308*(Pt 1), 1.

- Murata, N., Wada, H., & Gombos, Z. (1992). Modes of fatty-acid desaturation in cyanobacteria. *Plant and Cell Physiology*, 33(7), 933-941.
- Mutanda, T., Ramesh, D., Karthikeyan, S., Kumari, S., Anandraj, A., & Bux, F. (2011). Bioprospecting for hyper-lipid producing microalgal strains for sustainable biofuel production. *Bioresource Technology*, 102(1), 57-70.
- Naik, S. N., Goud, V. V., Rout, P. K., & Dalai, A. K. (2010). Production of first and second generation biofuels: a comprehensive review. *Renewable and Sustainable Energy Reviews*, 14(2), 578-597.
- Nazari, F., & Raheb, J. (2015). Genetic engineering of microalgae for enhanced biodiesel production suitable fuel replacement of fossil fuel as a novel energy source. *American Journal of Life Sciences*, 3(1), 32.
- Nomanbhay, S., & Ong, M. (2017). A review of microwave-assisted reactions for biodiesel production. *Bioengineering*, 4(2), 57.
- Nozzi, N. E., Oliver, J. W., & Atsumi, S. (2013). Cyanobacteria as a platform for biofuel production. *Frontiers in Bioengineering and Biotechnology*, 1, 7.
- O'Farrell, P. H. (1975). High resolution two-dimensional electrophoresis of proteins. *Journal of Biological Chemistry*, 250(10), 4007-4021.
- Olsson, M. (1995). Alterations in lipid composition, lipid peroxidation and anti-oxidative protection during senescence in drought stressed plants and non drought stressed plants of *Pisum sativum*. *Plant Physiol. Biochem.*, 33, 547-553.

- Oren, A. (1999). Bioenergetic aspects of halophilism. *Microbiol. Mol. Biol. Rev.*, 63(2), 334-348.
- Pade, N., & Hagemann, M. (2015). Salt acclimation of cyanobacteria and their application in biotechnology. *Life*, 5(1), 25-49.
- Padrova, K., Lukavský, J., Nedbalová, L., Čejková, A., Cajthaml, T., Sigler, K., Vítová, M. & Řezanka, T. (2015). Trace concentrations of iron nanoparticles cause overproduction of biomass and lipids during cultivation of cyanobacteria and microalgae. *Journal of Applied Phycology*, 27(4), 1443-1451.
- Pal, D., Khozin-Goldberg, I., Cohen, Z., & Boussiba, S. (2011). The effect of light, salinity, and nitrogen availability on lipid production by *Nannochloropsis* sp. *Applied Microbiology and Biotechnology*, 90(4), 1429-1441.
- Parmar, A., Singh, N. K., Pandey, A., Gnansounou, E., & Madamwar, D. (2011). Cyanobacteria and microalgae: a positive prospect for biofuels. *Bioresource Technology*, 102(22), 10163-10172.
- Pate, R., Klise, G., & Wu, B. (2011). Resource demand implications for US algae biofuels production scale-up. *Applied Energy*, 88(10), 3377-3388.
- Patel, V., Berthold, D., Puranik, P., & Gantar, M. (2015). Screening of cyanobacteria and microalgae for their ability to synthesize silver nanoparticles with antibacterial activity. *Biotechnology Reports*, 5, 112-119.
- Pattanaik, B., Busch, A. W., Hu, P., Chen, J., & Montgomery, B. L. (2014). Responses to iron limitation are impacted by light quality and regulated by RcaE in the chromatically acclimating cyanobacterium *Fremyella diplosiphon*. *Microbiology*, 160(5), 992-1005.

- Pattanaik, B., Whitaker, M. J., & Montgomery, B. L. (2011). Convergence and divergence of the photoregulation of pigmentation and cellular morphology in *Fremyella diplosiphon*. *Plant Signaling & Behavior*, 6(12), 2038-2041.
- Quintana, N., Van der Kooy, F., Van de Rhee, M. D., Voshol, G. P., & Verpoorte, R. (2011). Renewable energy from Cyanobacteria: energy production optimization by metabolic pathway engineering. *Applied Microbiology and Biotechnology*, 91(3), 471-490.
- Radakovits, R., Jinkerson, R. E., Darzins, A., & Posewitz, M. C. (2010). Genetic engineering of algae for enhanced biofuel production. *Eukaryotic Cell*, 9(4), 486-501.
- Riss, J., Décordé, K., Sutra, T., Delage, M., Baccou, J.C., Jouy, N., Brune, J.P., Oréal, H., Cristol, J.P. & Rouanet, J.M. (2007). Phycobiliprotein C-phycoocyanin from *Spirulina platensis* is powerfully responsible for reducing oxidative stress and NADPH oxidase expression induced by an atherogenic diet in hamsters. *J. of Agricultural and Food Chemistry*, 55(19), 7962-7967.
- Rizwan, M., Mujtaba, G., & Lee, K. (2017). Effects of iron sources on the growth and lipid/carbohydrate production of marine microalga *Dunaliella tertiolecta*. *Biotechnology and Bioprocess Engineering*, 22(1), 68-75.
- Sabaitis, J. E., & Powell, G. L. (1976). Acyl carrier protein metabolism and regulation of fatty acid biosynthesis by *Lactobacillus plantarum*. *Journal of Biological Chemistry*, 251(15), 4706-4712.

- Sakai, M., Ogawa, T., Matsuoka, M., & Fukuda, H. (1997). Photosynthetic conversion of carbon dioxide to ethylene by the recombinant cyanobacterium, *Synechococcus* sp. PCC 7942, which harbors a gene for the ethylene-forming enzyme of *Pseudomonas syringae*. *Journal of Fermentation and Bioengineering*, 84(5), 434-443.
- Sakamoto, T., Kumihashi, K., Kunita, S., Masaura, T., Inoue-Sakamoto, K., & Yamaguchi, M. (2011). The extracellular-matrix-retaining cyanobacterium *Nostoc verrucosum* accumulates trehalose, but is sensitive to desiccation. *FEMS Microbiology Ecology*, 77(2), 385-394.
- Sakamoto, T., Yoshida, T., Arima, H., Hatanaka, Y., Takani, Y., & Tamaru, Y. (2009). Accumulation of trehalose in response to desiccation and salt stress in the terrestrial cyanobacterium *Nostoc commune*. *Phycological Research*, 57(1), 66-73.
- Sayre, R. (2010). Microalgae: the potential for carbon capture. *Bioscience*, 60(9), 722-727.
- Seib, L. O., & Kehoe, D. M. (2002). A turquoise mutant genetically separates expression of genes encoding phycoerythrin and its associated linker peptides. *Journal of Bacteriology*, 184(4), 962-970.
- Sevcu, A., El-Temsah, Y. S., Joner, E. J., & Černík, M. (2009). Oxidative stress induced in microorganisms by zero-valent iron nanoparticles. *Microbes and Environments*, 1107220320-1107220320.

- Shcolnick, S., & Keren, N. (2006). Metal homeostasis in cyanobacteria and chloroplasts. Balancing benefits and risks to the photosynthetic apparatus. *Plant Physiology*, *141*(3), 805-810.
- Sheehan, J., Dunahay, T., Benemann, J., & Roessler, P. (1998). A look back at the US Department of Energy's aquatic species program: biodiesel from algae. *National Renewable Energy Laboratory*, 328.
- Shimajima, M., Ohta, H., & Nakamura, Y. (2009). Biosynthesis and function of chloroplast lipids. In *Lipids in Photosynthesis* (pp. 35-55). Springer, Dordrecht.
- Shukla, E., Singh, S. S., Singh, P., & Mishra, A. K. (2012). Chemotaxonomy of heterocystous cyanobacteria using FAME profiling as species markers. *Protoplasma*, *249*(3), 651-661.
- Siegenthaler, P. A. (1998). Molecular organization of acyl lipids in photosynthetic membranes of higher plants. In *Lipids in Photosynthesis: Structure, Function and Genetics* (pp. 119-144). Springer, Dordrecht.
- Singh, J. S., Kumar, A., Rai, A. N., & Singh, D. P. (2016). Cyanobacteria: a precious bio-resource in agriculture, ecosystem, and environmental sustainability. *Frontiers in Microbiology*, *7*, 529.
- Singh, S. C., Sinha, R. P., & Hader, D. P. (2002). Role of lipids and fatty acids in stress tolerance in cyanobacteria. *Acta Protozoologica*, *41*(4), 297-308.
- Singh, S. P., & Montgomery, B. L. (2013). Salinity impacts photosynthetic pigmentation and cellular morphology changes by distinct mechanisms in *Fremyella*

- diplosiphon*. *Biochemical and Biophysical Research Communications*, 433(1), 84-89.
- Sinha, R.P. (2011). Antioxidants as natural arsenal against multiple stresses in cyanobacteria. *Journal of Biotechnology*, 2(2), pp. 168-178.
- Sitther, V. & Gharai, F.S. (2018). Engineered cyanobacteria with enhanced lipid production. Non Provisional Patent Application No. 16/123,484.
- Sitther, V. & Gharai, F.S. (2018). *Fremyella diplosiphon* growth enhanced by metallic nanoparticles to produce biomass. Provisional Patent Application No. 62778617.
- Srivastava, A. K., Bhargava, P., & Rai, L. C. (2005). Salinity and copper-induced oxidative damage and changes in the antioxidative defence systems of *Anabaena doliolum*. *World journal of Microbiology and Biotechnology*, 21(6-7), 1291-1298.
- Srivastava, A. K., Bhargava, P., Kumar, A., Rai, L. C., & Neilan, B. A. (2009). Molecular characterization and the effect of salinity on cyanobacterial diversity in the rice fields of Eastern Uttar Pradesh, India. *Saline Systems*, 5(1), 4.
- Straus, N. A. (1994). Iron deprivation: physiology and gene regulation. In *The Molecular Biology of Cyanobacteria* (pp. 731-750). Springer, Dordrecht.
- Tabatabai, B. (2017). Biotechnological approaches to enhance halotolerance and photosynthetic efficacy in the cyanobacterium, *Fremyella diplosiphon*. *Dissertation. Morgan State University, p. 150*.
- Tabatabai, B., Fathabad, S. G., Bonyi, E., Rajini, S., Aslan, K., & Sitther, V. (2019). Nanoparticle-Mediated Impact on Growth and Fatty Acid Methyl Ester

- Composition in the Cyanobacterium *Fremyella diplosiphon*. *BioEnergy Research*, 1-10.
- Tabatabai, B., Arumanayagam, A.S., Enitan, O., Mani, A., Natarajan, S.S. & Sittther, V. (2017a). Identification of a halotolerant mutant via in vitro mutagenesis in the cyanobacterium *Fremyella diplosiphon*. *Current Microbiology*, 74(1), pp.77-83.
- Tabatabai, B., Arumanayagam, A.S., Enitan, O., Mani, A., Natarajan, S.S. & Sittther, V. (2017b). Overexpression of *hlyB* and *mdh* genes confers halotolerance in *Fremyella diplosiphon*, a freshwater cyanobacterium. *Enzyme and Microbial Technology*, 103, pp.12-17.
- Tabatabai, B., Chen, H., Lu, J., Giwa-Otusajo, J., McKenna, A. M., Shrivastava, A. K., & Sittther, V. (2018). *Fremyella diplosiphon* as a Biodiesel Agent: Identification of Fatty Acid Methyl Esters via Microwave-Assisted Direct in Situ Transesterification. *Bioenergy Research*, 11(3), 528-537.
- Takagi, M., & Yoshida, T. (2006). Effect of salt concentration on intracellular accumulation of lipids and triacylglyceride in marine microalgae *Dunaliella* cells. *Journal of Bioscience and Bioengineering*, 101(3), 223-226.
- Talebi, A. F., Tabatabaei, M., & Chisti, Y. (2014). BiodieselAnalyzer: a user-friendly software for predicting the properties of prospective biodiesel. *Biofuel Research Journal*, 1(2), 55-57.
- Tasaka, Y., Gombos, Z., Nishiyama, Y., Mohanty, P., Ohba, T., Ohki, K., & Murata, N. (1996). Targeted mutagenesis of acyl-lipid desaturases in *Synechocystis*: evidence

for the important roles of polyunsaturated membrane lipids in growth, respiration and photosynthesis. *The EMBO Journal*, 15(23), 6416-6425.

Terry, M. J., Linley, P. J., & Kohchi, T. (2002). Making light of it: the role of plant haem oxygenases in phytochrome chromophore synthesis.

The NCBI taxonomy database

<https://www.ncbi.nlm.nih.gov/Taxonomy/Browser/wwwtax.cgi?lvl=0&id=57143>

3

Tonk, L., Bosch, K., Visser, P. M., & Huisman, J. (2007). Salt tolerance of the harmful cyanobacterium *Microcystis aeruginosa*. *Aquatic Microbial Ecology*, 46(2), 117-123.

Tunnacliffe, A., & Lapinski, J. (2003). Resurrecting Van Leeuwenhoek's rotifers: a reappraisal of the role of disaccharides in anhydrobiosis. *Philosophical Transactions of the Royal Society of London. Series B: Biological Sciences*, 358(1438), 1755-1771.

United State Environmental Protection Agency (2017).

<https://www.epa.gov/ghgemissions/global-greenhouse-gas-emissions-data>

Vadivel, N., Yuvakkumar, R., Suriyaprabha, R., & Rajendran, V. (2012). Catalytic Effect of Iron Nanoparticles on Heterocyst, Protein and Chlorophyll Content of *Anabaena sp.* *International Journal of Green Nanotechnology*, 4(3), 326-338.

Valentine, D. L., & Reddy, C. M. (2015). Latent hydrocarbons from cyanobacteria. *Proceedings of the National Academy of Sciences*, 112(44), 13434-13435.

- Venegas-Calcerón, M., Sayanova, O., & Napier, J. A. (2010). An alternative to fish oils: metabolic engineering of oil-seed crops to produce omega-3 long chain polyunsaturated fatty acids. *Progress in Lipid Research*, 49(2), 108-119.
- Vermaas, W. F. (2001). Photosynthesis and respiration in cyanobacteria. *eLS*.
- Vimalarasan, A., Pratheeba, N., Ashokkumar, B., Sivakumar, N., & Varalakshmi, P. (2011). Production of biodiesel from cyanobacteria (*Oscillatoria annae*) by alkali and enzyme mediated transesterification.
- Voelker, T. A., Jones, A., Cranmer, A. M., Davies, H. M., & Knutzon, D. S. (1997). Broad-range and binary-range acyl-acyl-carrier-protein thioesterases suggest an alternative mechanism for medium-chain production in seeds. *Plant Physiology*, 114(2), 669-677.
- Wada, H., & Murata, N. (1990). Temperature-induced changes in the fatty acid composition of the cyanobacterium, *Synechocystis* PCC6803. *Plant Physiology*, 92(4), 1062-1069.
- Wada, N., Sakamoto, T., & Matsugo, S. (2013). Multiple roles of photosynthetic and sunscreen pigments in cyanobacteria focusing on the oxidative stress. *Metabolites*, 3(2), 463-483.
- Wahlen, B. D., Willis, R. M., & Seefeldt, L. C. (2011). Biodiesel production by simultaneous extraction and conversion of total lipids from microalgae, cyanobacteria, and wild mixed-cultures. *Bioresource Technology*, 102(3), 2724-2730.

- Wang, J., Fang, Z., Cheng, W., Yan, X., Tsang, P. E., & Zhao, D. (2016). Higher concentrations of nanoscale zero-valent iron (nZVI) in soil induced rice chlorosis due to inhibited active iron transportation. *Environmental Pollution*, *210*, 338-345.
- Whitaker, M. J., Bordowitz, J. R., & Montgomery, B. L. (2009). CpcF-dependent regulation of pigmentation and development in *Fremyella diplosiphon*. *Biochemical and Biophysical Research Communications*, *389*(4), 602-606.
- Xu, W., Tang, H., Wang, Y., & Chitnis, P. R. (2001). Proteins of the cyanobacterial photosystem I. *Biochimica et Biophysica Acta (BBA)-Bioenergetics*, *1507*(1-3), 32-40.
- Zhang, A., Carroll, A. L., & Atsumi, S. (2017). Carbon recycling by cyanobacteria: improving CO₂ fixation through chemical production. *FEMS Microbiology Letters*, *364*(16), fnx165.
- Zhang, M., Barg, R., Yin, M., Gueta-Dahan, Y., Leikin-Frenkel, A., Salts, Y., Shabtai, S. & Ben-Hayyim, G. (2005). Modulated fatty acid desaturation via overexpression of two distinct ω -3 desaturases differentially alters tolerance to various abiotic stresses in transgenic tobacco cells and plants. *The Plant Journal*, *44*(3), 361-371.